AFRL-RV-HA-TR-2010-1024

Improvements to a Major Digital Archive of Seismic Waveforms from Nuclear Explosions

Won-Young Kim
Paul G. Richards
Diane Baker
Howard Patton
George Randall

The Trustees of Columbia University in the City of New York
Research Administration
1700 Broadway
New York, NY 10019-5905

Final Report

23 March 2010

APPROVED FOR PUBLIC RELEASE; DISTRIBUTION IS UNLIMITED.

AIR FORCE RESEARCH LABORATORY
Space Vehicles Directorate
29 Randolph Rd
AIR FORCE MATERIEL COMMAND
HANSCOM AFB, MA 01731-3010

NOTICES

AFRL-RV-HA-TR-2010-1024 HAS BEEN REVIEWED AND IS APPROVED FOR PUBLICATION IN ACCORDANCE WITH ASSIGNED DISTRIBUTION STATEMENT.

//signature//	//signature//
ROBERT J. RAISTRICK Contract Manager	Domenic Thompson, Maj, USAF, Chief Battlespace Surveillance Innovation Center

REPORT DOCUMENTATION PAGE

Form Approved OMB No. 0704-0188

1. REPORT DATE *(DD-MM-YYYY)*	2. REPORT TYPE	3. DATES COVERED *(From - To)*
03-23-2010	Final Report	02-023-2007 to 02-23-2010

4. TITLE AND SUBTITLE
Improvements to a Major Digital Archive of Seismic Waveforms from Nuclear Explosions

5a. CONTRACT NUMBER
FA8718-07-C-0004

5b. GRANT NUMBER

5c. PROGRAM ELEMENT NUMBER
62601F

6. AUTHOR(S)
Won-Young Kim[1], Paul G. Richards[1], Diane Baker[2], Howard Patton[2] and George Randall[2]

5d. PROJECT NUMBER
1010

5e. TASK NUMBER
SM

5f. WORK UNIT NUMBER
A1

7. PERFORMING ORGANIZATION NAME(S) AND ADDRESS(ES)

The Trustees of Columbia University in the City of New York
1700 Broadway
New York, NY 10019-5905

8. PERFORMING ORGANIZATION REPORT NUMBER

9. SPONSORING / MONITORING AGENCY NAME(S) AND ADDRESS(ES)

Air Force Research Laboratory
29 Randolph Rd.
Hanscom AFB, MA 01731-3010

10. SPONSOR/MONITOR'S ACRONYM(S)
AFRL/RVBYE

11. SPONSOR/MONITOR'S REPORT NUMBER(S)
AFRL-RV-HA-TR-2010-1024

12. DISTRIBUTION / AVAILABILITY STATEMENT

Approved for Public Release; Distribution Unlimited.

13. SUPPLEMENTARY NOTES

[1]Lamont-Doherty Earth Observatory of Columbia University, New York, NY
[2]Los Alamos National Laboratory, Los Alamos, NM

14. ABSTRACT
This project took advantage of Soviet-era digital seismic recordings, all of them made at the Borovoye Geophysical Observatory in Kazakhstan, of ground motion from numerous underground nuclear explosions that occurred in Eurasia over a period of three decades, from 1966 to 1995. We have prepared these recordings in a modern format, to make them usable by the seismic monitoring community for numerous ongoing and future studies of Earth structure, attenuation characteristics, and explosion source physics including source representation by body force equivalents and associated source spectra. To produce the newly-formatted signals required major efforts at Los Alamos National Laboratory to remove glitches in the original records, and at the Lamont-Doherty Geophysical Observatory to obtain instrument responses. Three different recording systems operated at Borovoye: the KOD system from 1973 to 1990; the SS system from 1973 to 1990; and the TSG system from 1974 to 1995. Each system included channels of low-gain and high-gain recording; and each system included vertical, north/south, and east/west channels. In this project, particular attention was paid to data from the KOD and SS systems, which had not previously been deglitched and instrument-corrected. We have prepared waveforms from nuclear explosions at the following five test sites: Balapan (1269 traces), Degelen (1146 traces), and Murzhik (160 traces), all in Kazakhstan on the Semipalatinsk Test site; Novaya Zemlya (461 traces) in Russia; and Lop Nor (120 traces) in China; and also from many Peaceful Nuclear Explosions (552 traces) in Russia. Although the dynamic range of specific channels is limited by the low number of bits in the recording system, the scientific content of the signals across the many different channels approaches that for modern recording systems. The improved Borovoye archive now provides many practical examples of the types of explosion signals that modern monitoring networks (which do not have large archives of explosion signals) must be designed to detect and identify.

15. SUBJECT TERMS
Digital seismograms, Instrument calibration, Soviet-era nuclear testing, Nuclear explosion monitoring

16. SECURITY CLASSIFICATION OF:			17. LIMITATION OF ABSTRACT	18. NUMBER OF PAGES	19a. NAME OF RESPONSIBLE PERSON
					Robert Raistrick
a. REPORT	b. ABSTRACT	c. THIS PAGE			19b. TELEPHONE NUMBER *(include area code)*
UNC	UNC	UNC	SAR	125	781-377-3726

Standard Form 298 (Rev. 8-98)
Prescribed by ANSI Std. Z39.18

Table of Contents

1. Summary 1

2. Introduction 1

    2.1. The Borovoye Station 20

3. Methods of Analysis 22

    3.1. Technical Approach to Deglitching 22

    3.2. The KOD Digital Seismograph System 24

    3.3. The STsR-SS Digital Seismograph System 38

4. Results 69

    4.1. Example seismograms

5. Conclusions 107

References 109

List of Symbols, Abbreviations, and Acronyms 111

Figures

1. Locations (red stars) of underground nuclear explosions (UNEs) recorded digitally by seismic monitoring systems at the Borovoye Geophysical Observatory (BRV) in Northern Kazakhstan. More detailed maps are given as Figures 2 – 5. 3

2. UNTs at Semipalatinsk Test Site (*circles*) recorded at Borovoye (BRV) during 1966-1989.The Balapan, Degelen, and Murzhik regions are indicated. 5

3. Locations of UNTs (*circles*) at Northern Novaya Zemlya Test Sites recorded at Borovoye during 1967-1990 are shown on topographic relief map. Southern and Northern Test Sites on Novaya Zemlya and great circle path between BRV and NZ test site is indicated (*inset*). 6

4. Soviet PNEs (*stars*) recorded at Borovoye during 1967-1988. Event id in Table 6 is indicated for each PNE. IMS primary (*double circle*), auxiliary (*single circle*), IRIS/GSN (*inverted triangle*) and Kazakstan Broadband Seismographic Network stations are indicated (*solid triangle*). Large circles around BRV indicate 1000 and 2000 km distance ranges from the staton. 78 frequency-amplitude calibration curves of the KODB system during 1967–1973 7

5. Locations of UNEs at the Lop Nor Chinese Test Site . Notice that UNTs are clustered into three groups: A, B and C. UNEs not contained in the BRV archive are plotted with crosses. 8

6. 78 frequency-amplitude calibration curves of the KODB system during 1967–1973. 26

7. 34 selected frequency-amplitude calibration curves of the KODB system during 1967–1973. 27

8. Frequency-amplitude calibration curves of short-period, vertical-component (channel #1, SHZ) of KODB system during 1967–1973. The averaged values at each frequency are plotted with their standard deviations. 28

9. Frequency-amplitude calibration curves of short-period, NS-component (channel #3, SHN) of KODB system during 1967–1973. The averaged values at each frequency are plotted with their standard deviations. 29

10. Frequency-amplitude calibration curves of short-period, EW-component (channel #4, SHE) of KODB system during 1967–1973. The averaged values at each frequency are plotted with their standard deviations. 30

11. Frequency-amplitude calibration curves of short-period, low-gain vertical-component (channel #2, SLZb) of KODB system during 1967–1973. The averaged values at each frequency are plotted with their standard deviations 31

12. Averaged frequency-amplitude calibration curves of the high-gain vertical-, NS- and EW-component as well as the low-gain vertical-component channels of the KODB system are plotted. 32

13. 64 frequency-amplitude calibration curves of the KODM system during 1967–1973. 33

14. 32 selected frequency-amplitude calibration curves of the KODM system during 1967–1973. 34

15. Averaged frequency-amplitude calibration curves of low-gain vertical-, NS- and EWcomponent as well as the high-gain vertical-component channels of the KODM system are plotted. 35

16. Frequency-amplitude calibration curve of the low-gain, short-period vertical component channel (SLZb) during 1967–1973 is compared with the theoretical amplitude response curve obtained by using the instrument response listed in Table 9. 37

17. Frequency-amplitude calibration curves of 10-channel STsR-SS system are plotted. 40

18. Frequency-amplitude calibration curves of 3-component short-period SKM-3 channels during 1973–1982. s07Z = vertical-component, s08N = NS-component, and s09E = EW-component. The curves for the NS-component are plotted with their amplitudes multiplied by 10, and EW-component are plotted by multiplying the amplitude by 100 to show the response curves separately. *Red lines* are for the curve on 1973-10-24 and *blue lines* are for the curve on 1981-08-04. 41

19. Comparisons of observed (*solid circles*) and theoretical (*solid lines*) frequency amplitude curves of 3-component short-period SKM-3 channels during 1973–1982. s07Z = vertical-component, s08N = NS-component, and s09E = EW-component. The curves for the NS-component are plotted with their amplitudes multiplied by 10, and EW-component are plotted by multiplying the amplitude by 100 to show the response curves separately. 43

20. Two frequency-amplitude calibration curves of the low-gain, vertical-component short-period SKM-3 channel during 1973–1982. s01Z = low-gain vertical-component. The curves are similar to those of channel 7 (s07Z) except the gain. 45

21. Comparisons of observed (*solid circles* with *dashed line*) and theoretical (*solid line*) frequency-amplitude curves of low-gain vertical-component short-period SKM-3 channel (s01Z) during 1973–1982. 46

22. Frequency-amplitude calibration curves of 3-component short-period SKM-3 channels during 1982–1991. s07Z = vertical-component, s08N = NS-component, and s09E = EW-component. The curves for the NS-component are plotted with their amplitudes multiplied by 10, and EW-component are plotted by multiplying the amplitude by 100 to show the response curves separately. 48

23. Comparison of frequency-amplitude calibration curves of 3-component short-period SKM-3 channels during 1973–1982 (*solid lines*) and 1982–1991 (*red lines*). Amplitude responses are nearly identical at frequencies up to 3 Hz for both periods. s07Z = vertical-component, s08N= NS-component, and s09E = EW-component. The curves for the NS-component are plotted with their amplitudes multiplied by 10, and EW-component are plotted by multiplying the amplitude by 100 to show the response curves separately. 49

24. Comparisons of observed (*solid circles*) and theoretical (*solid lines*) frequency amplitude curves of 3-component short-period SKM-3 channels during 1982–1989. s07Z = vertical-component, s08N = NS-component, and s09E = EW-component. The curves for the NS-component are plotted with their amplitudes multiplied by 10, and EW-component are plotted by multiplying the amplitude by 100 to show the response curves separately 50

25. A frequency-amplitude calibration curve of vertical-component, low-gain short-period SKM-3 channels during 1982–1991. s06Z = low-gain vertical-component. The curve is similar to those of channel 7 (s07Z) shown in Figure 22 except the gain. 53

26. Comparisons of observed (*solid circles* with *dashed line*) and theoretical (*solid line*) frequency-amplitude curves of low-gain vertical-component short-period SKM-3 channels (s06Z) during 1982–1991. 54

27. Frequency-amplitude calibration curves of 3-component extended-period SKD channels during 1973–1982. l02Z = vertical-component, l03N = NS-component, and l04E = EW-component. The curves for the NS-component are plotted with their amplitudes multiplied by 10, and EW-component are plotted by multiplying the amplitudes by 100 to show the response curves separately. 56

28. Comparisons of observed (*solid circles*) and theoretical (*solid lines*) frequency-amplitude curves of 3-component extended-period SKD channels during 1973–1982. l02Z = vertical-component, l03N = NS-component, and l04E = EW-component. The theoretical amplitude response is calculated using the instrument response for the later time period 1982–1991. The curves for the NS-component are plotted with their amplitudes multiplied by 10, and EW-component are plotted by multiplying the amplitude by 100 to show the response curves separately. 57

29. Frequency-amplitude calibration curves of 3-component extended-period SKD channels during 1982–1991. l02Z = vertical-component, l03N = NS-component, and l04E = EW-component. The curve for the NS-component is plotted with their amplitudes

multiplied by 10, and EW-component is plotted by multiplying the amplitude by 100 to show the response curves separately. 60

30. Comparisons of observed (*solid circles*) and theoretical (*solid lines*) frequency-amplitude curves of 3-component extended-period SKD channels during 1982–1991. l02Z = vertical-component, l03N = NS-component, and l04E = EW-component. The curves for the NS-component are plotted with their amplitudes multiplied by 10, and EW-component are plotted by multiplying the amplitude by 100 to show the response curves separately. 61

31. Frequency-amplitude calibration curves of 3-component extended-period SKD channels during 1982–1991. l01Z = vertical-component, l05N = NS-component, and l10E = EW-component. The curve for the NS-component is plotted with its amplitudes multiplied by 10, and EW-component is plotted by multiplying the amplitude by 100 to show the response curves separately. 63

32. Comparisons of observed (*solid circles*) and theoretical (*solid lines*) frequency-amplitude curves of low-gain, 3-component extended-period SKD channels during 1982–1991. l01Z = vertical-component, l05N = NS-component, and l10E = EW-component. The curves for the NS-component are plotted with their amplitudes multiplied by 10, and EW-component are plotted by multiplying the amplitude by 100 to show the response curves separately. 64

33. A summary plot of the averaged frequency-amplitude calibration curves of all data streams of the STsR-SS system (*open circles*=SKD and *solid circles*=SKM-3 seismometers). Theoretical amplitude responses are plotted by *solid lines*. SKM-3 data streams: s07Z 1982=3-component (s07Z, s08N and s09E, 1982–1991); s07Z 1973= 3-component (s07Z, s08N and s09E, 1973–1982); s01Z 1973= low-gain vertical-component, 1973–1982; s06Z 1982= low-gain vertical-component, 1982–1991. SKD data stream: l02Z 1973= 3-component (l02Z, l03N and l04E, 1973–1982); l02Z 1982= 3-component (l02Z, l03N and l04E, 1982–1991); l01Z 1982=low-gain 3-component (l01Z, l05N and l10E, 1982–1991). 66

34. First of seven sets of BRV seismograms on the KOD system for a UNE at the Balapan area of the Semipalatinsk Test Site, Kazakhstan; test of 1968 June 19 70

35. Last of seven sets of BRV seismograms on the KOD system for a UNE at the Balapan area of the Semipalatinsk Test Site, Kazakhstan; test of 1973 July 23 71

36. First of 78 sets of BRV seismograms on the SS system for a UNE at the Balapan area of the Semipalatinsk Test Site, Kazakhstan; test of 1975 October 29 72

37. Last of 78 sets of BRV seismograms on the SS system for a UNE at the Balapan area of the Semipalatinsk Test Site, Kazakhstan; test of 1989 October 19 73

38. First of 73 sets of BRV seismograms on the TSG system for a UNE at the Balapan area of the Semipalatinsk Test Site, Kazakhstan; test of 1974 December 27 74

39. BRV seismograms on the TSG system for an overburied UNE at the Balapan area of the Semipalatinsk Test Site, Kazakhstan; test of 1989 July 8 75

40. Last of 73 sets of BRV seismograms on the TSG system for a UNE at the Balapan area of the Semipalatinsk Test Site, Kazakhstan; test of 1989 October 19 76

41. First of 45 sets of BRV seismograms on the KOD system for a UNE at the Degelen area of the Semipalatinsk Test Site, Kazakhstan; test of 1967 February 26 77

42. Last of 45 sets of BRV seismograms on the KOD system for a UNE at the Degelen area of the Semipalatinsk Test Site, Kazakhstan; test of 1973 October 26 78

43. First of 59 sets of BRV seismograms on the SS system for a UNE at the Degelen area of the Semipalatinsk Test Site, Kazakhstan; test of 1975 December 13 79

44. Last of 59 sets of BRV seismograms on the SS system for a UNE at the Degelen area of the Semipalatinsk Test Site, Kazakhstan; test of 1989 October 4 80

45. First of 59 sets of BRV seismograms on the TSG system for a UNE at the Degelen area of the Semipalatinsk Test Site, Kazakhstan; test of 1974 December 16 81

46. Last of 59 sets of BRV seismograms on the TSG system for a UNE at the Degelen area of the Semipalatinsk Test Site, Kazakhstan; test of 1989 October 4 82

47. First of 14 sets of BRV seismograms on the KOD system for a UNE at the Murzhik area of the Semipalatinsk Test Site, Kazakhstan; test of 1966 December 18 (the earliest Eurasian nuclear test digitally recorded at Borovoye) 83

48. Last of 14 sets of BRV seismograms on the KOD system for a UNE at the Murzhik area of the Semipalatinsk Test Site, Kazakhstan; test of 1973 April 19 84

49. First of five sets of BRV seismograms on the SS system for a UNE at the Murzhik area of the Semipalatinsk Test Site, Kazakhstan; test of 1976 August 4 85

50. Last of five sets of BRV seismograms on the SS system for a UNE at the Murzhik area of the Semipalatinsk Test Site, Kazakhstan; test of 1980 April 4 86

51. First of four sets of BRV seismograms on the TSG system for a UNE at the Murzhik area of the Semipalatinsk Test Site, Kazakhstan; test of 1978 March 19 87

52. Last of four sets of BRV seismograms on the TSG system for a UNE at the Murzhik area of the Semipalatinsk Test Site, Kazakhstan; test of 1980 April 4 88

53. First of nine sets of BRV seismograms on the KOD system for a UNE at the Novaya Zemlya Test Site, Russia; test of 1967 October 21 89

54. Last of nine sets of BRV seismograms on the KOD system for a UNE at the Novaya Zemlya Test Site, Russia; test of 1973 October 27 90

55. First of 17 sets of BRV seismograms on the SS system for a UNE at the Novaya Zemlya Test Site, Russia; test of 1973 September 27 91

56. Last of 17 sets of BRV seismograms on the SS system for a UNE at the Novaya Zemlya Test Site, Russia; test of 1990 October 24 92

57. First of 19 sets of BRV seismograms on the TSG system for a UNE at the Novaya Zemlya Test Site, Russia; test of 1975 August 23 93

58. Last of 19 sets of BRV seismograms on the TSG system for a UNE at the Novaya Zemlya Test Site, Russia; test of 1990 October 24 94

59. First of 27 sets of BRV seismograms on the KOD system for a PNE in the Soviet Union; test of 1967 October 6, at (57.7°N, 65.2°E), depth 172 m, 0.3 kt, mb 4.7 95

60. Last of 27 sets of BRV seismograms on the KOD system for a PNE in the Soviet Union; test of 1973 October 26, at (53.65°N, 55.4°E), depth 2036, 10 kt, mb 4.8 96

61. First of 38 sets of BRV seismograms on the SS system for a PNE in the Soviet Union; test of 1973 August 15, at (42.775°N, 67.408°E), depth 600 m, 6.3 kt, mb 5.3 97

62. Last of 38 sets of BRV seismograms on the SS system for a PNE in the Soviet Union; tests of 1984 July 21, being three separate shots five minutes apart, centered at (51.37°N, 53.34°E), depth 900, 15 kt, mb 5.4 98

63. First of 27 sets of BRV seismograms on the TSG system for a PNE in the Soviet Union; test of 1976 March 29, at (47.897°N, 48.133°E), depth 986 m, 8 to 10 kt, mb 4.3. This was a partially decoupled shot in Azgir, Western Kazakhstan, but although it was detected teleseismically there is minimal signal at BRV. Signals are also available on the SS system. The 64 kiloton mb 6.0 shot on 1971 December 22 which made the cavity was well recorded on the KOD system. 99

64. Last of 27 sets of BRV seismograms on the TSG system for a Soviet PNE; test of 1984 October 27, at (46.9°N, 48.10°E), depth 1000, 3.2 kt, mb 5.0 in salt 100

65. The only set of BRV seismograms on the KOD system for a UNE at the Lop Nor Test Site, China; China's first UNE, of 1969 September 22 101

66. First of seven sets of BRV seismograms on the SS system for a UNE at the Lop Nor Test Site, China; test of 1976 October 17 102

67. Last of seven sets of BRV seismograms on the SS system for a UNE at the Lop Nor Test Site, China; test of 1983 October 06 103

68. First of eight sets of BRV seismograms on the TSG system for a UNE at the Lop Nor Test Site, China; test of 1978 October 14 104

69. Last of eight sets of BRV seismograms on the TSG system for a UNE at the Lop Nor Test Site, China; test of 1995 May 15 105

Tables

1. Numbers of deglitched waveforms by region, as recorded by each of the three systems (KOD, SS, TSG) at the Borovoye Geophysical Observatory from 1966 to 1989. Note that some underground nuclear explosions are listed here as events that may have been recorded by more than one instrument system. Tables 2 through 7 list each event for which there is Borovoye data, and the systems that recorded them. 4

2. Deglitched Borovoye data for underground nuclear tests in the Balapan subarea of STS, 1968–1988 9–11

3. Deglitched Borovoye data for underground nuclear test at Degelen subarea of STS, 1967–1989 12–14

4. Deglitched Borovoye data for underground nuclear test at Murzhik subarea of STS, 1967–1980 15

5. Deglitched Borovoye data for underground nuclear test at Novaya Zemlya Test Sites, 1967–1990 16

6. Deglitched Borovoye data for Peaceful Nuclear Explosions in the Former Soviet Union, 1967–1988 17–18

7. Deglitched Borovoye data for Chinese Underground Nuclear Tests at Lop Nor, 1969–1995 19

8. Instrument Characteristics and Gains of the KOD System at Borovoye 25

9. Instrument Constants of SKM-3 high-gain, KODB and low-gain, KODM Seismographs, 1967–1973 36

10. Gains at 2 Hz for Channels 7, 8 and 9 during 1973–1982 39

11. Instrument constants of the high-gain SKM channels 7, 8 and 9, 1973–1982 42

12. Poles and Zeros for the instrument response of the high-gain SKM channels 7, 8 and 9, 1973–1982 42

13. The gain at 2 Hz for channel 1 during 1973–1982 44

14. The gains at 2 Hz for channels 7, 8 and 9 during 1982–1991 47

15. Instrument constants of the high-gain SKM channels 7, 8 and 9, 1982–1991 51

16. Gains, Poles and Zeros of the instrument response of the Extended-period SKD Channels 2, 3 and 4, 1973–1982 58

17. Instrument Constants of the Extended-period SKD Channels 2, 3 and 4, 1982–1991 59

18. The gains of the Extended-period SKD Channels 1, 5 and 10, 1982–1991 62

19. Instrument Characteristics at Borovoye (BRV) 67–68

Acknowledgments

The writing of this report and production of an openly available modern format archive of digital seismograms of hundreds of underground nuclear explosions in Eurasia represent the culmination of an effort that has engaged many people beginning in 1965, forty-five years ago, when recording efforts began at the Borovoye location. Involvement with western scientists began in 1991, when Paul Richards and Göran Ekström were hosted at meetings at the Borovoye Geophysical Observatory, then operated by the Institute of Dynamics of the Geosphere (IDG) of the USSR Academy of Sciences. Shortly thereafter, when Kazakhstan became an independent country, personnel of that country's National Nuclear Centre became heavily engaged in the operation of the Borovoye Observatory, and in efforts to make its digital archive of use to the wider world.

We thank the original station operators who acquired the data we have processed in this project, in particular Vadim An of IDG who helped us by supplying many details of the station operation. We thank Vitaly Adushkin, who, as director of IDG for many years, introduced western scientists to the Borovoye operation when it was still being run from Moscow. We thank his colleagues Vadim An, Vladimir Ovtchinnikov, and Peter Kasik, who worked with us on efforts funded by the International Science and Technology Centre to save the seismogram archive by transferring the original records from thousands of deteriorating magnetic tapes to modern recording media. Participants in this operation included Nadezhda Belyashova and Natalya Mikhailova of the National Nuclear Centre of the Republic of Kazakhstan, whom we thank for continuing to supply us with information on the Borovoye Geophysical Observatory operation in several visits by Won-Young Kim and Paul Richards. And we thank Scott Phillips of the Los Alamos National Laboratory for his work on the software used for much of the deglitching work described in this report.

1. SUMMARY

In 2007 Columbia University entered into a contract with the Air Force Research Laboratory to prepare in modern format a major archive of digitally recorded seismic waveforms, generated by hundreds of underground nuclear explosions in Eurasia conducted by the Soviet Union from 1966 to 1990, and by China from 1969 to 1995.

This contract built upon more than 25 years of operation of the Borovoye Geophysical Observatory by the Academy of Sciences of the USSR beginning in 1965. The Observatory has been operated by the National Nuclear Center (NNC) of the Republic of Kazakhstan since 1992. The contract built also upon several years of cooperative efforts between the Russian Academy of Sciences' Institute of Dynamics of the Geosphere (the organization which operated the Observatory in the Soviet era), the NNC, and the Lamont-Doherty Earth Observatory of Columbia University (LDEO), which was invited to begin researches with Borovoye personnel in 1991. Specifically, these three institutions worked together from 1997 to 2000 in a preliminary effort to salvage the digital recordings of the Borovoye archive from their original recording medium consisting of thousands of deteriorating magnetic tapes.

The archive was made available to researchers in 2001, but it had two substantial defects, both of which have been corrected in the present project. First, the digital data suffered from numerous glitches. Second, information on the instrument responses of the numerous different recording channels was incomplete, thus preventing about two-thirds of the archive from being used.

Issuance of the archive in 2001 promoted efforts at the Los Alamos National Laboratory (LANL) to remove the glitches, and scientific results based upon the deglitched records, for those recordings for which the instrument responses were known, found many uses. Consequently the present project was initiated, with the intent to complete work on deglitching and instrument responses. This work has now been concluded, and the deglitched waveforms are available for the research community at http://www.ldeo.columbia.edu/res/pi/Monitoring/Arch/BRV_arch_deglitched.html.

2. INTRODUCTION

Seismology was developed in Kazakhstan by the USSR from the mid-1960s to the end of the Soviet era in 1991 with central planning from Moscow, in the context of military programs to monitor nuclear weapons testing at sites around the world. Under these programs, high quality work was performed in seismometer design and construction, in field surveys to discover suitable sites for instrument deployment, and in the development of methods of data analysis and interpretation.

Kazakhstan turned out to provide superb sites for seismometer operation, because: (a) the whole country is deep within the interior of the Eurasian continent, a long way from any ocean, and sites could readily be found that were seismologically very quiet; and (b) the geological structures, particularly of Northern Kazakhstan, allow seismic waves to propagate very efficiently, with minimal attenuation and minimal scattering. As a result, seismographic stations in Kazakhstan began as early as the 1960s to acquire high-quality data from nuclear explosions, which occurred somewhere around the world

at a rate of approximately once a week for the 30-year period from 1961-1990. The seismic data (then secret in the Soviet Union) was used by the USSR to monitor nuclear explosions carried out by the USA, France, the UK, and China, using signals that propagated in the Earth for thousands of kilometers from nuclear test sites used by these countries, to the seismometer sites in Kazakhstan. Such signals are called teleseismic, and it is a testament to the detection capability of stations in Kazakhstan that they could record teleseismic signals from distant explosions with yield down to about one kiloton (about magnitude 4). The monitoring facilities also recorded nuclear explosions carried out by the USSR itself, many of them within Kazakhstan (for example at the Semipalatinsk Test Site, the location of about 350 underground nuclear explosions), using seismic signals that propagated in many instances only a few hundred kilometers to the in-country recording sites.

At several sites in Kazakhstan, funded and/or operated in the 1970s and 1980s by military organizations, the seismic data were obtained with digital recording systems. Seismic data can be recorded in analog form, for example by pen on paper, or photographically. But digital recording is much preferred over analog since digital data can more readily be analyzed for their frequency content, and for signals of interest in the presence of other signals and noise. Digital recording did not become widespread in western countries until the 1970s, and there are no western archives of digital data that document earthquakes and explosions prior to 1975 except for a limited number of seismic events in regions of special study.

Although nuclear weapons testing has occurred only at greatly reduced levels in recent years (India and Pakistan in May 1998; North Korea in October 2006 and May 2009), Kazakhstan still has an important role to play in seismic monitoring for nuclear explosions. Thus, Russia has observed a moratorium since carrying out the Soviet Union's last nuclear explosion in 1990. Moratoria on testing have also been instituted by the USA, the UK, France, and China, in the context of these nuclear weapons states having all signed (and in some cases ratified) the Comprehensive Nuclear-Test-Ban Treaty (CTBT) of 1996. The context for explosion monitoring is now arms control, and monitoring to demonstrate the absence of nuclear explosions.

Kazakhstan is superbly located for purposes of acquiring teleseismic and regional seismic signals to monitor the territories of China, Russia, and countries of South Asia (India and Pakistan) plus Central Asia and the Middle East.

Under the Soviet regime, one of the primary nuclear testing sites was in eastern Kazakhstan near the town of Semipalatinsk. At that time seismology throughout much of Central Asia was heavily controlled by Russian groups from the Ministry of Defense and Soviet Academy of Sciences. While there were well-established earthquake studies programs in the most seismically active areas along the southern border in Tadjikistan, Kyrgyzstan and the Tien Shan mountains of southern Kazakhstan, most of the seismological observations in central and northern Kazakhstan were focused on classified monitoring of the Soviet and foreign nuclear test sites.

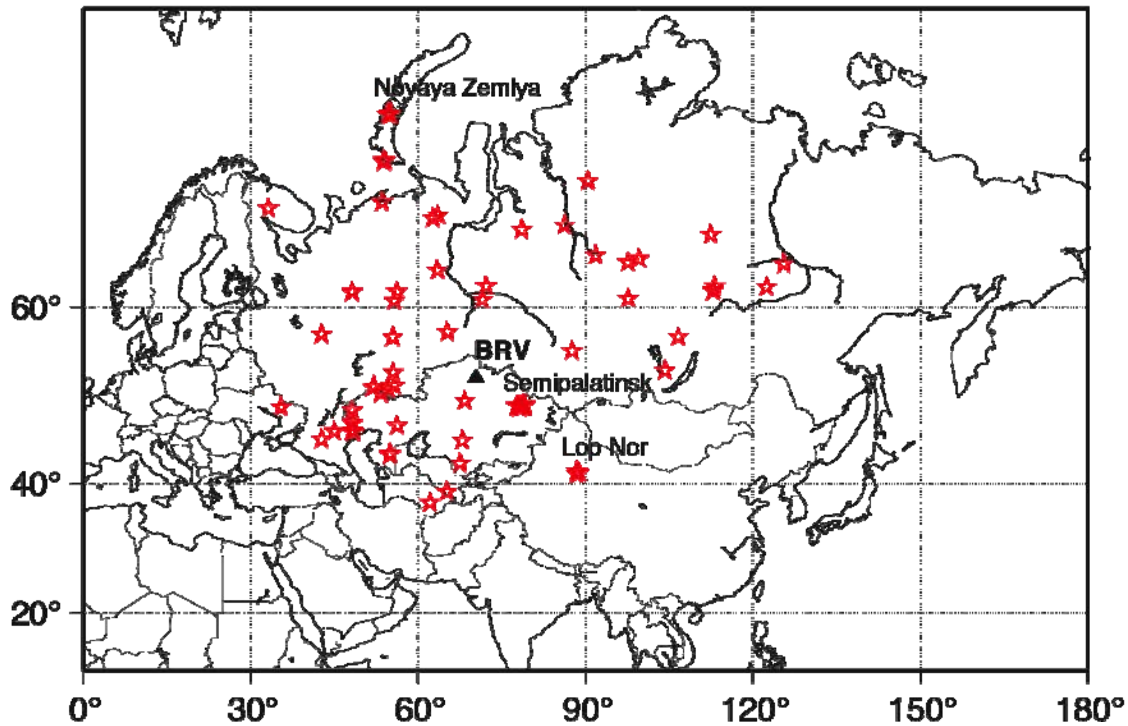

Figure 1. Locations (red stars) of underground nuclear explosions (UNEs) recorded digitally by seismic monitoring systems at the Borovoye Geophysical Observatory (BRV) in Northern Kazakhstan. More detailed maps are given as Figures 2 – 5.

In the mid 1980s, the Soviet government agreed to allow US university groups to make seismic observations at temporary locations surrounding the Semipalatinsk nuclear test site in Kazakhstan. This work was part of a program sponsored by the US-based Natural Resources Defense Council and the Soviet Academy of Sciences. An outgrowth of that program was an agreement between the Soviet Academy of Sciences and IRIS, a consortium of US universities, to establish permanent seismic observatories throughout the USSR as part of the Global Seismographic Network being developed by IRIS and the US Geological Survey. Seismic stations were established in Tadjikistan and Kyrgyzstan, but Kazakhstan remained closed for permanent observatories.

With the gradual opening of the USSR in the early 1990s, details began to emerge about some extensive Soviet seismological facilities in Kazakhstan. In June 1991, Paul Richards of LDEO/Columbia University and Göran Ekström, then of Harvard University, visited the Borovoye Geophysical Observatory, previously a secret operation, and were introduced to the monitoring facilities and data archive there. In 1993, the National Nuclear Center of Kazakhstan was created and given authority for many facilities, including that at Borovoye (BRV), built in the Soviet era.

Figure 1 shows the location of Borovoye, and of the hundreds of nuclear explosions in Eurasia recorded by the Observatory. Table 1 summarizes the numbers of explosions and the numbers of recordings (traces) associated with six different groups, namely the Balapab, Degelen, and Murzhik sub-regions of the Semipalatinsk Test Site in

Kazakhstan; the Novaya Zemlya Test Site in Russia; the wide-ranging locations of the Peaceful Nuclear Explosions (PNEs) conducted by the Soviet Union; and the Lop Nor Test Site in China.

Table 1. Numbers of deglitched waveforms by region, as recorded by each of the three systems (KOD, SS, TSG) at the Borovoye Geophysical Observatory from 1966 to 1989. Note that some underground nuclear explosions are listed here as events that may have been recorded by more than one instrument system. Tables 2 through 7 list each event for which there is Borovoye data, and the systems that recorded them.

Region	**System**	**Events**	**Traces**	**Dates**
Balapan (Kazakhstan,	KOD	7	51	680619-730723
Semipalatinsk	SS	78	664	751029-891019
Test Site)	TSG	73	575	741227-891019
subtotal		158	1290	
Degelen (Kazakhstan,	KOD	45	290	670226-731026
Semipalatinsk	SS	59	469	751213-891004
Test Site)	TSG	59	382	741216-891004
subtotal		163	1141	
Murzhik (Kazakhstan,	KOD	14	102	661218-730419
Semipalatinsk	SS	4	34	760804-800404
Test Site)	TSG	4	24	780319-800404
subtotal		22	160	
Novaya Zemlya (Russia)	KOD	9	68	671021-731027
	SS	17	114	730927-901024
	TSG	19	279	750823-901024
subtotal		45	461	
PNEs (Former Soviet	KOD	27	152	671006-731026
Union)	SS	38	259	730815-880906
	TSG	28	157	760329-880906
subtotal		93	568	
Lop Nor (China)	KOD	1	4	690922
	SS	7	58	761017-900816
	TSG	8	58	781014-950515
subtotal		16	120	
Total		**497**	**3740**	

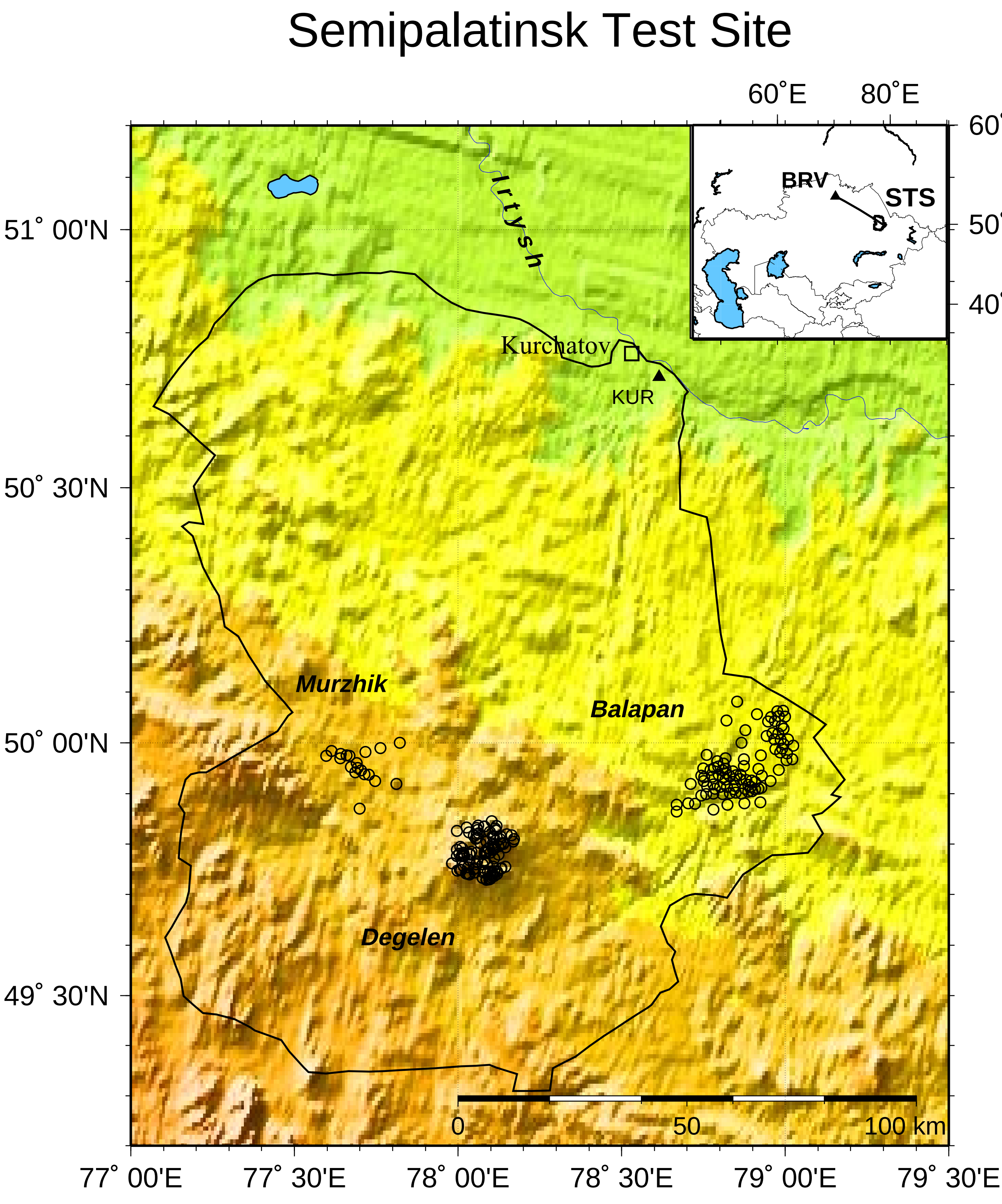

Figure 2: UNTs at Semipalatinsk Test Site (*circles*) recorded at Borovoye (BRV) during 1966-1989.The Balapan, Degelen, and Murzhik regions are indicated.

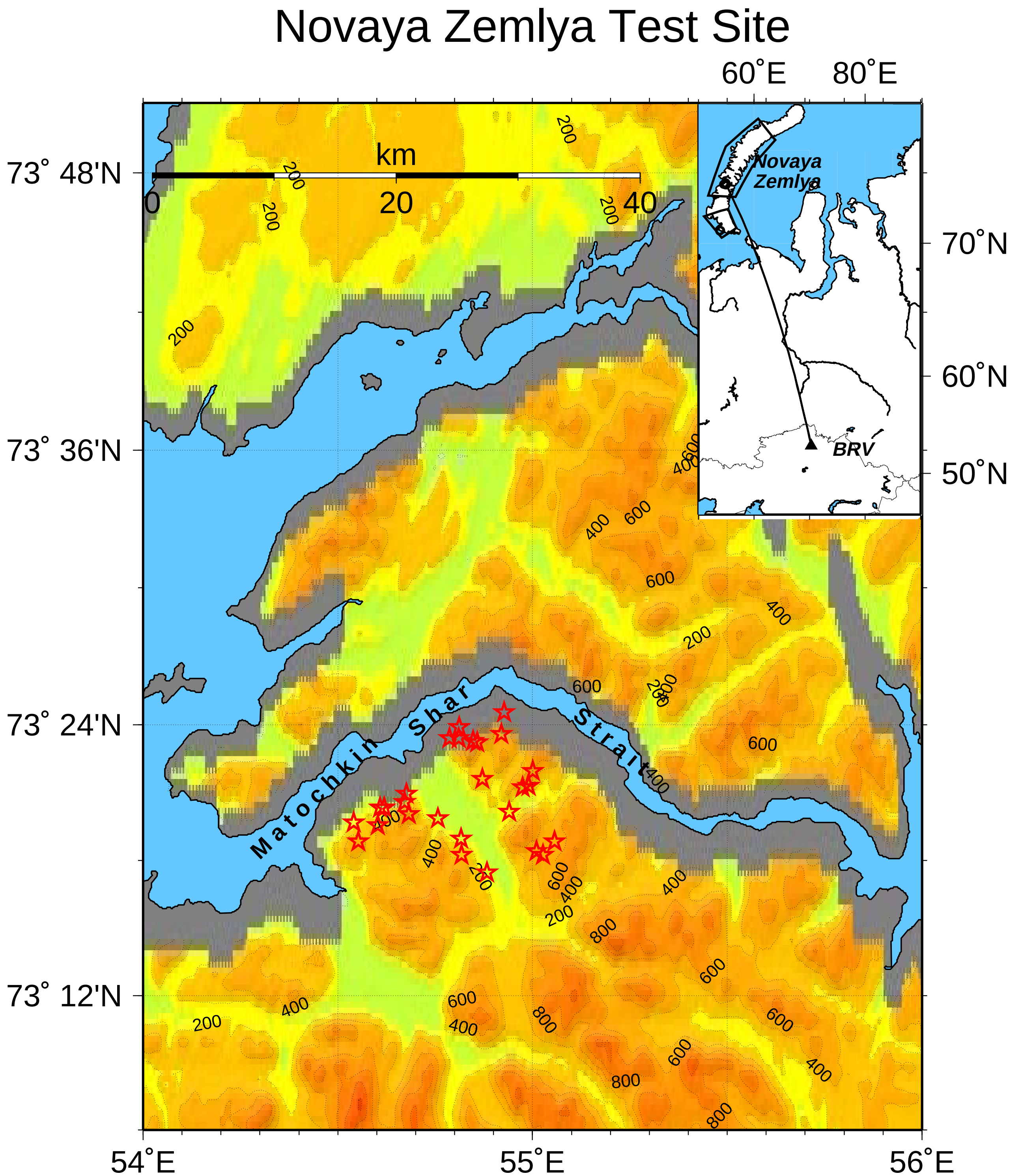

Figure 3: Locations of UNTs (*circles*) at Northern Novaya Zemlya Test Sites recorded at Borovoye during 1967-1990 are shown on topographic relief map. Southern and Northern Test Sites on Novaya Zemlya and great circle path between BRV and NZ test site is indicated (*inset*).

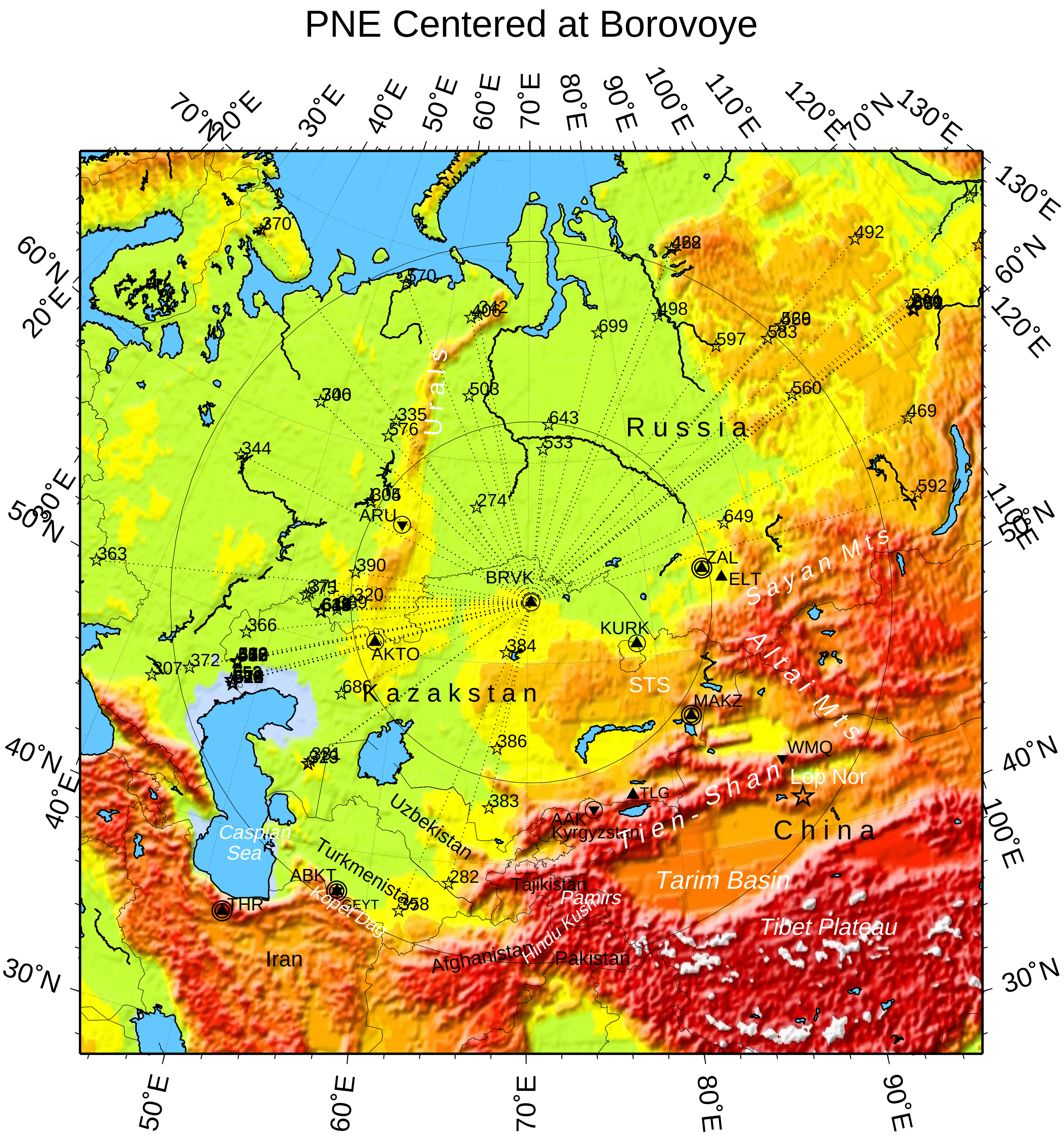

Figure 4: Soviet PNEs (*stars*) recorded at Borovoye during 1967-1988. Event id in Table 6 is indicated for each PNE. IMS primary (*double circle*), auxiliary (*single circle*), IRIS/GSN (*inverted triangle*) and Kazakstan Broadband Seismographic Network stations are indicated (*solid triangle*). Large circles around BRV indicate 1000 and 2000 km distance ranges from the staton.

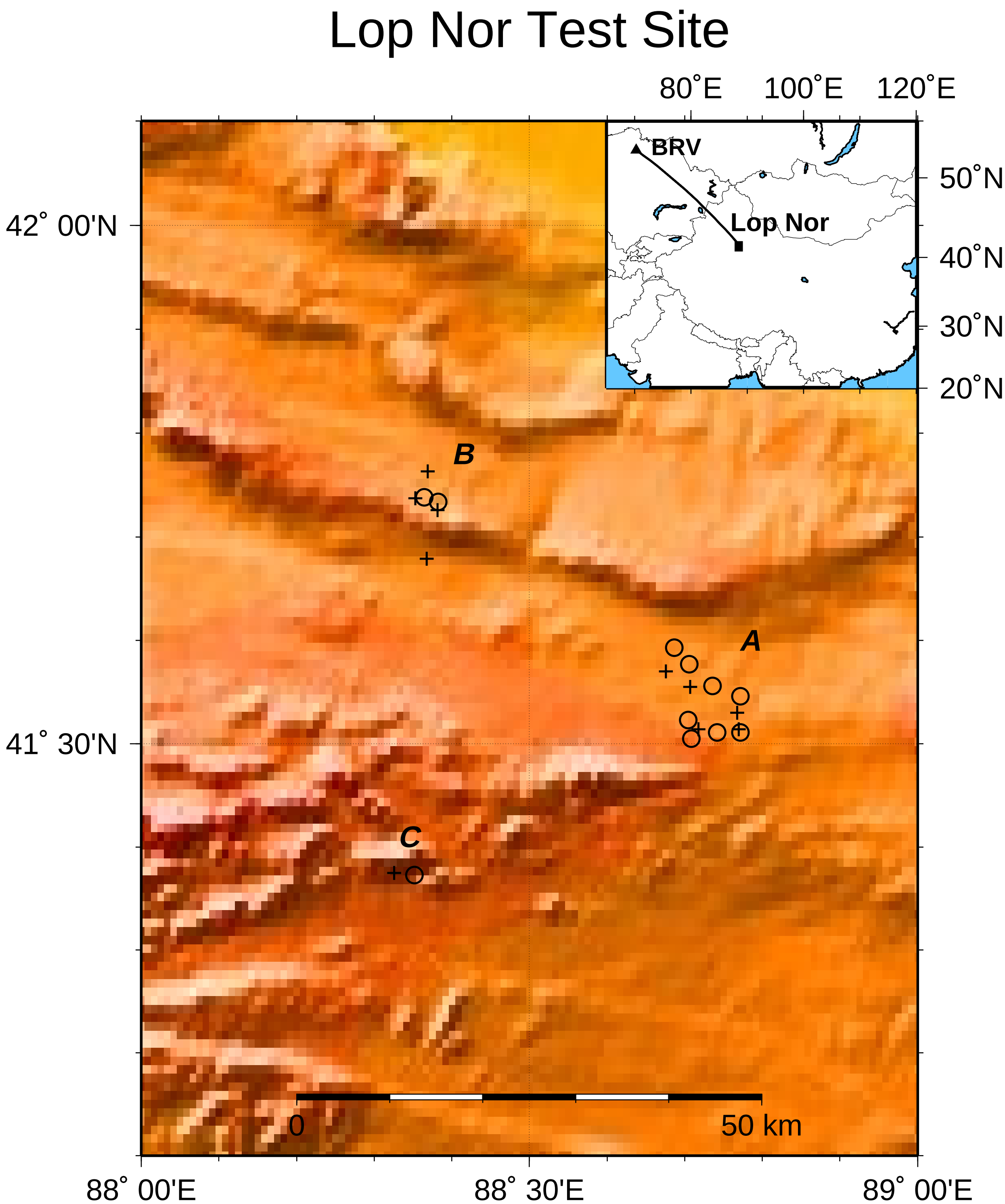

Figure 5: Locations of UNEs at the Lop Nor Chinese Test Site . Notice that UNTs are clustered into three groups: A, B and C. UNEs not contained in the BRV archive are plotted with crosses.

Table 2: Deglitched Borovoye data for underground nuclear test at Balapan subarea of STS, 1968–1988[1]

Test No.	Date Year-Mo-Da	Time (hr:mn:sec)	Latitude (°N)	Longitude (°E)	m_b (P)	Instrument type[2]	Comments
285	1968-06-19	05:05:59.8	49.98025	78.98550	5.28	KODB/M	Bocharov
312	1969-11-30	03:32:59.7	49.92428	78.95575	6.02	KODB/M	Bocharov
341	1971-06-30	03:56:59.8	49.94600	78.98047	4.94	KODB/M	Bocharov
355	1972-02-10	05:03:00.0	50.02428	78.87808	5.27	KODB/M	Bocharov
373	1972-11-02	01:27:00.2	49.92697	78.81725	6.16	KODB	Bocharov
377	1972-12-10	04:27:10.0	50.02700	78.99556	5.96	KODB/M	Bocharov/Double
382	1973-07-23	01:23:00.11	49.96889	78.81750	6.17	KODB/M	AWE/NNC
416	1974-12-27	05:46:59.35	49.96583	79.00333	5.50	TSG	AWE/NNC
433	1975-10-29	04:46:59.82	49.95389	78.87389	5.61	SS/TSG	AWE/NNC
435	1975-12-25	05:16:59.65	50.04389	78.82000	5.69	TSG	AWE/NNC
440	1976-04-21	05:02:59.70	49.90056	78.83083	5.12	SS/TSG	AWE/NNC
443	1976-06-09	03:02:59.75	49.99361	79.02444	5.07	TSG	AWE/NNC
444	1976-07-04	02:56:59.94	49.90417	78.89944	5.85	SS/TSG	AWE/NNC
448	1976-08-28	02:56:59.99	49.97500	78.92639	5.74	SS/TSG	AWE/NNC
453	1976-11-23	05:02:59.75	50.01306	78.94333	5.79	SS	AWE/NNC
454	1976-12-07	04:56:59.85	49.94389	78.83917	5.80	SS/TSG	AWE/NNC
460	1977-05-29	02:57:00.01	49.94639	78.77167	5.75	SS/TSG	AWE/NNC
461	1977-06-29	03:07:00.35	49.99944	78.86667	5.20	SS/TSG	AWE/NNC
468	1977-09-05	03:02:59.86	50.05556	78.91417	5.73	SS/TSG	AWE/NNC
474	1977-10-29	03:07:04.92	50.05222	78.98028	5.56	SS/TSG	AWE/NNC/Double
478	1977-11-30	04:06:59.85	49.96722	78.87444	5.89	SS/TSG	AWE/NNC
487	1978-06-11	02:57:00.08	49.91333	78.80194	5.83	SS/TSG	AWE/NNC
488	1978-07-05	02:46:59.97	49.90000	78.86667	5.77	SS/TSG	AWE/NNC
496	1978-09-15	02:36:59.90	49.92833	78.86167	5.89	SS/TSG	AWE/NNC
505	1978-11-04	05:05:59.81	50.04167	78.94722	5.56	SS/TSG	AWE/NNC
506	1978-11-29	04:33:04.99	49.95333	78.79528	5.96	SS/TSG	AWE/NNC/Double
514	1979-02-01	04:13:00.17	50.08083	78.85333	5.29	SS/TSG	AWE/NNC
521	1979-06-23	02:57:00.02	49.91472	78.84583	6.16	TSG	AWE/NNC
522	1979-07-07	03:46:59.81	50.03306	78.98917	5.84	SS	AWE/NNC
526	1979-08-04	03:56:59.97	49.90306	78.88778	6.13	SS/TSG	AWE/NNC
528	1979-08-18	02:51:59.61	49.94806	78.91889	6.13	SS/TSG	AWE/NNC
538	1979-10-28	03:16:59.45	49.99667	78.99500	5.98	SS/TSG	AWE/NNC
540	1979-12-02	04:36:59.95	49.90944	78.78444	5.99	SS/TSG	AWE/NNC
542	1979-12-23	04:56:59.93	49.93222	78.75278	6.13	SS/TSG	AWE/NNC
546	1980-04-25	03:57:00.03	49.97639	78.75944	5.45	SS	AWE/NNC
548	1980-06-12	03:27:00.11	49.98872	78.99108	5.52	SS/TSG	AWE/NNC
552	1980-06-29	02:33:00.19	49.94861	78.81806	5.69	SS/TSG	AWE/NNC
554	1980-09-14	02:42:41.63	49.93667	78.79750	6.21	SS	AWE/NNC
558	1980-10-12	03:34:16.58	49.96750	79.02250	5.88	SS/TSG	AWE/NNC
564	1980-12-14	03:47:08.91	49.90889	78.91861	5.93	SS/TSG	AWE/NNC
566	1980-12-27	04:09:10.56	50.06194	78.97528	5.87	SS/TSG	AWE/NNC
568	1981-03-29	04:03:52.51	50.01806	78.97881	5.49	SS/TSG	AWE/NNC
569	1981-04-22	01:17:13.82	49.89889	78.80861	5.94	SS/TSG	AWE/NNC
571	1981-05-27	03:58:14.82	49.98694	78.97056	5.30	SS/TSG	AWE/NNC

continue on next page

Test No.	Date Year-Mo-Da	Time (hr:mn:sec)	Latitude (°N)	Longitude (°E)	m_{b} (P)	Instrument type[(2)]	Comments
577	1981-09-13	02:17:20.76	49.91333	78.89444	6.06	SS/TSG	AWE/NNC
582	1981-10-18	03:57:05.14	49.92806	78.84472	6.00	SS/TSG	AWE/NNC
585	1981-11-29	03:35:11.11	49.90194	78.84889	5.62	SS/TSG	AWE/NNC
587	1981-12-27	03:43:16.62	49.93306	78.77833	6.16	SS/TSG	AWE/NNC
589	1982-04-25	03:23:07.88	49.91694	78.88778	6.03	SS/TSG	AWE/NNC
591	1982-07-04	01:17:16.65	49.95861	78.81167	6.08	SS/TSG	AWE/NNC
594	1982-08-31	01:31:03.17	49.91417	78.76139	5.20	SS/TSG	AWE/NNC
604	1982-12-05	03:37:15.04	49.93083	78.80972	6.08	SS/TSG	AWE/NNC
606	1982-12-26	03:35:16.68	50.06306	78.99389	5.58	SS/TSG	AWE/NNC
611	1983-06-12	02:36:46.01	49.92500	78.89806	6.02	SS/TSG	AWE/NNC
625	1983-10-06	01:47:09.08	49.92458	78.75069	5.95	SS	AWE/NNC
626	1983-10-26	01:55:07.33	49.91250	78.82167	6.04	SS/TSG	AWE/NNC
628	1983-11-20	03:27:06.86	50.05083	78.99917	5.33	SS/TSG	AWE/NNC
632	1984-02-19	03:57:05.85	49.89611	78.74306	5.77	SS	AWE/NNC
633	1984-03-07	02:39:08.80	50.05000	78.95611	5.56	SS	AWE/NNC
634	1984-03-29	05:19:10.66	49.91111	78.92694	5.86	SS/TSG	AWE/NNC
636	1984-04-25	01:09:05.99	49.93583	78.85056	5.90	SS/TSG	AWE/NNC
637	1984-05-26	03:13:14.85	49.97889	79.00556	6.01	SS/TSG	AWE/NNC
638	1984-07-14	01:09:12.99	49.90944	78.87722	6.10	SS/TSG	AWE/NNC
654	1984-10-27	01:50:12.93	49.93472	78.92806	6.19	SS/TSG	AWE/NNC
656	1984-12-02	03:19:08.85	50.00611	79.00889	5.77	SS/TSG	AWE/NNC
657	1984-12-16	03:55:05.07	49.94583	78.80861	6.12	SS/TSG	AWE/NNC
658	1984-12-28	03:50:13.09	49.88028	78.70389	6.00	SS/TSG	AWE/NNC
659	1985-02-10	03:27:09.98	49.89917	78.78056	5.83	SS	AWE/NNC
660	1985-04-25	00:57:08.97	49.92667	78.88083	5.84	SS	AWE/NNC
661	1985-06-15	00:57:03.25	49.90861	78.84278	6.05	SS/TSG	IDG/NNC
663	1985-06-30	02:39:05.26	49.86444	78.66861	5.92	SS/TSG	IDG/NNC
667	1985-07-20	00:53:16.91	49.94972	78.78389	5.89	SS/TSG	AWE/NNC
670	1987-03-12	01:57:19.57	49.93528	78.82889	5.31	SS/TSG	AWE/NNC
671	1987-04-03	01:17:10.28	49.91806	78.78028	6.12	SS/TSG	AWE/NNC
673	1987-04-17	01:03:07.09	49.87778	78.66889	5.92	SS/TSG	AWE/NNC
678	1987-06-20	00:53:07.09	49.93528	78.74417	6.03	SS/TSG	AWE/NNC
683	1987-08-02	00:58:09.27	49.88056	78.87472	5.83	SS/TSG	IDG/NNC
688	1987-11-15	03:31:09.08	49.89861	78.75806	5.98	SS	AWE/NNC
689	1987-12-13	03:21:07.31	49.96306	78.79306	6.06	SS	IDG/NNC
691	1987-12-27	03:05:07.00	49.87944	78.72500	6.00	SS	IDG/NNC
693	1988-02-13	03:05:08.327	49.93667	78.86389	5.97	SS/TSG	IDG/NNC
694	1988-04-03	01:33:08.294	49.90833	78.90833	5.99	SS/TSG	IDG/NNC
696	1988-05-04	00:57:09.261	49.94944	78.75028	6.09	SS/TSG	IDG/NNC
698	1988-06-14	02:27:08.98	50.01889	78.96056	4.80	SS/TSG	AWE/NNC
701	1988-09-14	03:59:59.69	49.87778	78.82306	6.03	SS/TSG	AWE/NNC
703	1988-11-12	03:30:06.26	50.04306	78.96889	5.24	SS/TSG	AWE/NNC
706	1988-12-17	04:18:09.291	49.88194	78.92472	5.83	SS/TSG	IDG/NNC
708	1989-01-22	03:57:09.02	49.93944	78.81944	6.10	SS/TSG	AWE/NNC
709	1989-02-12	04:15:09.342	49.91861	78.71111	5.86	SS/TSG	IDG/NNC
711	1989-07-08	03:47:00.03	49.86778	78.78028	5.55	SS/TSG	AWE/NNC
712	1989-09-02	04:16:59.85	50.00583	78.98556	4.94	SS/TSG	AWE/NNC

continue on next page

Test No.	Date Year-Mo-Da	Time (hr:mn:sec)	Latitude (°N)	Longitude (°E)	m_b (P)	Instrument type[2]	Comments
714	1989-10-19	09:49:59.81	49.92222	78.90833	5.86	SS/TSG	AWE/NNC

[1] Test No.=unique test number given in Mikhailov et al. (1996) for 715 nuclear tests in USSR; body-wave magnitude, $m_b(P)$, from Marshall et al. (1985); Bocharov=ground truth data from Bocharov et al (1989); NNC=ground truth location by the National Nuclear Center, RK (1999); AWE=origin time from Lilwall & Farthing (1990); Double=double tests either proceeded or followed by another test at Degelen by few seconds; [2] Instrument type=instrument used, KODB= KOD low-gain system; KODM= KOD high-gain system; SS=STsR-SS system; TSG=STsR-TSG system (see Kim & Ekström, 1996); Precision of the seismically determined origin times are indicated by their decimal points and the accuracy of the groundtruth information is also indicated by the decimal point.

Table 3: Deglitched Borovoye data for underground nuclear test at Degelen subarea of STS, 1967–1989[1]

Test No.	Date Year-Mo-Da	Time (hr:mn:sec)	Latitude (°N)	Longitude (°E)	m_b (P)	Instrument type[2]	Comments
264	1967-02-26	03:57:59.8	49.74569	78.08231	6.03	KODB	Bocharov
266	1967-04-20	04:08:01.0	49.74161	78.10542	5.56	KODB	Bocharov
267	1967-05-28	04:07:59.6	49.75642	78.01689	5.46	KODB	Bocharov
268	1967-06-29	02:56:59.9	49.81669	78.04903	5.34	KODB/M	Bocharov
269	1967-07-15	03:26:59.9	49.83592	78.11817	5.39	KODB	Bocharov
270	1967-08-04	06:58:00.3	49.76028	78.05550	5.32	KODB/M	Bocharov
271	1967-09-02	04:04:00.0	49.74194	78.02556	4.10	KODB	Khalturin
275	1967-10-17	05:04:00.2	49.78089	78.00383	5.63	KODB/M	Bocharov
277	1967-10-30	06:04:00.0	49.79436	78.00786	5.41	KODB/M	Bocharov
279	1967-12-08	06:03:59.8	49.81714	78.16378	5.31	KODB	Bocharov
280	1968-01-07	03:46:59.9	49.75442	78.03094	4.98	KODB	Bocharov
281	1968-04-24	10:35:59.7	49.84519	78.10322	4.91	KODB	Bocharov
284	1968-06-11	03:05:59.7	49.79300	78.14508	5.24	KODB/M	Bocharov
294	1968-11-09	02:54:00.1	49.80053	78.13911	4.75	KODB	Bocharov
296	1968-12-18	05:01:59.7	49.74594	78.09203	5.04	KODB/M	Bocharov
297	1969-03-07	08:26:59.8	49.82147	78.06267	5.66	KODB/M	Bocharov
300	1969-05-16	04:02:59.7	49.75942	78.07578	5.26	KODB/M	Bocharov
302	1969-07-04	02:46:59.6	49.74603	78.11133	5.24	KODB/M	Bocharov
303	1969-07-23	02:47:00.2	49.81564	78.12961	5.50	KODB/M	Bocharov
306	1969-09-11	04:02:00.0	49.77631	77.99669	4.91	KODB/M	Bocharov
308	1969-10-01	04:02:59.9	49.78250	78.09831	5.26	KODB/M	Bocharov
315	1969-12-29	04:02:00.0	49.73367	78.10225	4.22	KODB	Bocharov
316	1970-01-29	07:03:00.0	49.79558	78.12389	5.60	KODB/M	Bocharov
318	1970-03-27	05:02:59.6	49.74781	77.99897	4.93	KODB/M	Bocharov
319	1970-05-27	04:03:00.0	49.73131	78.09861	4.20	KODB	Bocharov
321	1970-06-28	01:58:00.0	49.80150	78.10681	5.87	KODB/M	Bocharov
324	1970-07-24	03:57:00.0	49.80972	78.12839	5.34	KODB/M	Bocharov
326	1970-09-06	04:02:59.9	49.78889	77.99750	5.53	KODB/M	Bocharov
330	1970-12-17	07:01:00.0	49.74564	78.09917	5.43	KODB/M	Bocharov
332	1971-01-29	05:03:00.0	49.80528	78.16861	4.47	KODB	Khalturin
333	1971-03-22	04:33:00.3	49.79847	78.10897	5.77	KODB/M	Bocharov
337	1971-04-25	03:32:59.9	49.76853	78.03392	6.08	KODB/M	Bocharov
338	1971-05-25	04:03:00.4	49.80164	78.13883	5.05	KODB/M	Bocharov
350	1971-11-29	06:02:59.9	49.74342	78.07850	5.46	KODB/M	Bocharov
351	1971-12-15	07:52:59.8	49.82639	77.99731	4.90	KODB	Bocharov
353	1971-12-30	06:21:00.2	49.74917	78.00611	5.84	KODB/M	Bocharov
356	1972-03-10	04:56:59.8	49.74531	78.11969	5.45	KODM	Bocharov
357	1972-03-28	04:22:00.1	49.73306	78.07569	5.18	KODB/M	Bocharov
360	1972-06-07	01:28:00.0	49.82675	78.11547	5.42	KODB/M	Bocharov
365	1972-08-16	03:16:59.8	49.76547	78.05883	5.11	KODB/M	Bocharov
376	1972-12-10	04:27:00.0	49.81939	78.05822	5.72	KODB/M	Bocharov/Double
378	1972-12-28	04:27:00.0	49.73919	78.10625	4.60	KODB	Bocharov
379	1973-02-16	05:03:00.0	49.81583	78.10667	5.48	KODB/M	AWE/Leith
381	1973-07-10	01:27:00.15	49.79111	78.01278	5.34	KODB	AWE/Leith

continue on next page

Test No.	Date Year-Mo-Da	Time (hr:mn:sec)	Latitude (°N)	Longitude (°E)	m_b (P)	Instrument type[(2)]	Comments
391	1973-10-26	04:27:00.14	49.75222	78.13250	5.23	KODB/M	AWE/Leith
414	1974-12-16	06:23:00.14	49.76778	78.08167	4.94	TSG	AWE/Leith
415	1974-12-16	06:41:00.34	49.83306	78.02667	4.89	TSG	AWE/Leith
434	1975-12-13	04:56:59.99	49.81333	78.10861	5.00	SS/TSG	AWE/Leith
436	1976-01-15	04:46:59.97	49.81000	78.17139	5.18	SS/TSG	AWE/Leith
441	1976-04-21	04:58:00.16	49.75472	78.10750	4.94	SS/TSG	AWE/Leith
442	1976-05-19	02:57:00.2	49.77750	78.01556	4.72	SS	AWE/Leith
445	1976-07-23	02:33:00.19	49.74333	78.05167	4.96	SS	AWE/Leith
451	1976-10-30	04:57:00.21	49.83139	78.05722	4.62	SS/TSG	AWE/Leith
456	1976-12-30	03:57:00.31	49.78028	78.03667	5.09	TSG	AWE/Leith
457	1977-03-29	03:56:59.95	49.77639	78.01750	5.41	SS/TSG	AWE/Leith
459	1977-04-25	04:07:00.16	49.81333	78.10861	5.07	SS/TSG	AWE/Leith
463	1977-07-30	01:57:00.11	49.75056	78.04917	5.13	SS/TSG	AWE/Leith
465	1977-08-17	04:26:59.97	49.83083	78.11389	5.01	SS/TSG	AWE/Leith
479	1977-12-26	04:03:00.24	49.81083	78.05417	4.91	SS/TSG	AWE/Leith
482	1978-03-26	03:56:59.96	49.76194	77.98250	5.69	SS/TSG	AWE/Leith
483	1978-04-22	03:07:00.01	49.75167	78.13167	5.35	TSG	AWE/Leith
485	1978-05-29	04:56:59.85	49.79139	78.09444	4.68	SS/TSG	AWE/Leith
489	1978-07-28	02:46:59.89	49.75500	78.14500	5.75	TSG	AWE/Leith
493	1978-08-29	02:36:59.95	49.81333	78.10861	5.20	SS	AWE/Leith/Double
501	1978-10-15	05:37:00.14	49.73667	78.11111	5.15	SS/TSG	AWE/Leith
504	1978-10-31	04:17:00.19	49.78861	78.10750	5.25	SS/TSG	AWE/Leith
509	1978-12-14	04:43:00.03	49.81583	78.10667	4.74	SS/TSG	AWE/Leith
511	1978-12-20	04:33:00.04	49.81083	78.05417	4.71	SS/TSG	AWE/Leith
518	1979-05-06	03:17:00.07	49.76194	77.98250	5.22	SS/TSG	AWE/Leith
519	1979-05-31	05:55:00.05	49.81278	78.05944	5.27	SS/TSG	AWE/Leith
532	1979-09-27	04:13:00.00	49.75056	78.04917	4.42	SS/TSG	AWE/Leith
535	1979-10-18	04:17:00.11	49.82417	78.09750	5.23	SS/TSG	AWE/Leith
539	1979-11-30	04:53:00.58	49.78306	78.08667	4.42	SS/TSG	AWE/Leith
541	1979-12-21	04:42:00.09	49.79222	78.11300	4.71	SS/TSG	AWE/Leith
545	1980-04-10	04:07:00.19	49.78250	78.05722	4.98	SS/TSG	AWE/Leith
547	1980-05-22	03:57:00.14	49.77972	78.03639	5.53	SS/TSG	AWE/Leith
553	1980-07-31	03:33:00.07	49.79056	78.09083	5.33	SS/TSG	AWE/Leith
555	1980-09-25	06:21:13.06	49.78333	78.08056	4.83	SS/TSG	AWE/Leith
573	1981-06-30	01:57:15.34	49.76750	78.08083	5.16	SS/TSG	AWE/Leith
574	1981-07-17	02:37:18.12	49.80139	78.13139	5.07	TSG	AWE/Leith
575	1981-08-14	02:27:15.24	49.75222	78.05306	4.88	SS/TSG	AWE/Leith
584	1981-11-20	04:57:05.07	49.73667	78.10417	5.00	SS	AWE/Leith
586	1981-12-22	04:31:05.27	49.83417	78.08028	4.96	SS/TSG	AWE/Leith
588	1982-02-19	03:56:13.42	49.82333	78.03333	5.40	SS/TSG	AWE/Leith
590	1982-06-25	02:03:07.16	49.77139	78.11083	4.57	SS/TSG	AWE/Leith
593	1982-08-23	02:43:06.70	49.74028	78.03083	4.44	SS	AWE/Leith
596	1982-09-21	02:57:03.17	49.77917	78.12472	5.15	SS/TSG	AWE/Leith
605	1982-12-25	04:23:08.38	49.78111	78.03500	4.47	SS/TSG	AWE/Leith
608	1983-03-30	04:17:10.22	49.78500	78.04056	4.61	SS/TSG	AWE/Leith
609	1983-04-12	03:41:08.26	49.78556	78.08472	4.65	SS/TSG	AWE/Leith
610	1983-05-30	03:33:47.04	49.74111	78.12028	5.43	SS	AWE/Leith

continue on next page

Test No.	Date Year-Mo-Da	Time (hr:mn:sec)	Latitude (°N)	Longitude (°E)	m_b (P)	Instrument type[2]	Comments
612	1983-06-24	02:56:13.85	49.73972	78.03583	4.46	SS/TSG	AWE/Leith
617	1983-09-11	06:33:13.10	49.78472	78.08417	4.48	SS/TSG	AWE/Leith
629	1983-11-29	02:19:08.80	49.73028	78.09583	5.31	SS	AWE/Leith
631	1983-12-26	04:29:09.25	49.79000	78.10917	5.48	SS/TSG	AWE/Leith
635	1984-04-15	03:17:11.46	49.76056	78.08917	5.72	SS/TSG	AWE/Leith
648	1984-09-09	02:59:08.85	49.80444	78.08750	4.89	SS/TSG	AWE/Leith
650	1984-10-18	04:57:08.32	49.72944	78.08639	4.25	SS/TSG	AWE/Leith
655	1984-11-23	03:55:07.48	49.81250	78.05944	4.38	SS/TSG	AWE/Leith
668	1985-07-25	03:11:09.23	49.81917	78.14944	4.82	SS/TSG	AWE/Leith
669	1987-02-26	04:58:24.32	49.83417	78.08111	5.40	SS/TSG	AWE/Leith
676	1987-05-06	04:02:08.11	49.77583	78.01222	5.60	SS/TSG	AWE/Leith
677	1987-06-06	02:37:09.25	49.83667	78.06167	5.40	SS/TSG	AWE/Leith
680	1987-07-17	01:17:09.18	49.77583	78.01972	5.80	SS	AWE/Leith
685	1987-09-18	02:32:10.01	49.80444	78.08750	4.30	SS	AWE/Leith
687	1987-10-16	06:06:06.99	49.72972	78.08667	4.60	SS/TSG	AWE/Leith
690	1987-12-20	02:55:09.14	49.77583	78.01222	4.80	SS/TSG	AWE/Leith
692	1988-02-06	04:19:09.13	49.77583	78.01972	4.70	SS/TSG	AWE/Leith
695	1988-04-22	09:30:09.44	49.79028	78.10694	4.90	SS/TSG	AWE/Leith
702	1988-10-18	03:40:09.16	49.78000	78.01722	4.90	SS/TSG	AWE/Leith
704	1988-11-23	03:57:08.99	49.77944	78.03722	5.40	SS/TSG	AWE/Leith
707	1988-12-28	05:28:10	49.80111	78.06861	3.74	SS/TSG	Khalturin/Leith
710	1989-02-17	04:01:09.22	49.82778	78.05972	5.00	SS/TSG	AWE/Leith
713	1989-10-04	11:30:00.16	49.74833	78.00944	4.60	SS/TSG	AWE/Leith

[1] Test No.=unique test id number given in Mikhailov et al. (1996) for nuclear tests in USSR; Body-wave magnitude, $m_b(P)$, from Marshall et al. (1985) and Ringdal et al. (1992). Bocharov=ground truth data from Bocharov et al (1989); Leith=ground truth location by Leith (1998) for entrance to the tunnels; AWE=origin time from Lilwall & Farthing (1990); Khalturin=location and origin time from Khalturin et al. (2001); Double=double tests either proceeded or followed by another test at Balapan by few seconds; [2] Instrument type=instrument used, KODB= KOD low-gain system; KODM= KOD high-gain system; SS=STsR-SS system; TSG=STsR-TSG system (see Kim & Ekström, 1996); Precision of the seismically determined origin times are indicated by their decimal points and the accuracy of the groundtruth information is also indicated by the decimal point.

Table 4: Deglitched Borovoye data for underground nuclear test at Murzhik subarea of STS, 1967–1980[(1)]

Test No.	Date Year-Mo-Da	Time (hr:mn:sec)	Latitude (°N)	Longitude (°E)	m_b (P)	Instrument type[(2)]	Comments
262	1966-12-18	04:58:00.0	49.92458	77.74722	5.92	KODB	Bocharov
272	1967-09-16	04:04:00.3	49.93719	77.72811	5.25	KODB/M	Bocharov
273	1967-09-22	05:04:00.0	49.95964	77.69106	5.16	KODB	Bocharov
278	1967-11-22	04:03:59.9	49.94194	77.68683	4.41	KODB	Bocharov
301	1969-05-31	05:01:59.4	49.95031	77.69422	5.29	KODB/M	Bocharov
314	1969-12-28	03:47:00.2	49.93733	77.71422	5.79	KODB/M	Bocharov
323	1970-07-21	03:02:59.7	49.95242	77.67289	5.38	KODB/M	Bocharov
328	1970-11-04	06:02:59.8	49.98922	77.76244	5.44	KODB/M	Bocharov
339	1971-06-06	04:02:59.7	49.97542	77.66028	5.53	KODB/M	Bocharov
340	1971-06-19	04:04:00.1	49.96903	77.64081	5.54	KODB/M	Bocharov
347	1971-10-09	06:02:59.7	49.97789	77.64144	5.37	KODB/M	Bocharov
348	1971-10-21	06:02:59.7	49.97381	77.59733	5.58	KODB/M	Bocharov
367	1972-08-26	03:46:59.7	49.98197	77.71661	5.36	KODB/M	Bocharov
380	1973-04-19	04:32:59.92	49.984	77.614	5.36	KODB/M	AWE
447	1976-08-04	02:57:00	49.87	77.70	4.20	SS	Khalturin
481	1978-03-19	03:46:59.82	49.945	77.704	5.19	SS/TSG	AWE
515	1979-02-16	04:04:00.50	49.974	77.668	5.39	SS/TSG	AWE
524	1979-07-18	03:17:04.92	49.919	77.812	5.16	SS/TSG	AWE
544	1980-04-04	05:32:59.83	50.000	77.823	4.90	SS/TSG	AWE

[(1)] Test No.=nuclear test number given in Mikhailov et al. (1996), which lists 715 nuclear tests conducted by USSR; Bocharov=ground truth data from Bocharov et al (1989); AWE=origin time and location from Lilwall & Farthing (1990); Khalturin=location and origin time from Khalturin et al. (2000); Body-wave magnitude, $m_b(P)$, from Marshall et al. (1985) and Ringdal et al. (1992). [(2)] Instrument type=instrument used, KODB= KOD low-gain system; KODM= KOD high-gain system; SS=STsR-SS system; TSG=STsR-TSG system.

Table 5: Deglitched Borovoye data for underground nuclear test at Novaya Zemlya Test Sites, 1967–1990[1]

Test No.	Date Year-Mo-Da	Time (hr:mn:sec)	Lat. (°N)	Long. (°E)	m_b (P)	Inst. type[2]	Comments
276	1967-10-21	04:59:58.49	73.390	54.810	5.98	KODB/M	salvo exp. in two tunnels
293	1968-11-07	10:02:05.49	73.387	54.858	6.13	KODB/M	salvo exp. in single tunnel
309	1969-10-14	07:00:06.61	73.390	54.787	6.18	KODB/M	3 explosions
327	1970-10-14	05:59:57.57	73.304	55.027	6.79	KODB/M	3 explosions 150-1500 kt
345	1971-09-27	05:59:55.75	73.393	54.920	6.67	KODB/M	4 explosions 150-1500 kt
368	1972-08-28	05:59:56.87	73.388	54.847	6.49	KODB/M	4 explosions
385	1973-09-12	06:59:54.81	73.314	55.056	6.97	KODB/M	hightest yield Soviet UNT
388	1973-09-27	07:00:01.12	70.731	53.827	5.89	KODB/SS	Southern Test Site
392	1973-10-27	07:00:00.61	70.780	54.026	6.98	KODB/M/SS	Southern Test Site
427	1975-08-23	08:59:58.25	73.334	54.682	6.55	TSG	salvo exp. with 8 explosions
430	1975-10-18	08:59:59.40	70.816	53.744	6.75	TSG	2 expls. shaft Yu-6N
431	1975-10-18	Single explosion in shaft Yu-7 simultaneously with test #430 both Sothern Test Site					
432	1975-10-21	11:59:58.03	73.307	55.010	6.60	SS/TSG	5 explosions
449	1976-09-29	02:59:57.70	73.360	54.871	5.83	SS/TSG	2 expls. reference for JED
450	1976-10-20	07:59:58.07	73.398	54.812	4.98	SS/TSG	4 explosions
467	1977-09-01	02:59:57.97	73.339	54.619	5.66	TSG	4 explosions
471	1977-10-09	10:59:58.12	73.409	54.927	4.36	SS/TSG	single explosion 0.001-20 kt
491	1978-08-10	07:59:57.93	73.291	54.883	6.00	SS/TSG	6 explosions
499	1978-09-27	02:04:58.60	73.349	54.676	5.63	SS/TSG	7 explosions
531	1979-09-24	03:29:59.75	73.343	54.672	5.77	TSG	3 explosions
536	1979-10-18	07:09:58.75	73.316	54.816	5.79	SS/TSG	4 explosions
557	1980-10-11	07:09:57.47	73.336	54.940	5.76	SS	7 explosions
580	1981-10-01	12:14:57.23	73.304	54.818	5.97	TSG	4 explosions
599	1982-10-11	07:14:58.63	73.339	54.608	5.58	TSG	4 explosions
616	1983-08-18	16:09:58.90	73.354	54.974	5.91	SS	5 explosions
624	1983-09-25	13:09:58.22	73.328	54.541	5.77	SS/TSG	4 explosions
651	1984-10-25	06:29:58.12	73.355	54.990	5.82	SS/TSG	4 explosions
682	1987-08-02	02:00:00.20	73.326	54.602	5.82	SS/TSG	5 explosions
697	1988-05-07	22:49:58.34	73.314	54.553	5.58	SS/TSG	3 explosions
705	1988-12-04	05:19:53.30	73.366	55.001	5.89	SS/TSG	5 explosions
715	1990-10-24	14:57:58.45	73.331	54.757	5.70	SS/TSG	8 expls. last Sovie test

[1] Test No.=unique test id number given in Mikhailov et al. (1996) for nuclear tests in USSR; Body-wave magnitude, $m_b(P)$, from Marshall et al. (1994); location and origin time from Marshall et al. (1994) and Richards (2000). [2] Inst. type= instrument used; KODB= KOD low-gain system; KODM= KOD high-gain system; SS=STsR-SS system; TSG=STsR-TSG system. [3] salvo exp.= salvo explosion means two or more separate explosions where a period of time between successive individual explosions does not exceed 5 seconds and where the burial points of all explosive devices can be connected by segments of straight lines, each of them connecting two burial points and does not exceed 40 kilometers in length.

Table 6: Deglitched Borovoye data for Peaceful Nuclear Explosions in the Former Soviet Union, 1967–1988[(1)]

Test No.	Date Year-Mo-Da	Time (hr:mn:sec)	Latitude (°N)	Longitude (°E)	Depth (m)	m_b (P)	Distance (°)	Az (°)	Instrument type
274	1967-10-06	06:59:57.5	57.70	65.20	172	4.7	5.46	330.2	KODB
282	1968-05-21	03:59:11.98	38.918	65.032	2440	5.4	14.59	196.4	KODB
304	1969-09-02	04:59:58.61	57.220	55.393	1212	4.8	9.45	302.1	KODB
305	1969-09-08	04:59:58.70	57.220	55.417	1208	4.8	9.44	302.1	KOD
307	1969-09-26	06:59:58.14	45.848	42.600	712	5.6	19.23	259.2	KOD
313	1969-12-06	07:02:59.85	43.867	54.800	407	5.8	13.73	234.2	KOD
320	1970-06-25	04:59:55.5	52.20	55.70	702	4.9	8.88	270.3	KODB
329	1970-12-12	07:00:59.83	43.85	54.80	497	6.0	13.74	234.2	KOD
331	1970-12-23	07:00:59.76	44.025	54.933	470	6.0	13.55	234.3	KOD
335	1971-03-23	06:59:58.38	61.40	56.20	127	5.5	11.25	323.4	KOD
342	1971-07-02	17:00:01.13	67.283	63.467	542	4.7	14.60	349.5	KODB
344	1971-09-19	11:00:01.08	57.508	42.643	610	4.5	16.23	296.9	KODB
346	1971-10-04	10:00:00.14	61.358	48.092	595	4.6	14.49	313.6	KODB
352	1971-12-22	06:59:59.0	47.897	48.133	986	6.0	14.94	258.7	KOD
358	1972-04-11	06:00:01.92	37.35	62.05	1720	4.9	16.72	203.3	KODB
363	1972-07-09	07:00:01.25	49.80	35.40	2483	4.8	21.77	275.6	KODB
366	1972-08-20	03:00:00.01	49.400	48.142	489	5.7	14.28	264.1	KOD
370	1972-09-04	07:00:00	67.75	33.10	131	4.6	22.92	324.0	KODB
371	1972-09-21	09:00:00.31	52.118	52.068	485	5.0	11.08	272.4	KODB
372	1972-10-03	09:00:00.18	46.853	44.938	485	5.6	17.34	259.3	KODB
375	1972-11-24	09:00:00.04	51.990	51.867	675	4.5	11.22	271.9	KODB
383	1973-08-15	02:00:00.02	42.775	67.408	600	5.3	10.46	191.7	KOD/SS
384	1973-08-28	03:00:00.04	50.527	68.323	395	5.2	2.81	206.4	KOD/SS
386	1973-09-19	03:00:00.18	45.758	67.825	615	5.1	7.47	193.3	KOD/SS
389	1973-09-30	05:00:00.35	51.65	54.55	1145	5.2	9.69	268.0	KODB
390	1973-10-26	05:59:59.5	53.65	55.40	2026	4.8	8.89	279.8	KODB
406	1974-08-29	15:00:00.39	67.085	62.625	583	5.0	14.51	348.1	SS
428	1975-09-29	11:00:00.43	69.578	90.337	834	4.8	18.91	21.7	SS
438	1976-03-29	07:00:00.23	47.897	48.133	986	4.3	14.94	258.7	SS/TSG
446	1976-07-29	05:00:00.5	47.870	48.150	1000	5.9	14.94	258.6	SS/TSG
452	1976-11-05	03:59:59.98	61.458	112.860	1522	5.3	24.00	52.6	SS
462	1977-07-26	17:00:00.22	69.575	90.375	850	5.0	18.92	21.7	SS/TSG
466	1977-08-20	22:00:00.78	64.108	99.558	600	5.0	18.57	42.1	TSG
469	1977-09-10	16:00:00.18	57.251	106.551	550	4.8	20.88	63.9	SS/TSG
470	1977-09-30	06:59:58.43	47.897	48.161	1500	5.0	14.92	258.7	SS
490	1978-08-09	18:00:00.79	63.678	125.522	567	5.6	29.74	47.3	SS
492	1978-08-24	18:00:00.35	65.925	112.338	577	5.1	24.25	41.7	SS/TSG
498	1978-09-21	15:00:00.19	66.598	86.210	886	5.2	15.62	23.9	SS/TSG
500	1978-10-08	00:00:00.0	61.55	112.85	1545	5.2	23.99	52.4	SS
502	1978-10-17	04:59:59.06	47.850	48.120	1040	5.8	14.97	258.6	SS
503	1978-10-17	14:00:00.16	63.185	63.432	593	5.5	10.74	343.2	SS
510	1978-12-18	07:59:58.5	47.860	48.160	630	5.9	14.94	258.6	SS/TSG
513	1979-01-17	07:59:58.5	47.920	48.120	995	6.0	14.93	258.8	SS/TSG
523	1979-07-14	04:59:58.0	47.880	48.120	849	5.6	14.95	258.7	SS/TSG

continue on next page

Test No.	Date Year-Mo-Da	Time (hr:mn:sec)	Latitude (°N)	Longitude (°E)	Depth (m)	m_b (P)	Distance (°)	Az (°)	Instrument type
527	1979-08-12	18:00:00.21	61.803	122.430	982	4.9	28.52	51.4	SS/TSG
529	1979-09-06	18:00:00.31	64.110	99.562	599	4.9	18.57	42.1	SS/TSG
533	1979-10-04	16:00:00.03	60.675	71.455	837	5.4	7.64	4.3	SS/TSG
534	1979-10-07	21:00:00.22	61.85	113.10	1545	5.0	24.12	51.7	SS/TSG
537	1979-10-24	05:59:59.0	47.850	48.140	915	5.8	14.96	258.6	SS/TSG
556	1980-10-08	06:00:00.29	46.757	48.275	1050	5.2	15.43	254.8	SS
560	1980-11-01	13:00:00.42	60.80	97.55	720	5.2	16.60	51.5	TSG
570	1981-05-25	05:00:00.32	68.20	53.50	1511	5.5	17.10	338.6	SS
576	1981-09-02	03:59:59.99	60.60	55.70	2088	4.4	10.94	319.3	TSG
578	1981-09-26	05:00:00.28	46.790	48.313	1050	5.2	15.39	254.8	TSG
579	1981-09-26	05:03:59.94	46.771	48.304	1050	5.3	15.41	254.8	TSG
583	1981-10-22	14:00:00.36	63.80	97.55	581	5.1	17.64	41.9	TSG
592	1982-07-30	21:00:00.00	53.80	104.15	554	5.0	20.00	74.2	TSG
597	1982-09-25	18:00:00.18	64.35	91.80	554	5.2	15.74	35.8	TSG
613	1983-07-10	04:00:00.00	51.363	53.306	907	5.3	10.51	267.5	SS
614	1983-07-10	04:04:59.94	51.367	53.327	917	5.3	10.50	267.5	SS
615	1983-07-10	04:09:59.85	51.380	53.340	841	5.3	10.49	267.6	SS
618	1983-09-24	05:00:00.03	46.783	48.315	1050	5.2	15.39	254.8	SS
619	1983-09-24	05:05:00.03	46.788	48.297	1050	5.1	15.40	254.8	SS
620	1983-09-24	05:10:00.08	46.767	48.310	920	5.0	15.40	254.8	SS
621	1983-09-24	05:15:00.14	46.749	48.303	1100	5.2	15.42	254.7	SS
622	1983-09-24	05:19:59.93	46.754	48.288	950	5.4	15.42	254.8	SS
623	1983-09-24	05:25:00.00	46.766	48.274	1100	5.3	15.43	254.8	SS
639	1984-07-21	02:59:59.81	51.358	53.319	846	5.4	10.51	267.5	SS
640	1984-07-21	03:04:59.71	51.371	53.337	955	5.3	10.49	267.6	SS
641	1984-07-21	03:09:59.85	51.391	53.351	844	5.4	10.48	267.6	SS
643	1984-08-25	19:00:00.33	61.90	72.10	726	5.3	8.89	5.5	SS
649	1984-09-17	21:00:00.03	55.834	87.526	557	5.0	10.37	67.6	TSG
652	1984-10-27	06:00:00.10	46.90	48.15	1000	5.0	15.43	255.4	SS/TSG
653	1984-10-27	06:05:00.00	46.95	48.10	1000	5.0	15.43	255.6	SS/TSG
681	1987-07-24	02:00:00.0	61.45	112.80	1515	5.1	23.97	52.7	SS
684	1987-08-12	01:30:00.5	61.45	112.80	815	5.0	23.97	52.7	SS
686	1987-10-03	15:15:00.03	47.60	56.20	1002	5.3	10.49	244.3	SS/TSG
699	1988-08-22	16:20:00.07	66.280	78.491	829	5.3	13.83	13.9	SS/TSG
700	1988-09-06	16:19:59.94	61.361	48.092	820	4.8	14.49	313.7	SS/TSG

$^{(1)}$ Test No.=nuclear test number given in Mikhailov et al. (1996); Date and Time=origin time of the tests given in Sultanov et al. (1999); Latitude and Lognitude=location the tests given in Sultanov et al. (1999); $m_b(P)$=body-wave magnitude of the tests given in Sultanov et al. (1999); Distance=epicentral distance in degrees from the PNE to Borovoye; Az=azimuth in degrees from the station to PNE; Precision of the origin time[1] is indicated by their decimal point. Location accuracies are also indicated by the decimal point.

[1] whole second or one hundredth of a second

Table 7: Deglitched Borovoye data for Chinese Underground Nuclear Tests at Lop Nor, 1969–1995[1]

N	Date Year-Mo-Da	Time (hr:mn:sec)	Latitude (°N)	Longitude (°E)	m_b (P)	Event id	Instrument type[2]	Comments
01	1969-09-22	16:15:01.57	41.373	88.352	5.2	CH01	KODB	C, tunnel
02	1976-10-17	05:00:01.37	41.734	88.383	4.9	CH04	SS	B, tunnel
03	1978-10-14	01:00:00.25	41.511	88.772	4.9	CH05	SS/TSG	A, shaft
04	1983-10-06	10:00:00.52	41.523	88.705	5.5	CH07	SS/TSG	A, shaft
05	1984-10-03	06:00:00.58	41.577	88.706	5.4	CH08	SS	A, shaft
06	1984-12-19	06:00:00.86	41.738	88.365	4.7	CH09	SS/TSG	B, tunnel
07	1987-06-05	05:00:00.73	41.505	88.709	6.2	CH10	SS/TSG	A, shaft
08	1990-08-16	05:00:00.16	41.511	88.742	6.2	CH13	SS/TSG	A, shaft
09	1993-10-05	01:59:58.99	41.593	88.687	5.9	CH16	TSG	A, shaft
10	1994-10-07	03:26:00.37	41.556	88.736	5.9	CH18	TSG	A, shaft
11	1995-05-15	04:06:00.31	41.546	88.772	6.1	CH19	TSG	A, shaft

[1] location and origin time from Engdahl (2001), teleseismic body-wave magnitude from PDE. [2] Instrument type= instrument used, KODB= KOD low-gain system; KODM= KOD high-gain system; SS=STsR-SS system; TSG=STsR-TSG system.

2.1. The Borovoye Station

The Borovoye Geophysical Observatory began recording seismic signals in digital form in 1965 under the auspices of a field program of the USSR Academy of Sciences. A description of operations is given by Richards et al. (1992). Seismic observations continued to about 2008 when the Observatory grounds were taken over by organizations planning hotels and possibly casinos.

The digital data at Borovoye were mostly written on 35 mm tapes and were stored at the Observatory. This digital seismogram archive holds data from one of the few digital seismographic stations operated anywhere in the world during the late 1960s and early 1970s, and provides unique data for the Central Asia region for the whole 30-year period from commencement of recording, up to the end of regular nuclear weapons testing by the recognized nuclear weapons states in 1996. The archive is invaluable for global seismological studies, due to its longevity of homogeneous observation over more than 25 years and the low-noise conditions in northern Kazakhstan.

There are about 8,000 digital seismogram archive tapes. Each magnetic tape has about 10 megabytes of digital seismogram data. Digital data were recorded by three Russian different systems, called KOD, STsR-SS, and STsR-TSG; and in a few cases by IBM personal computer formats (PCs). Signals come from about 100,000 seismic events, which include earthquakes, industrial and nuclear explosions, and industrial accidents. The archive also contains some recordings from a former Soviet Army base near Borovoye and digital data from seismograph stations in Central Asia—including Talgar (TLG), Bishkek (formerly Frunze, FRU) and Naryn (NRN). Since underground nuclear explosions were carried out in a wide variety of geological conditions as part of the Soviet Peaceful Nuclear Explosion program, as well as at the USSR's nuclear weapons test sites, the BRVK archive of nuclear explosion data is invaluable for purposes of research on CTBT verification. Only with good data on explosions carried out in a variety of environments, is it possible to accomplish a rational design for an explosion monitoring network.

The original wide tapes used as the archive medium have been deteriorating for many years and it was realized that the signals should be copied to more stable media, otherwise these valuable seismic observations would be lost forever. In order to save the digital seismogram archive at Borovoye and to make this valuable data available to interested scientists worldwide, Paul Richards and Won-Young Kim of the Lamont-Doherty Earth Observatory, Columbia University, worked with personnel at the National Nuclear Centre (NNC), Republic of Kazakhstan, and of the Institute of Dynamics of the Geosphere (IDG), Russian Academy of Sciences, in the 1990s. This plan recognized that NNC, IDG and LDEO had to work closely together, since the Borovoye Observatory had become a facility of the NNC in Kazakhstan, but personnel of IDG were most familiar with the content of the archive, and LDEO had designed (with IDG) the necessary hardware and software systems for modernization.

In sections below, we further describe:

- the specific methods and procedures applied in the present project;
- the results obtained in terms of specific information about numerous different instrument systems and their different channels, with instrument responses and

how they were changed at different times;
- some representative seismograms; and
- our conclusions.

The BRV digital archive of nuclear explosion waveforms from 711 underground nuclear explosions was made available in April 2001 (for example, via http://www.ldeo.columbia.edu/res/pi/Monitoring/Arch/BRV_arch_exp.html), as an outcome of the International Science and Technology Center project mentioned above, which ran from 1997 to 2000. That project was initiated by Lamont, and provided 180 man-years of funding to scientists and technicians in Kazakhstan and Russia for several different projects, of which the most time-consuming was saving the Borovoye waveform archive.

The archive of nuclear explosion signals was issued as a series of modern databases, described by Kim et al. (2001), in a report available today as a 41-page pdf file via http://www.ldeo.columbia.edu/Monitoring/Data/Brv_arch_ex/brv_text_table.pdf . The archive was derived from original Soviet-era magnetic tapes that in many cases were in very bad condition, and for which only a limited number of tape readers existed. The tapes were written in complicated formats that had not been used even in the USSR for decades. For example, many tapes were 35 mm wide, and had 24 channels of information written across 17 separate tracks. The first steps in salvaging the archive were reading all the bits one last time from the original tapes using one of the few available tape readers, and then writing them to a mid-1990s mass store hard drive. Later steps entailed extraction of timing information, de-multiplexing, and re-formatting.

Here, we may note that three different sets of Soviet-style instruments and recording systems were deployed at BRV from 1966 to 1996. They are known as the KOD, STsR-SS, and STsR-TSG systems (sometimes abbreviated to KO or KOD, SS, and TS or TSG). The first BRV digital seismic system, KOD, began recording in 1966 and operated continuously from 1967 to 1973. It is based on three component, short-period seismometers, and is important as one of the few digital seismic systems anywhere in the world in the late 1960s and early 1970s. The other Soviet-era BRV digital systems began operation in February 1973. STsR-SS is intended mainly for low-gain recording. STsR-TSG includes six long-period and seven short-period Kirnos seismometers, most recorded at two gain levels, for a total (SS + TS) of 20 data channels. The highest sensitivity is 100,000 counts/micron based on a short-period Kirnos with a special magnet and a low-noise amplifier. This instrument was important at BRV for teleseismic monitoring of numerous French and US UNEs. Kim and Ekström (1996) have published details of the STsR-TSG instrument responses (many channels, extending across almost 3 decades in frequency). All of these main systems are approximately flat to ground displacement over a range of frequencies.

We note that numerous modern broadband sensors are deployed today at Borovoye, the first of which was installed by Won-Young Kim in July 1994. These modern sensors recorded the final underground nuclear explosions conducted by China, and the May 1998 tests of India and Pakistan. They have also recorded numerous earthquakes at regional distances. The station code BRVK is used to represent Borovoye today.

3. METHODS OF ANALYSIS

3.1. Technical Approach to Deglitching

When the BRV archive was made generally available in 2001, the decision was made that it be essentially in its original unprocessed form (though with the addition of basic header information), but converted to a modern and widely used format for digital seismic data (CSS3.0). The original Soviet-era recordings had some severe problems, most notoriously that the digitizer typically did not write a count value on seismic waveform channels at the time when the time channel was writing the marker for an integer second. The waveform data therefore ended up with numerous glitches. Also, the original recording system addressed the practical problem of input signal with wide dynamic range, by having several different channels set at different gain levels, each recording with a limited number of bits (often, only 11 bits), so that although each UNE was usually recorded on several channels, in practice these channels were often either clipped or had inadequate resolution.

Despite these defects, ways to extract the underlying information have been found. For example, empirical travel-time information, needed to generate Source Specific Station Corrections for the BRV station (which today is part of the International Monitoring System) can be obtained by picking first and secondary arrivals from a high-gain channel. But the spectrum of the strongest ground motion is often best obtained from one of the lower-gain channels. Coda can be measured from both high gain and low gain channels.

Prior to the execution of the present project, personnel at Los Alamos National Laboratory (including Howard Patton, Scott Phillips, George Randall, Steve Taylor) had become familiar with the BRV archive, had processed approximately one third of it to remove glitches, had used the results of Kim and Ekström (1996) to correct for instrument response for one of the instrument response/recording systems in use at BRV, and had used the resulting corrected waveforms in a variety of practical studies to improve nuclear explosion monitoring in Central Asia and the surrounding regions.

These corrected waveforms were used for regional seismic discrimination studies, coda wave magnitude studies, and regional *Ms* studies, primarily using the STsR-TSG or TS instrumentation. LANL personnel had also used a limited subset of the earlier KOD and STsR-SS data for discrimination studies of selected events, but were unable to use discriminants based on ratios of different frequency bands as the archive did not then contain response information for those instruments (KOD, SS).

Raw waveforms of the Borovoye archive are contaminated with glitches on all seismometer channels and their different gain levels, for the entire time period that data are available. Many glitches are not visible to the naked eye on the vertical scale of these plots, so the problem is more extensive than it may appear from just plotting the seismogram trace.

There appear to be at least two sources of glitches. The most easily corrected and explained are time marks (see above) characterized by a distinct period and the largest amplitude glitches. There are some waveforms for which the time-mark glitch is the primary problem.

The more difficult and time consuming glitches appear in some cases to be bit errors. During interactive passes over problematic waveforms, we found many glitches where the difference between the glitch and the apparent waveform is either a power of 2 (e.g. 16, 32, 64, 128 ...) or a sum of powers of 2 (e.g. 48 = 16 + 32, 96 = 32 + 64, 80 = 16 + 64, ...) which represent bit failures either in the original data stream or in the long-term deterioration of the archive. Many of these small bit errors are readily found by the deglitcher that will be discussed below. The labor to do this work is time-consuming and still requires technical judgements.

The most common defects in the salvaged Borovoye waveform archive resulting from the ISTC project are single point glitches and multiple point glitches of short duration. Certain glitches appear to be associated with timing, while others could be simple 1-bit errors. We did not investigate the sources of the glitches, but simply resolved to repair them via interpolation to allow subsequent analysis of the digital data. We discovered a range of glitch amplitudes in these data, many smaller than waveform amplitudes, which compelled us to design an automated, interactive script to perform the repair work.

The repair procedure developed and applied at Los Alamos National Laboratory by W. Scott Phillips relies upon a high passed, differentiated trace to identify glitches, and a fourth-order polynomial fit to find the glitch edge points and perform the repair. Prior to analysis, we marked poor data, such as saturated intervals, that the automated procedure should ignore. We also removed the median and applied ten-point tapers to the beginning and end of the entire waveform. To identify glitches, we differentiated the trace, then applied a two-pole, causal, high pass Butterworth filter with a corner set to two-thirds the Nyquist frequency, removed the median, and took absolute values. This procedure brought out small glitches that would otherwise be buried in the waveform. The user sets a threshold and a time window, and the procedure cycles through that subset of glitches. Additional passes with lower thresholds or different time windows may be run until the user decides that repair is complete.

For each glitch that is identified using the high-pass, differentiated trace, we set an initial analysis window of length ten times the sample interval. A fourth-order polynomial is fit to the waveform data in this window, using L1 minimization to avoid effects of the glitch. Glitches are defined using a three-sigma threshold based on a robust residual spread estimate (median absolute deviation, MAD; e.g., Rousseeuw and Croux, 1993), and are replaced using the polynomial coefficients. The L1 fit procedure matches five waveform points exactly, and those points may or may not include the nearest edge points on either side of the glitch. As a fine adjustment, we add a linear function to the polynominal to ensure that those edge points are matched exactly. The original glitch and repaired waveform are then displayed, whereupon the user may: 1) accept the repair, 2) pick one or more of the glitch edge points and window endpoints, and refit the waveform, 3) expand the window, pick as above, and refit the waveform, or 4) skip the repair of that segment. The user is allowed to mark additional unfixable waveform segments noted during the interactive processing after the procedure is finished.

The work of deglitching in this project was carried out at Los Alamos National Laboratory by Diane Baker, Howard Patton, and George Randall.

The next two sub-sections describe in detail the two earliest seismographic systems used at Borovoye.

3.2 KOD Digital Seismograph System

The KOD digital seismograph system consists of a three-component set of long-period SKD seismometers (T_0=30 sec) and a three-component set of short-period SKM-3 seismometers (T_0=3.5 sec), galvanometer phototube amplifier, three-channel KOD-I amplifier system, analog-to-digital converter and a tape recorder (Shishkevish, 1975). The KOD system, which was operating at several locations in the former Soviet Union since 1966, is important as one of the few digital systems anywhere in the world in the late 1960s and early 1970s. The KOD-I amplifier system consists of a postamplifer, a low-pass RC (resistor-capacitor) filter with a drop of 40 dB at 50 Hz, and a RC notch filter with notch frequency around 0.145 Hz ($\sim$ 6.9 s period) with an attenuation rate of 32 dB/octave and a drop of 40 dB at the notch (Shishkevish, 1975). The KOD-I has two outputs per channel with a gain of 10 and 100. However, excluding the sawtooth control voltage, only four data channels can be recorded on magnetic tapes, with the usual combination being three-component high gain and a vertical-component low-gain, or vice versa.

Seismic signals from the KOD-I amplifier system are sampled sequentially by an analog-to-digital (A/D) converter at a rate of 33 samples per second. The A/D converter is a 10-channel (only 5 are used), 11-bit unit with a dynamic range of $\pm$5 V (volts) and hence, the least significant bit represents $\pm$4.88 mV/count (= $\pm$ 5 V /$\pm$ 1024 counts). The five data channels are recorded in parallel in 11-bit code on 17-track 35-mm magnetic tape of a LMR type recorder. The 12th bit on the tape is a parity check.

The absolute time in 12-bit time code is recorded at every 30 s intervals, resulting in the loss of a data point from each of the five channels every 1,000 conversions. A quartz clock synchronized by radio wave signal once every 12 hours maintains an overall accuracy of 0.1 s per day (Osadchiy & Daragan, 1966).

The KOD seismograph system at Borovoye had only three-component, short-period seismometers – SKM-3, which had natural period, T_0 = 3.5 s and damping constant, D_s = 0.7 (Adushkin & An, 1990). The KOD system at Borovoye operated from 1966 to Nov. 1973 and had nominal gains of 3,000 counts/μm and 300 counts/μm for high- and low-gain channels, respectively (Adushkin & An, 1990). It is noted that the KOD system at Borovoye had polarity reversal on all channels. Four data channels and a sawtooth control voltage channel are recorded with the usual combination being three-component high-gain and a vertical-component low-gain (called KODB) and three-component low-gain and a vertical-component high-gain system (KODM) (Osadchiy & Daragan, 1966). The de-glitched Borovoye waveform archive includes records from KODB (high-gain channels) and KODM (low-gain channels) systems during 1967–1973.

KODB: 3-Component High-Gain and a Low-Gain Vertical-Component System

This is the main data stream for 3-component, short-period signals from SKM-3 seismometers with a vertical-component low-gain recording. Signals are recorded on channels 1, 3 and 4, for high-gain vertical-, NS-, and EW-component, respectively. Although we do not know the exact instrument response and gains of the KOD system, the Borovoye waveform data archive included instrument responses in discrete frequencies as in the fap (frequency, amplitude and period) files (see Kim et al., 2001). Figure 6 shows all 78 fap files available for the KODB system. These fap files are not associated with any events or specific time periods. 44 fap files do not cover notch filter bands and cover insufficient frequency band, and we selected 34 fap files that

cover complete frequency bands between 0.05 and 10 Hz. The selected fap response files are plotted in Figure 7 and are used to determine the nominal response of each channel. Figures 8, 9 and 10 show nine selected frequency-amplitude calibration curves for these channels and the average value at each frequency with its standard deviation. Figure 11 shows seven frequency-amplitude calibration curves for low-gain vertical-component channel and the average value at each frequency with its standard deviation.

These channels had the listed nominal gains of 3,000 counts/μm and 300 counts/μm for high- and low-gain channels, respectively and recorded with sampling interval of 30 msec during their operation (Adushkin & An, 1990). The gains of each channel are obtained by averaging values from these calibration curves and the peak amplitude at 1.8 Hz are listed in Table 8 as the gains.

KODM: 3-Component Low-Gain and a High-Gain Vertical-Component System

This is an additional data stream for 3-component, short-period signals from SKM-3 seismometers on low-gain with a vertical-component high-gain recording. Signals are recorded on channels 1, 3 and 4, for low-gain vertical-, NS-, and EW-component, respectively.

Figure 13 shows all 64 fap files available for the KODM system. These fap files are not associated with any events or specific time periods. 32 fap files do not cover notch filter bands and cover insufficient frequency band, and we selected 32 fap files that cover complete frequency bands between 0.05 and 10 Hz. The selected fap response files are plotted in Figure 14 and are used to determine the nominal response of each channel.

Figure 15 shows averaged frequency-amplitude calibration curves for low-gain vertical-component (SLZ), NS-component (SLN), and EW-component (SLE) as well as a high-gain vertical-component channel. Seven to nine calibration curves were available for each channel and the averaged values at each frequency are plotted with their standard deviation. The gains of each channel are obtained by averaging values from seven to nine calibration curves and the peak amplitude at 1.8 Hz are listed in Table 8.

Table 8: Instrument Characteristics and Gains of the KOD System at Borovoye$^{(*)}$

System	Seismometer	T_0 (s)	D_s	Channel name	Gain (counts/μm)	fn$^{(1)}$ (Hz)	Chan no.	Time period
KODB	SKM-3	3.5	0.7	SHZ	3,385.7 ± 277.0	1.8	1	67-02-26
				SHN	2,939.8 ± 342.8	1.8	3	–73-10-26
				SHE	3,353.6 ± 233.8	1.8	4	
				SLZb	423.4 ± 35.9	1.8	2	
KODM	SKM-3	3.5	0.7	SLZ	421.3 ± 33.8	1.8	1	67-06-29
				SLN	321.4 ± 31.3	1.8	3	–73-10-26
				SLE	371.1 ± 30.7	1.8	4	
				SHZm	3,385.7 ± 277.0	1.8	2	

$^{(1)}$ fn = Normalization frequency where gain (=sensitivity) is measured.

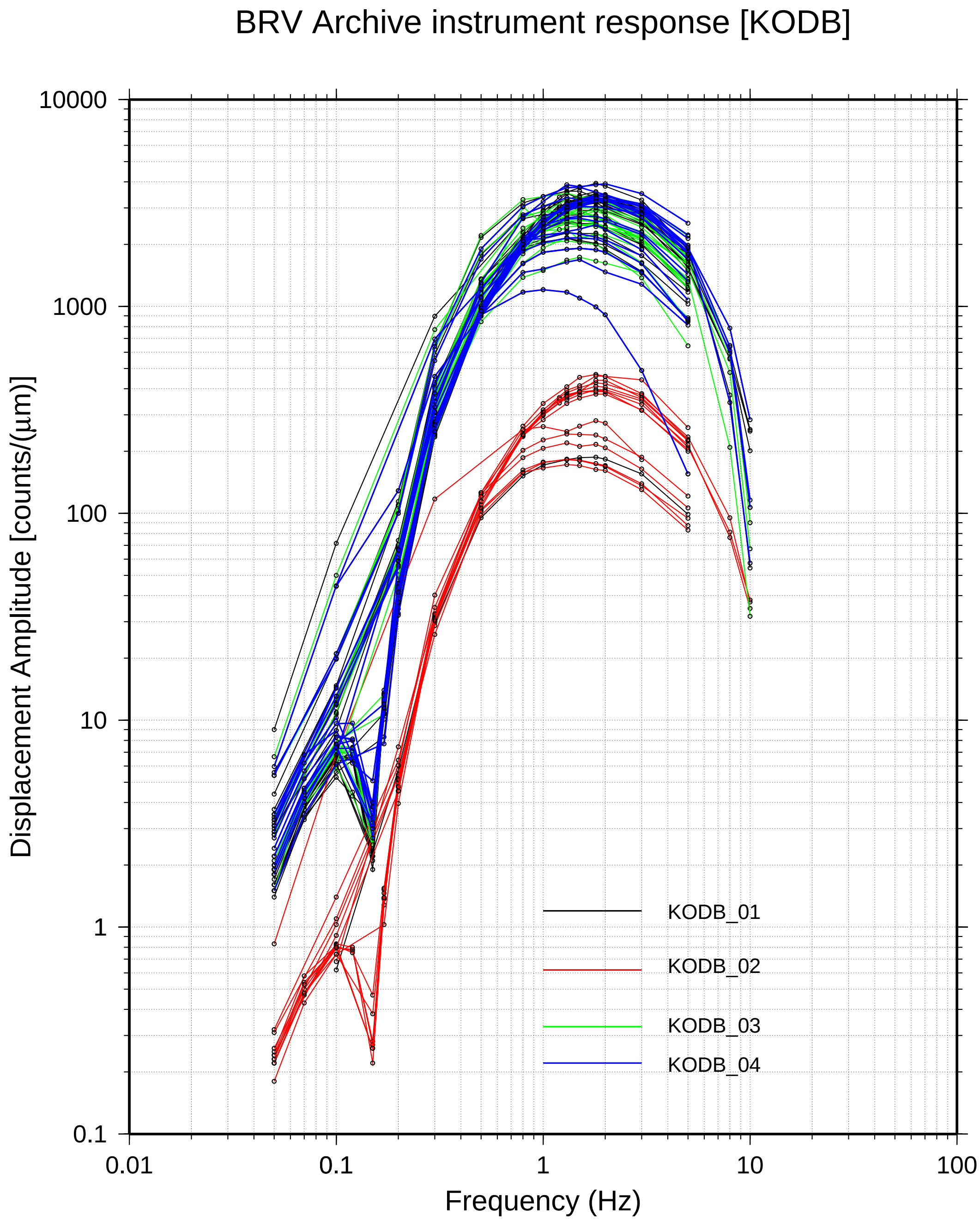

Figure 6: 78 frequency-amplitude calibration curves of the KODB system during 1967–1973.

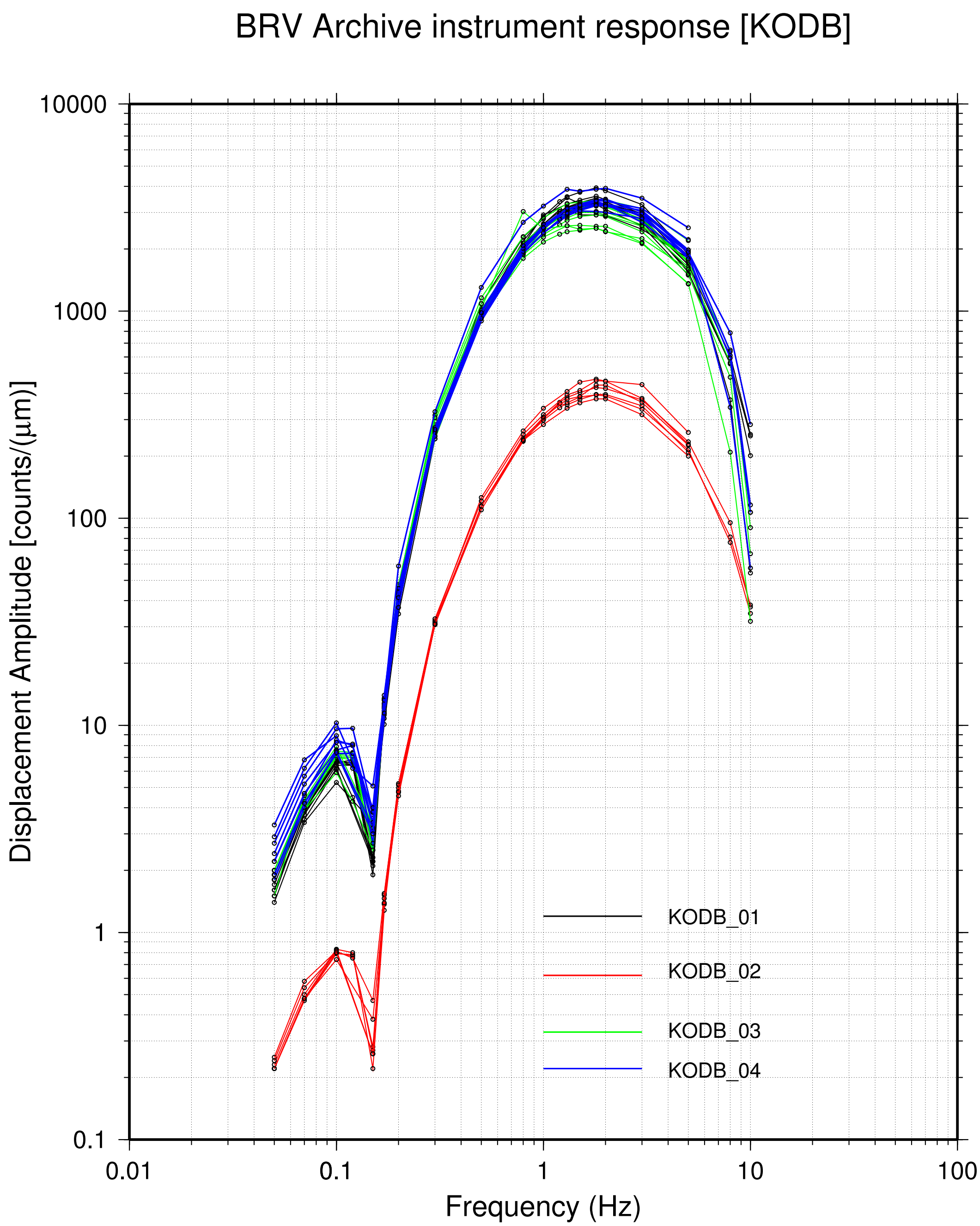

Figure 7: 34 selected frequency-amplitude calibration curves of the KODB system during 1967–1973.

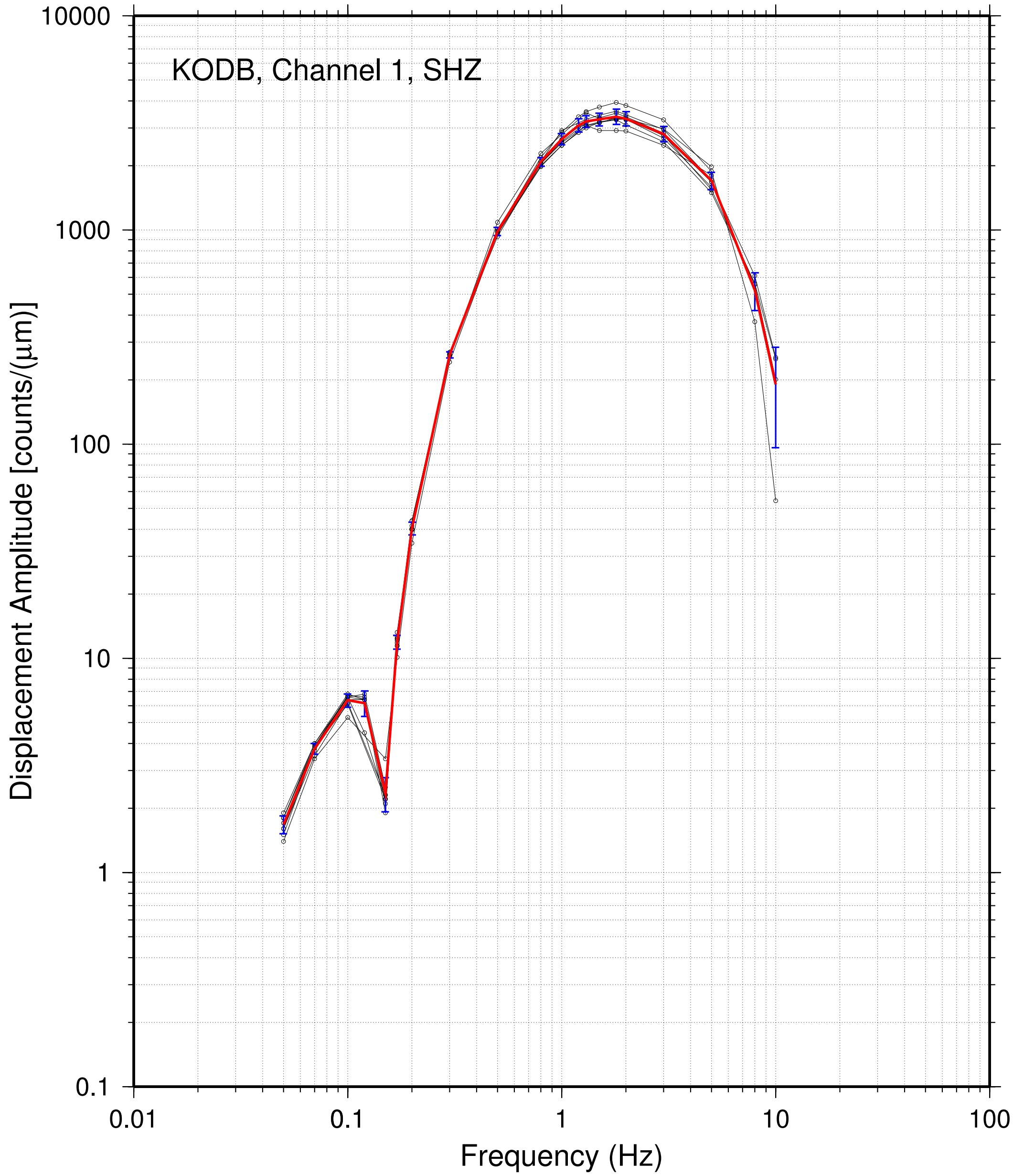

Figure 8: Frequency-amplitude calibration curves of short-period, vertical-component (channel #1, SHZ) of KODB system during 1967–1973. The averaged values at each frequency are plotted with their standard deviations.

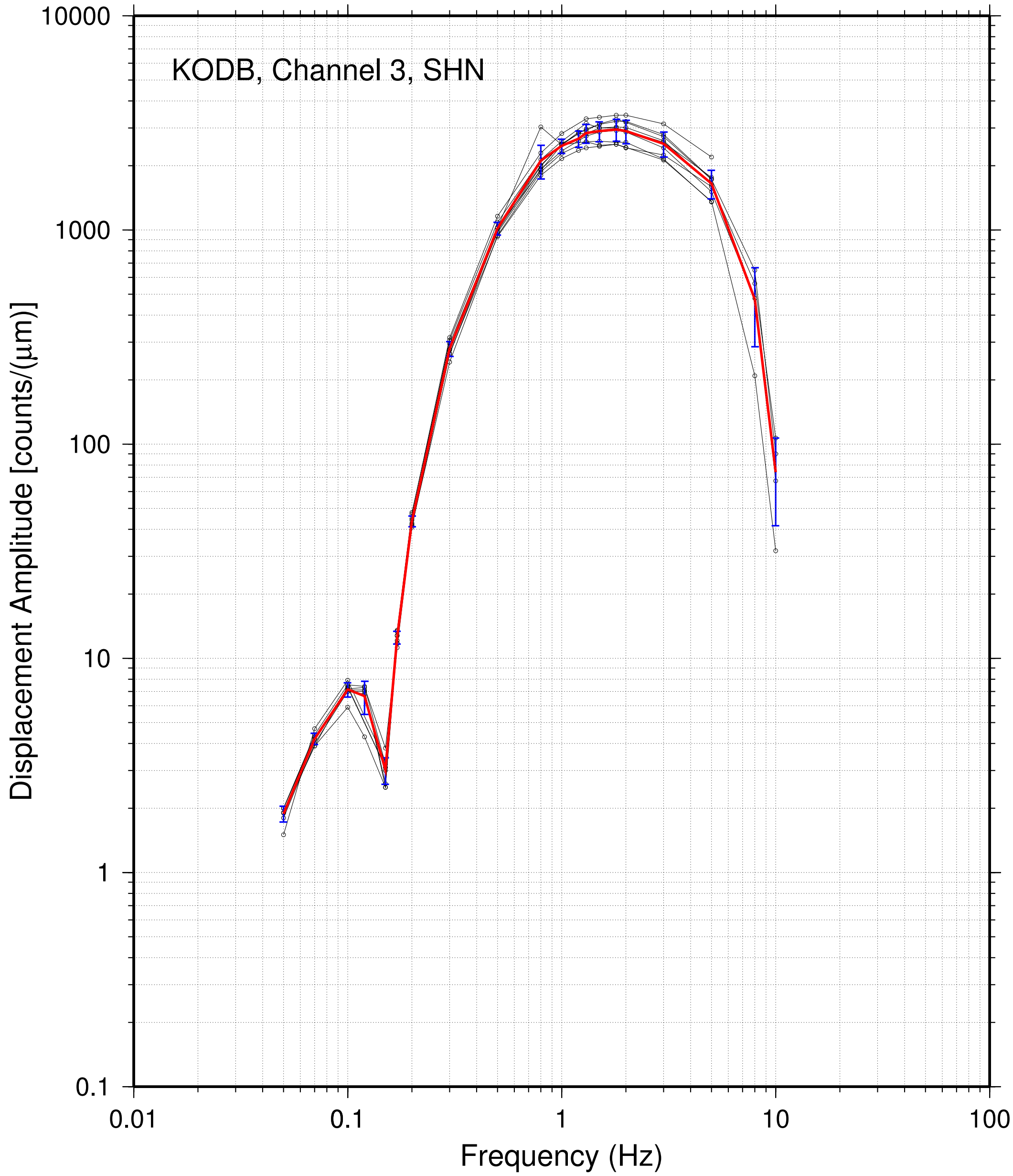

Figure 9: Frequency-amplitude calibration curves of short-period, NS-component (channel #3, SHN) of KODB system during 1967–1973. The averaged values at each frequency are plotted with their standard deviations.

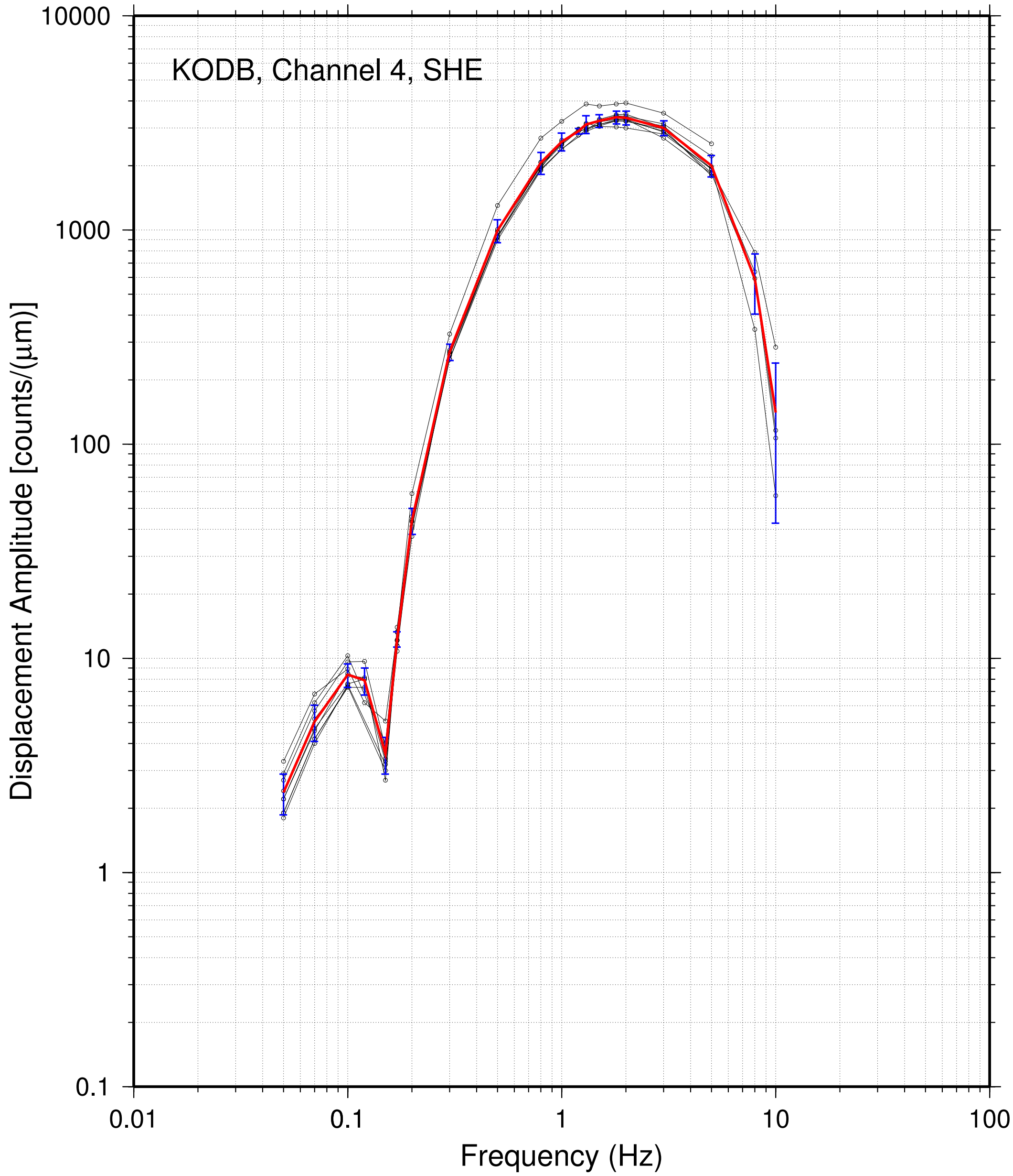

Figure 10: Frequency-amplitude calibration curves of short-period, EW-component (channel #4, SHE) of KODB system during 1967–1973. The averaged values at each frequency are plotted with their standard deviations.

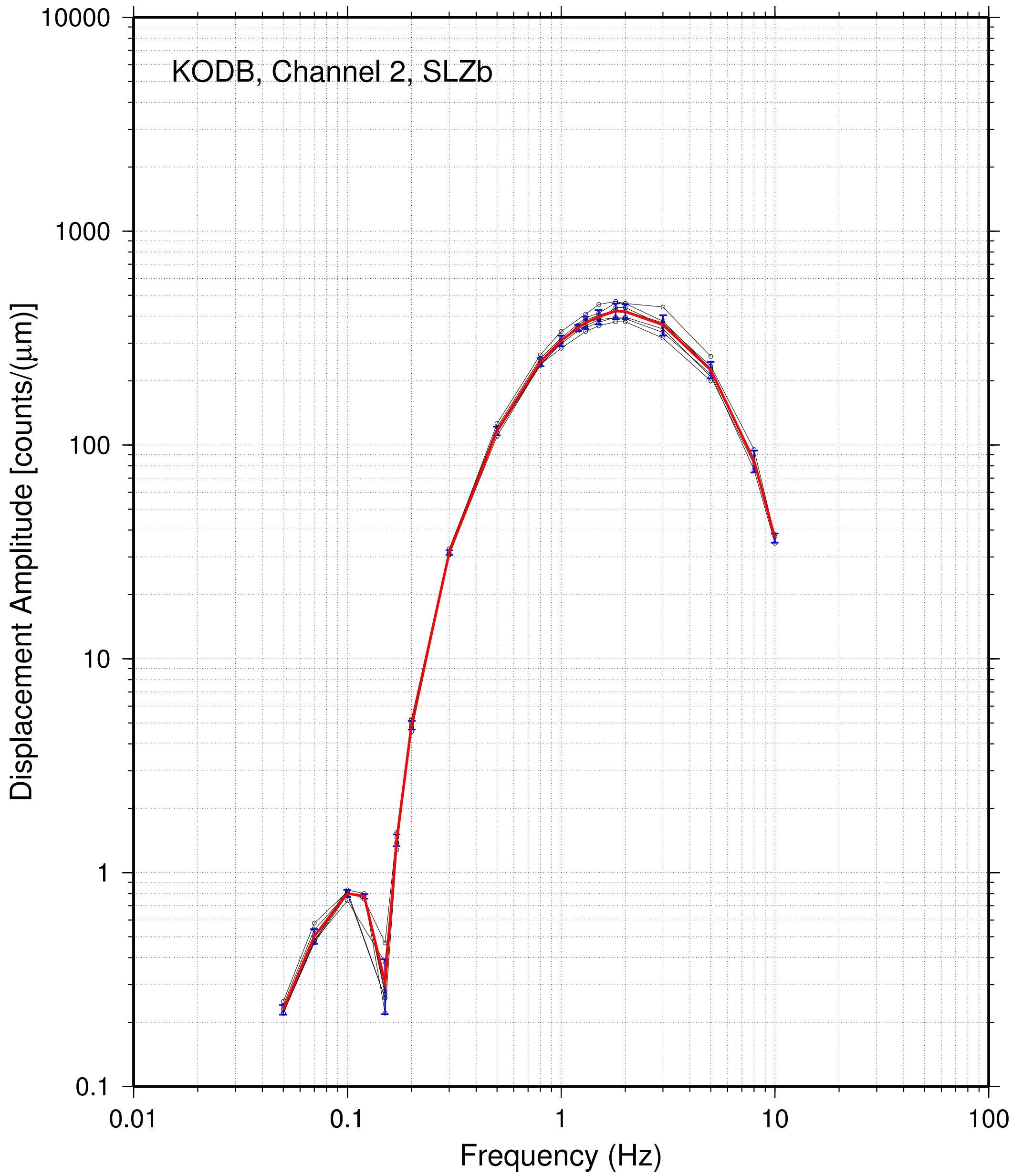

Figure 11: Frequency-amplitude calibration curves of short-period, low-gain vertical-component (channel #2, SLZb) of KODB system during 1967–1973. The averaged values at each frequency are plotted with their standard deviations.

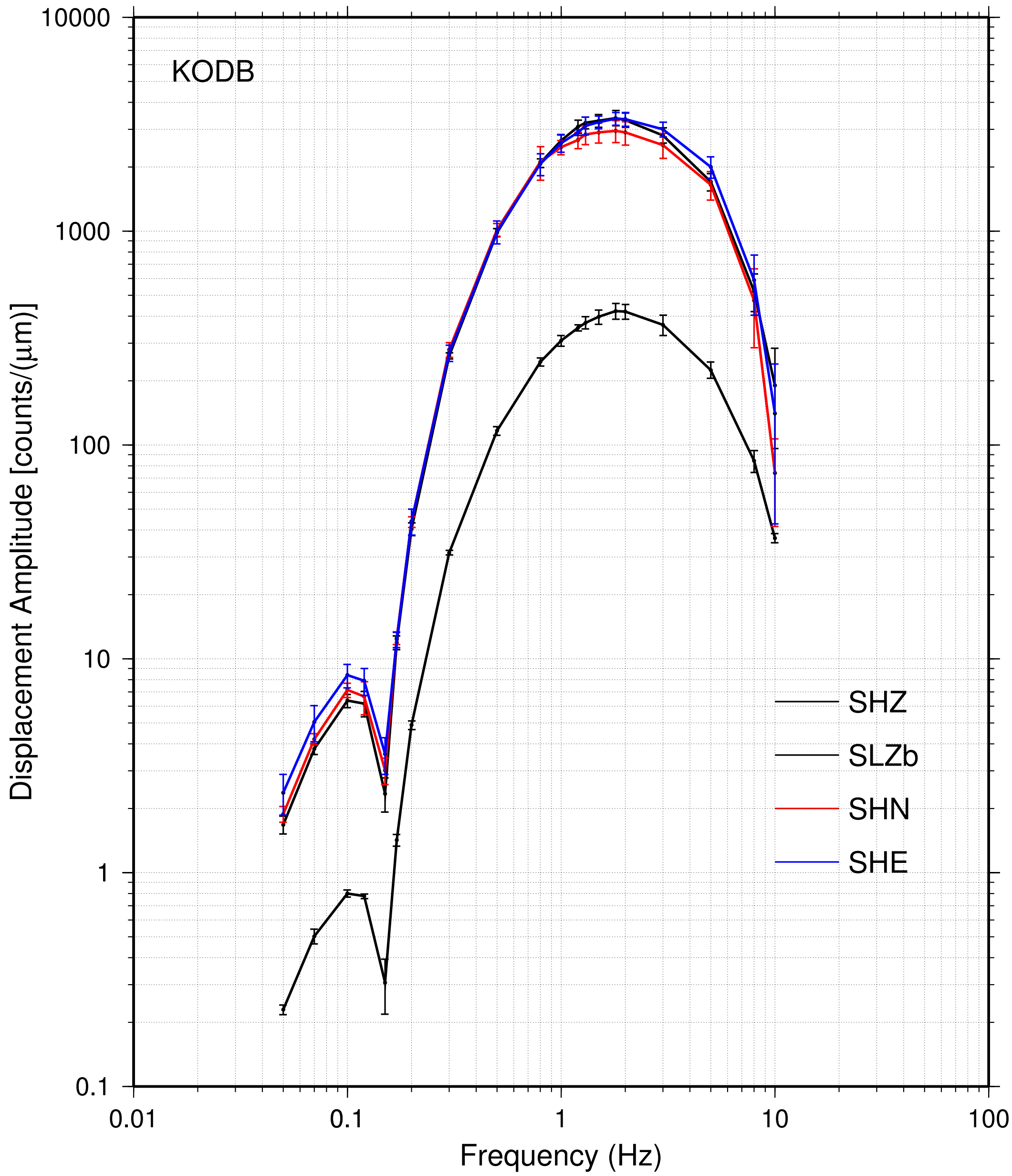

Figure 12: Averaged frequency-amplitude calibration curves of the high-gain vertical-, NS- and EW-component as well as the low-gain vertical-component channels of the KODB system are plotted.

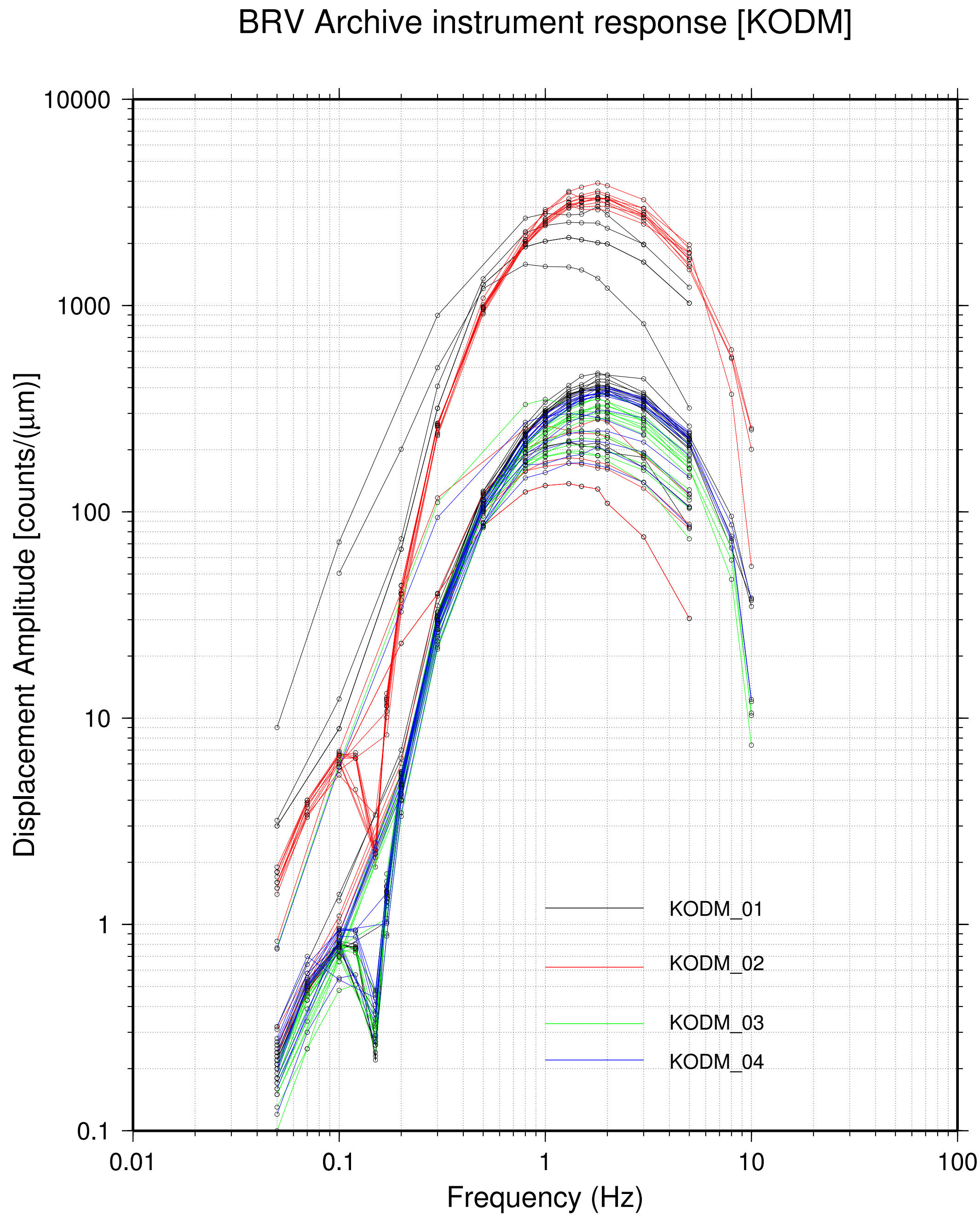

Figure 13: 64 frequency-amplitude calibration curves of the KODM system during 1967–1973.

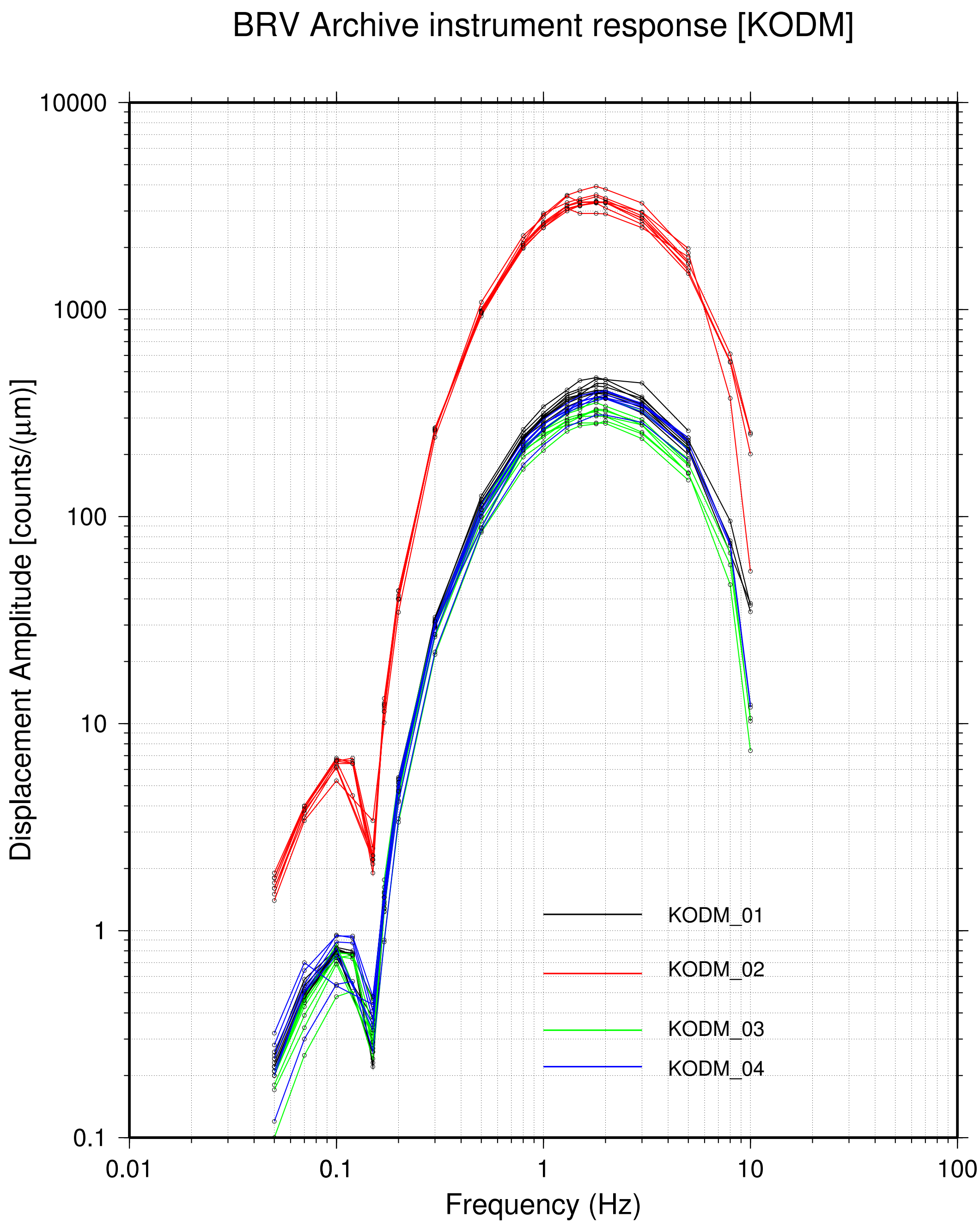

Figure 14: 32 selected frequency-amplitude calibration curves of the KODM system during 1967–1973.

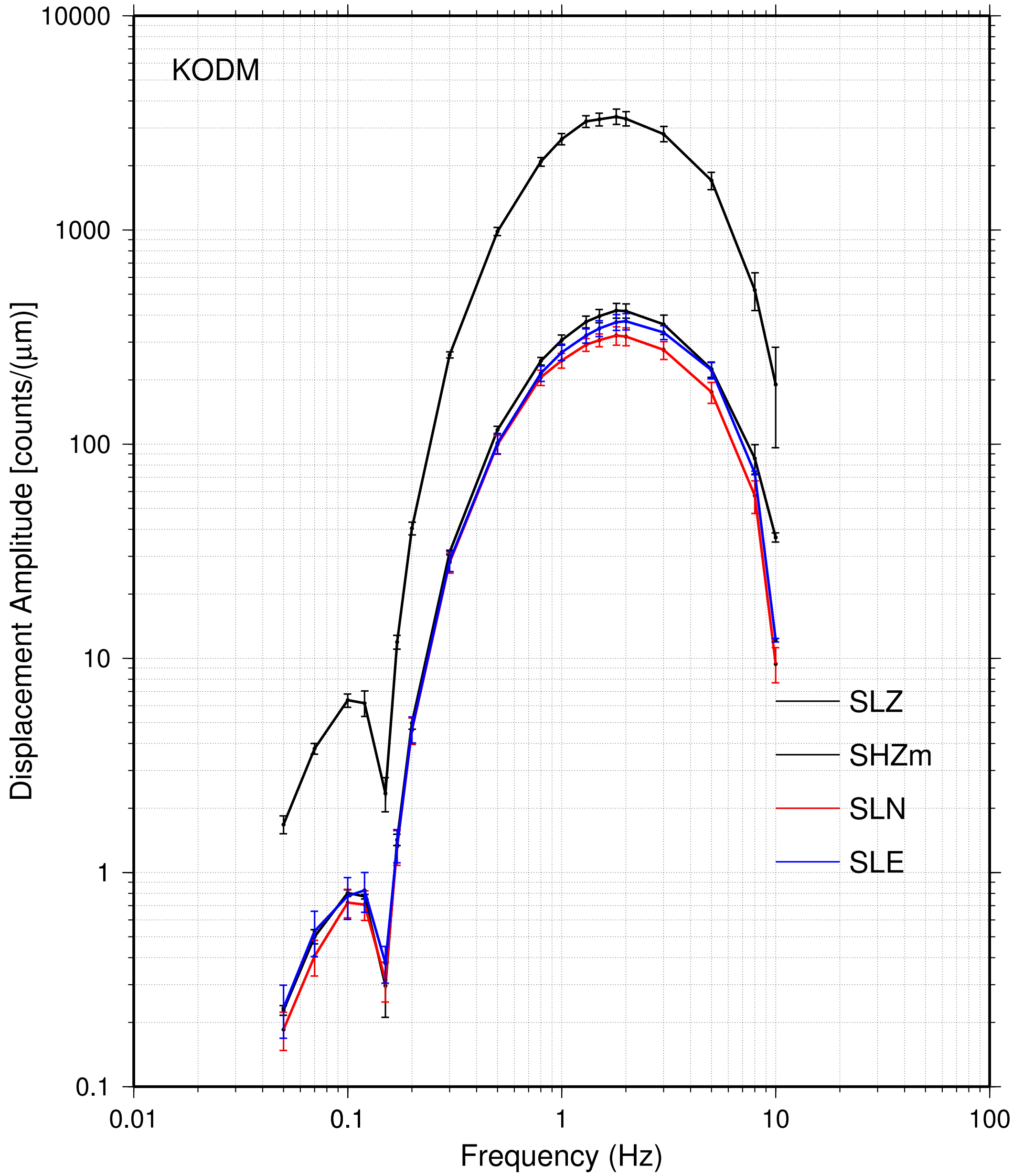

Figure 15: Averaged frequency-amplitude calibration curves of low-gain vertical-, NS- and EW-component as well as the high-gain vertical-component channels of the KODM system are plotted.

Instrument Response of KOD System

The KODB (high-gain channels) and KODM (low-gain channels) systems at Borovoye consist of SKM-3 short-period seismometers, a notch filter with notch at 0.145 Hz ($\sim$ 6.9 s period), and low-pass RC filter (Shishkevish, 1975). We fit the observed frequency-amplitude calibration curves with additional component such as, a first order RC high-pass filter with cutoff at 0.06 Hz, a first order RC high-pass filter with cutoff at 0.7 Hz, 2nd order Butterworth low-pass filter with cutoff at 3.0 Hz and a 2nd order Butterworth low-pass filter with cutoff at 8 Hz. The instrument response can be represented by 10 complex poles and 6 complex zeros as listed in Table 9. A comparison between the observed frequency-amplitude calibration curve and theoretical amplitude response calculated using these poles and zeros is shown in Figure 16. This is the most used channel due to its unclipped waveform traces produced by low-gain setting of 423.3 $\pm$ 35.9 counts/μm at 1.8 Hz.

Table 9: Instrument Constants of SKM-3 high-gain, KODB and low-gain, KODM Seismographs, 1967–1973

<table>
<tr><th>Component</th><th>Z-component (SHZ)</th><th>NS-component (SHN)</th><th>EW-component (SHE)</th></tr>
<tr><td>SKM-3
Seismometer
T_0=3.5s, D_S=0.5</td><td colspan="3">two poles (-1.269395, 1.269395), (1.269395, -1.269395)
two zeros at origin (0.00, 0.00), (0.00, 0.00)</td></tr>
<tr><td>Notch filter with
notch at 0.145 Hz</td><td colspan="3">two poles (-7.172775, 0.00), (-0.115720, 0.00)
two zeros (-0.0364424, 0.910333), (-0.0364424, -0.910333)</td></tr>
<tr><td>1st order high-pass
filter cutoff 0.06 Hz</td><td colspan="3">(-0.3769910, 0.00)
a zero at origin (0.00, 0.00)</td></tr>
<tr><td>1st order high-pass
filter cutoff 0.7 Hz</td><td colspan="3">(-4.398230, 0.00)
a zero at origin (0.00, 0.00)</td></tr>
<tr><td>2nd order Butterworth
low-pass filter</td><td colspan="3">(-13.3286, 13.3286), (-13.3286, -13.3286)
cutoff frequency at 3 Hz</td></tr>
<tr><td>2nd order Butterworth
low-pass filter</td><td colspan="3">(-35.5431, 35.5431), (-35.5431, -35.5431)
cutoff frequency at 8 Hz</td></tr>
</table>

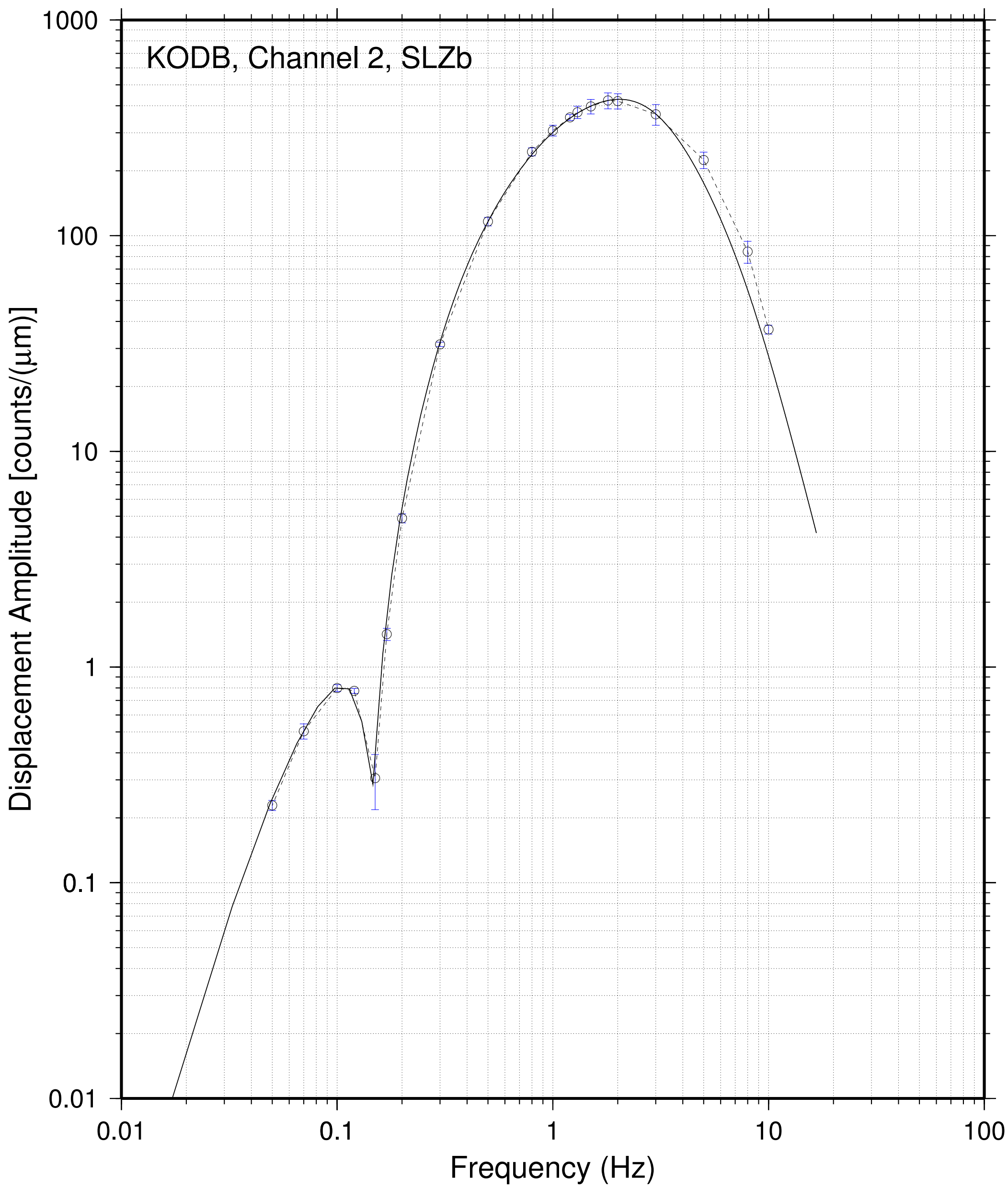

Figure 16: Frequency-amplitude calibration curve of the low-gain, short-period vertical-component channel (SLZb) during 1967–1973 is compared with the theoretical amplitude response curve obtained by using the instrument response listed in Table 9.

3.3 The STsR-SS Digital Seismograph System

The STsR-SS system consists of a 3-component, short-period seismometer – SKM-3 (Kirnos high-gain) and a 3-component, extended-period seismometer – SKD (Kirnos-Arkhangel'skiy broadband) (Shishkevish, 1974). The STsR-SS system recorded a total of 10 channels on 17-track tape with 11-bit analog-to-digital conversion. Usually, the data streams consisted of signals from 3-component short-period, 3-component extended-period, and a low-gain short-period vertical-component. Shishkevish (1974) called the SKD seismometer with the natural period, T_0=25 s, as *extended-period* seismometer and we will adopt this term throughout this report. SKM-3 seismometer is the later model of SKM seismometer and has adjustable natural period, T_0, between 1.5 to 3.5 s (Shishkevish, 1974). Hence, it is also called short-to-intermediate-period high-gain seismometer. We will call it a high-gain *short-period* seismometer throughout this report.

During 1973-06-06 – 1981-06-30, 3-component short-period signals from SKM-3 seismometer were recorded on channels 7, 8 and 9 for vertical-, NS-, and EW-component, respectively. These three-component data are assigned with component names s07Z, s08N and s09E; low-gain vertical-component SKM-3 data is recorded on channel 1 (s01Z); 3-component extended-period signals from SKD seismometer are recorded on channels 2, 3, and 4 (l02Z, l03N and l04E); and channels 5, 6 and 10 were unused.

During 1981-08-14 – 1982-07-04, 3-component short-period signals from SKM-3 seismometer were recorded on channels 7, 8 and 9 for vertical-, NS-, and EW-component, respectively. The sampling interval for these channels were changed from 0.032 s to 0.024 s. The low-gain vertical-component SKM-3 data is recorded on channel 6 (s06Z) with a sampling interval of 0.096 s. 3-component extended-period signals from SKD seismometer are recorded on channels 2, 3, and 4 (l02Z, l03N and l04E); and channels 1, 5 and 10 were unused. Although the sampling intervals have changed for short-period channels (6, 7, 8, and 9), the shapes of the amplitude responses for these channels followed the previous period.

During 1982-08-23 – 1991-07-15, 3-component short-period signals from SKM-3 seismometer were recorded on channels 7, 8 and 9 (component name: s07Z, s08N and s09E); low-gain vertical-component signals from the SKM-3 seismometer were recorded on channel 6 (s06Z); 3-component extended-period signals from SKD seismometer are recorded on channels 2, 3, and 4 (l02Z, l03N and l04E); and low-gain 3-component extended-period SKD data were recorded on channels 1, 5 and 10 (l01Z, l05N and l10E); hence all of the 10 channels of the STsR-SS system were utilized during this period (see Table 19). The shapes of the amplitude responses for all channels have changed from the previous periods.

Figure 17 show 40 available frequency-amplitude calibration curves for STsR-SS system given in the Borovoye waveform data archive.

SKM-3 High-gain Short-period Seismometer

1) Channels 7, 8 and 9 (s07Z, s08N and s09E; 1973–1982-07-04)

This is the main data stream for 3-component, short-period signals from the SKM-3 seismometer in the SS system. Signals are recorded on channels 7, 8 and 9, for vertical-, NS-, and EW-component, respectively. According to Adushkin & An (1990), these channels had the

nominal gains of 2,000 counts/μm and recorded with sampling interval of 24 msec during their operation. However, the waveform data and frequency-amplitude calibration curves given in the Borovoye waveform data archive indicate that there must have been at least two different instrument responses used for the 3-component short-period data from the SKM-3 seismometer. It is apparent that the sampling interval of these channels changed around August 04, 1981, and the instrument response of these channels changed around August 21, 1982.

During 1973–1981-06-30, these channels were recorded with the sampling interval of 32 msec and the gain at 2 Hz as listed in Table 10. The sampling interval of these channels changed to 24 msec around August 14, 1981, but the shapes of the amplitude responses for these channels remained the same.

Frequency-amplitude calibration curves during 1973-03-07–1982-07-04 are plotted in Figure 18.

Table 10: Gains at 2 Hz for Channels 7, 8 and 9 during 1973-1982

Time period	Z, s07Z (counts/μm)	NS, s08N (counts/μm)	EW, s09E (counts/μm)	sampling interval (msec)
1973-06-06–1973-09-27	1249	1330	1336	32
1973-10-27 07:04 (1.5 Hz)	75.3	73.4	75.4	32
1974-07-10–1979-06-28	1249	1330	1336	32
1979-07-07–1981-06-30	1489	1378	1416	32
1981-08-14 02:26	814	744	800	24
1981-09-13–1982-07-04	1301	1278	1263	24

Instrument Response: Poles and Zeros

The SKM-3 seismometer used in the STsR-SS system has natural period, T_0=2.0 s, and damping constant, D_s=0.5 (Table 19 and Adushkin & An, 1990). However, very little is known about its recording system and use of filters such as the anti-alias filters. For the STsR-SS system, we did not find any calibration pulse that can be used to determine instrument constants as shown by Kim & Ekström (1996) for STsR-TSG system. Examining the calibration curves plotted in Figure 18, we construct a preliminary instrument response consisting of a SKM-3 seismometer, a 2nd order RC (resistor capacitor) high-pass filter with cutoff frequency at 0.5 Hz, a 2nd order Bessel low-pass filter with cutoff at 3 Hz and a 2nd order Bessel low-pass filter with cutoff frequency at 8 Hz. We fit the averaged frequency-amplitude calibration curves in the frequency domain by a trial and error method. Figure 19 shows comparison of observed frequency-amplitude calibration curves with corresponding theoretical frequency-amplitude curves obtained by using the instrument constants constrained by the trial and error fit.

The instrument constants constrained for three components are listed in Table 11 for natural period and damping constant of SKM-3 seismometers as well as the gain of channels 7, 8 and 9.

Other instrument constants are: 2nd order high-pass filter with cutoff at 0.5 Hz, a 2nd order Bessel low-pass filter with cutoff at 3 Hz and a 2nd order Bessel low-pass filter with cutoff at 7

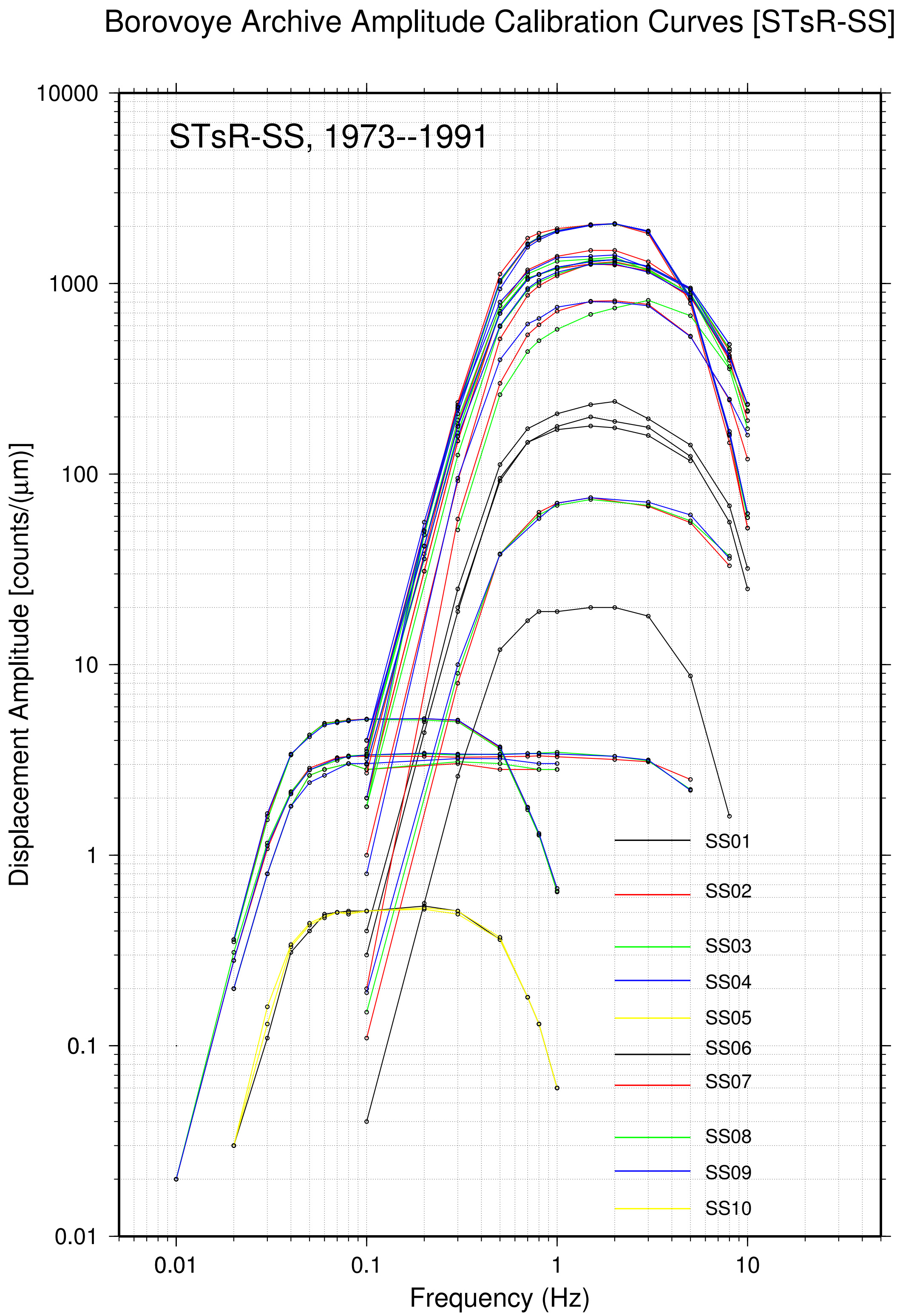

Figure 17: Frequency-amplitude calibration curves of 10-channel STsR-SS system are plotted.

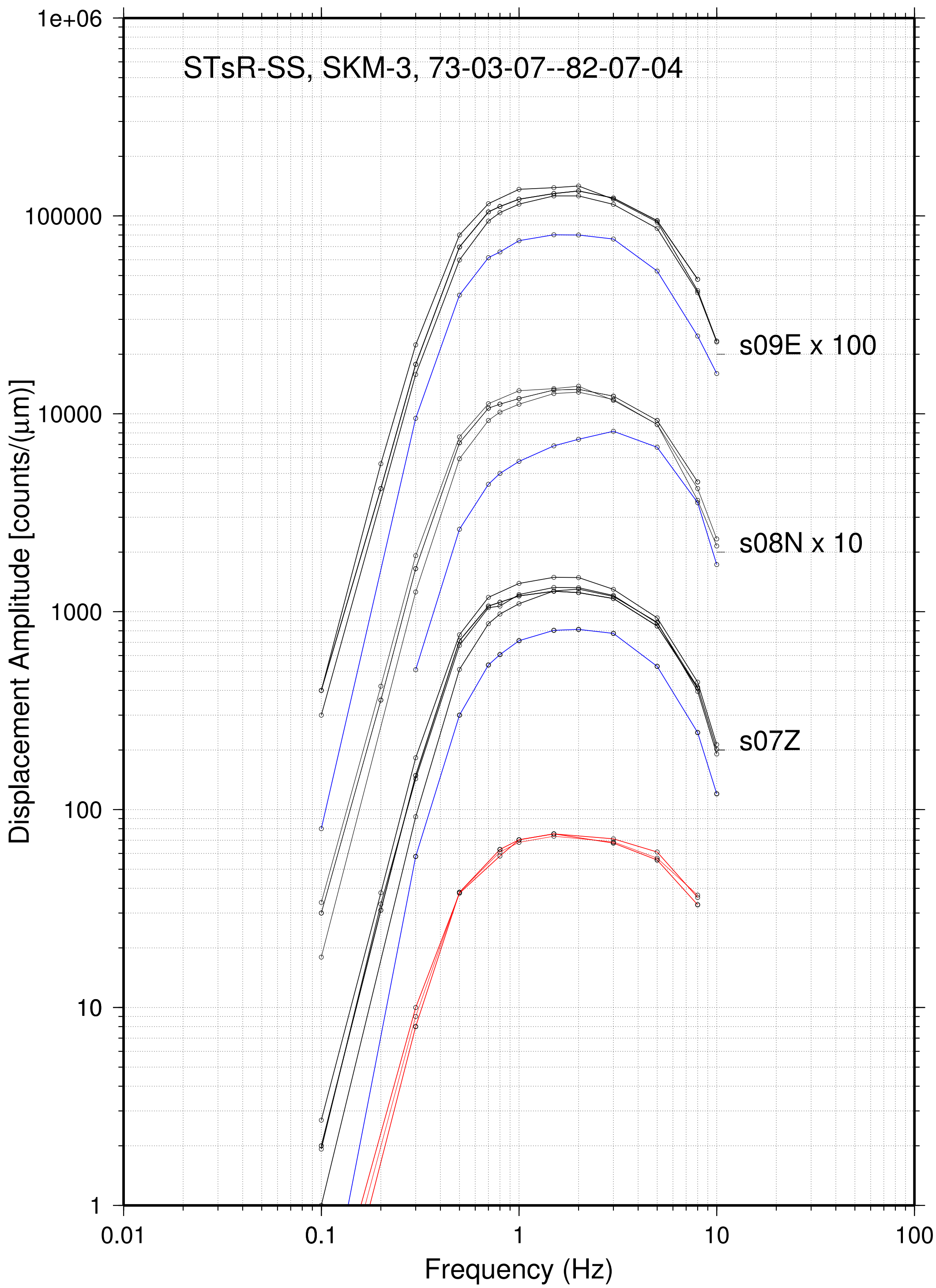

Figure 18: Frequency-amplitude calibration curves of 3-component short-period SKM-3 channels during 1973–1982. s07Z = vertical-component, s08N = NS-component, and s09E = EW-component. The curves for the NS-component are plotted with their amplitudes multiplied by 10, and EW-component are plotted by multiplying the amplitude by 100 to show the response curves separately. *Red lines* are for the curve on 1973-10-24 and *blue lines* are for the curve on 1981-08-04.

Table 11: Instrument constants of the high-gain SKM channels 7, 8 and 9, 1973–1982

Channel name	Natural period (sec)	Damping constant	Gain at 2 Hz (counts/μm)
s07Z	2.0	0.55	1249
s08N	2.2	0.55	1330
s09E	2.3	0.60	1336

Hz. Hence, the short-period high-gain channels of the SKM-3 seismometers can be represented by eight poles and four zeros as listed in Table 12. The theoretical frequency-amplitude curves in Figure 19 are calculated using poles and zeros for each component (Table 12).

Table 12: Poles and Zeros for the instrument response of the high-gain SKM channels 7, 8 and 9, 1973–1982

Component	Z-component (s07Z)	NS-component (s08N)	EW-component (s09E)
Seismometer SKM-3	(-1.72788, 2.62375) (-1.72788,-2.62375)	(-1.57080, 2.38523) (-1.57080,-2.38523)	(-1.63909, 2.18546) (-1.63909,-2.18546)
	two zeros at origin (0.0, 0.0), (0.0, 0.0)		
2nd order RC high-pass filter	(-3.14159, 0.00), (-3.14159, 0.0000) two zeros at origin (0.0, 0.0), (0.0, 0.0)		
2nd order Bessel low-pass filter	(-28.2743, -16.3242), (-28.2743, 16.3242) cutoff frequency= 3 Hz		
2nd order Bessel low-pass filter	(-65.9734, 38.0898), (-65.9734, -38.0898) cutoff frequency= 7 Hz		

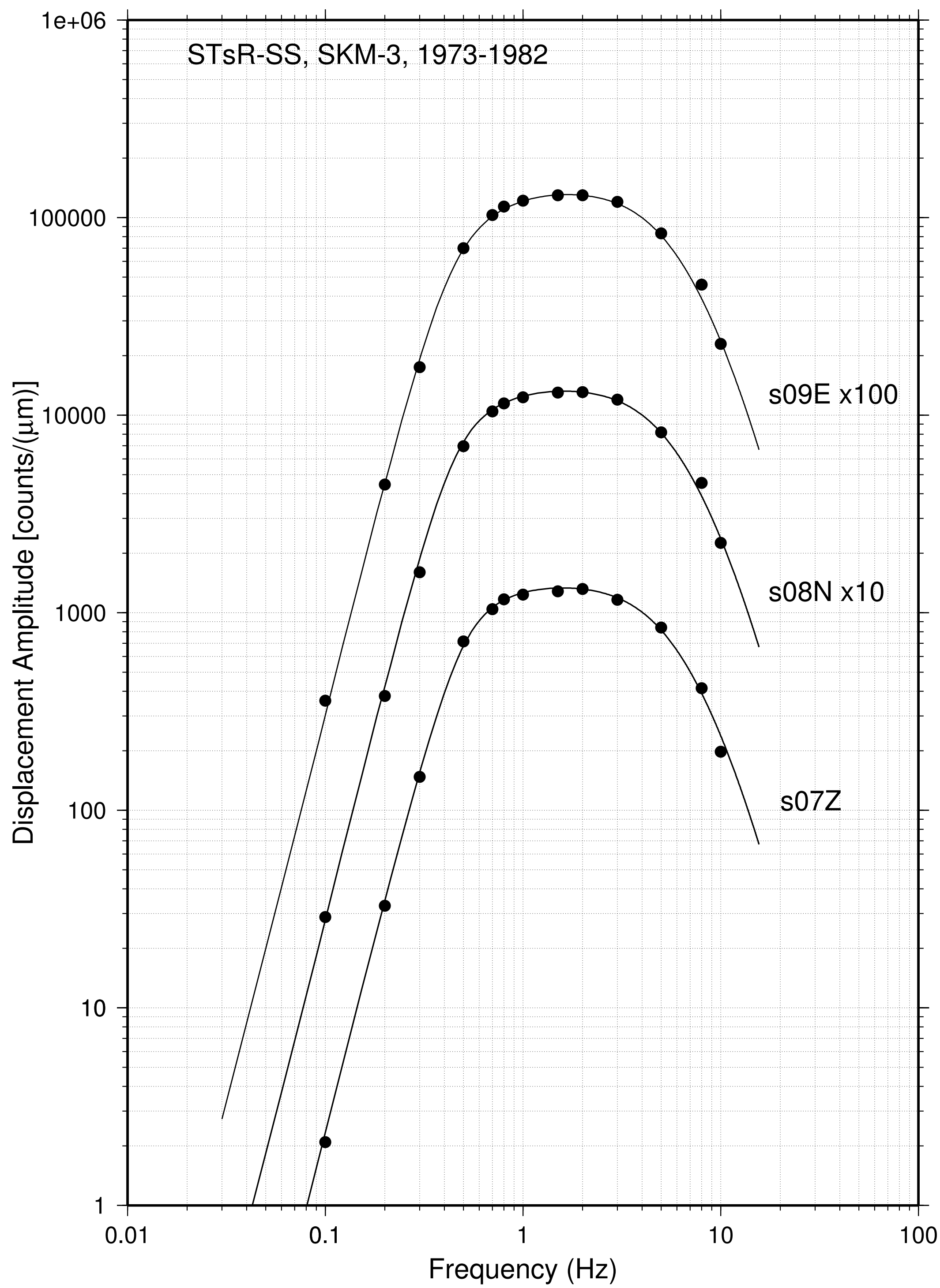

Figure 19: Comparisons of observed (*solid circles*) and theoretical (*solid lines*) frequency-amplitude curves of 3-component short-period SKM-3 channels during 1973–1982. s07Z = vertical-component, s08N = NS-component, and s09E = EW-component. The curves for the NS-component are plotted with their amplitudes multiplied by 10, and EW-component are plotted by multiplying the amplitude by 100 to show the response curves separately.

2) Channel 1 (s01Z; 1973–1981)

Channel 1 of the STsR-SS system was used to record short-period vertical-component signals from the SKM-3 seismometer during 1973–1981-01-15 with a nominal gain of 200 counts/μm at about 2 Hz (Adushkin & An, 1990). Two frequency-amplitude calibration curves are in the archive database: on 1973-04-19 and on 1979-07-02 (Table 13). Figure 20 shows the frequency-amplitude curves available for this period.

Table 13: The gain at 2 Hz for channel 1 during 1973-1981

Time period	Channel 1 (s01Z) (counts/μm)
1974-04-19–1979-06-28	175
1979-07-07–1981-01-15	241

Instrument Response: Poles and Zeros

Channel 1 of the STsR-SS system recorded vertical-component signals from the SKM-3 seismometer with a low-gain. Two frequency-amplitude curves available during 1973-1982 indicate that the channel has the same response as the high-gain vertical-component (s07Z). A comparison of observed and theoretical amplitude response curves are shown in Figure 21 (cf. Figure 19).

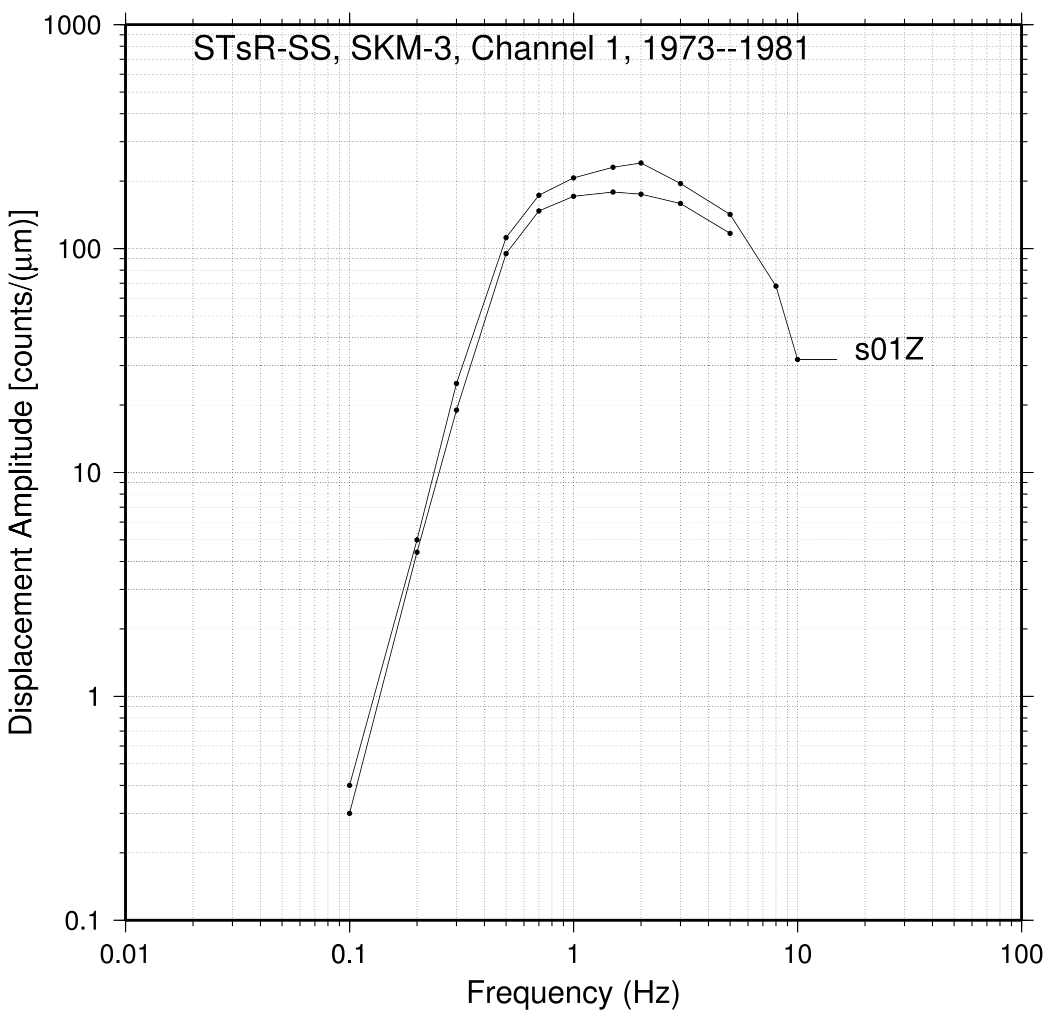

Figure 20: Two frequency-amplitude calibration curves of the low-gain, vertical-component short-period SKM-3 channel during 1973–1981. s01Z = low-gain vertical-component. The curves are similar to those of channel 7 (s07Z) except the gain.

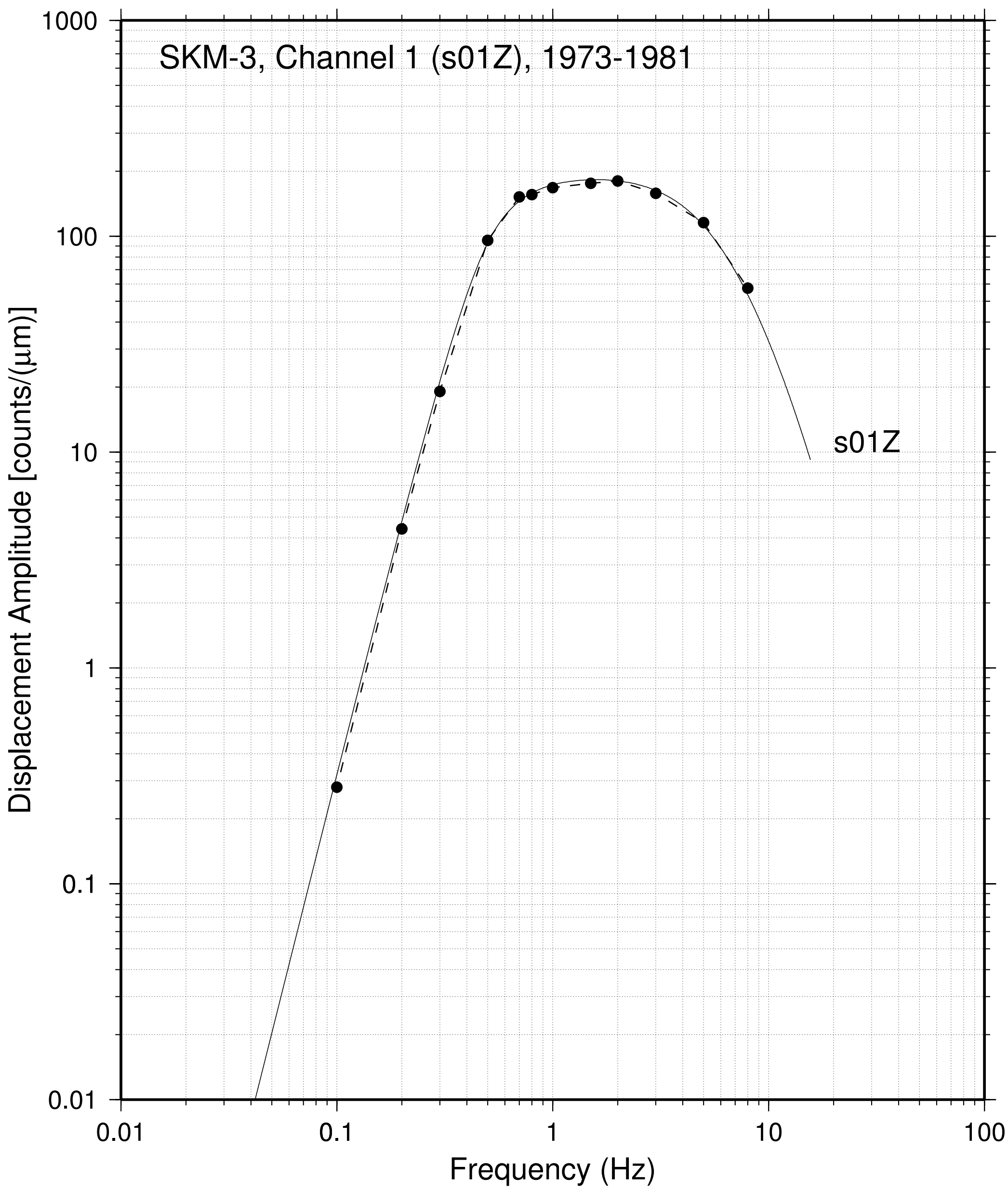

Figure 21: Comparisons of observed (*solid circles* with *dashed line*) and theoretical (*solid line*) frequency-amplitude curves of low-gain vertical-component short-period SKM-3 channel (s01Z) during 1973–1981-01-15.

3) Channels 7, 8 and 9 (s07Z, s08N and s09E; 1982–1991)

This is the main data stream for 3-component, short-period signals from the SKM-3 seismometers of the STsR-SS system during 1982–1991. Signals are recorded on channels 7, 8 and 9, for vertical-, NS-, and EW-component, respectively as before, but recorded with a sampling interval of 24 msec. The instrument characteristics and parameters reported in Adushkin & An (1990) for SKM-3 refer to this period.

Two frequency-amplitude calibration curves during 1982-08-21–1991-07-15 for these channels plotted in Figure 22 indicate that the gains are 2,059, 2,054 and 2,057 counts/μm at 2 Hz for vertical-, NS-, and EW-component, respectively for most of this period (Table 14).

Table 14: The gains at 2 Hz for channels 7, 8 and 9 during 1982-1991

Time period	Channel 7 (s07Z) (counts/μm)	Channel 8 (s08N) (counts/μm)	Channel 9 (s09E) (counts/μm)
1982-08-23–1985-06-30	2048	2067	2067
1985-07-20–1991-07-15	2059	2054	2057

Instrument Response: Poles and Zeros

The SKM-3 seismometer used in the STsR-SS system has natural period, T_0=2.0 s, and damping constant, D_s=0.5 (Table 19 and Adushkin & An, 1990). However, very little is known about its recording system and use of filters such as an anti-alias filter.

Comparing the calibration curves plotted in Figures 18 and 22 for 1973–1982 and 1982–1991, respectively, it is obvious that the amplitude response of the SKM-3 data stream has changed. The sampling interval is reduced to 0.024 s from 0.032 s, and the amplitude fall off at frequencies higher than 3 Hz is very significant – from about -20 dB to -40 dB. Perhaps, it may have been realized that the data stream from SKM-3 seismometer during 1973–1982 were somewhat aliased, due to insufficient amplitude attenuation at high frequencies prior to digitization with the Nyquist frequency=15.6 Hz. The amplitude responses at low frequencies – 0.1 – 3 Hz, are nearly identical for both periods (Figure 23).

The amplitude response for the 1982–1991 period must be the same as those during 1973-1982 at frequencies below 3 Hz, and we add a 4th order Butterworth low-pass filter with cutoff at 4 Hz to fit the amplitude response. We constrained instrument parameters by fitting the averaged frequency-amplitude calibration curves in the frequency domain by trial and error. Figure 24 shows comparison of observed frequency-amplitude calibration curves with corresponding theoretical frequency-amplitude curves obtained by using the instrument constants constrained by trial and error: seismometer with T_0=2.0 s and damping constant, D_s=0.5, 2nd order RC high-pass filter with cutoff at 0.5 Hz, and 4th order Butterworth low-pass filter with cutoff at 4 Hz. The instrument response of these channels can be represented by eight poles and four zeros as given in Table 15.

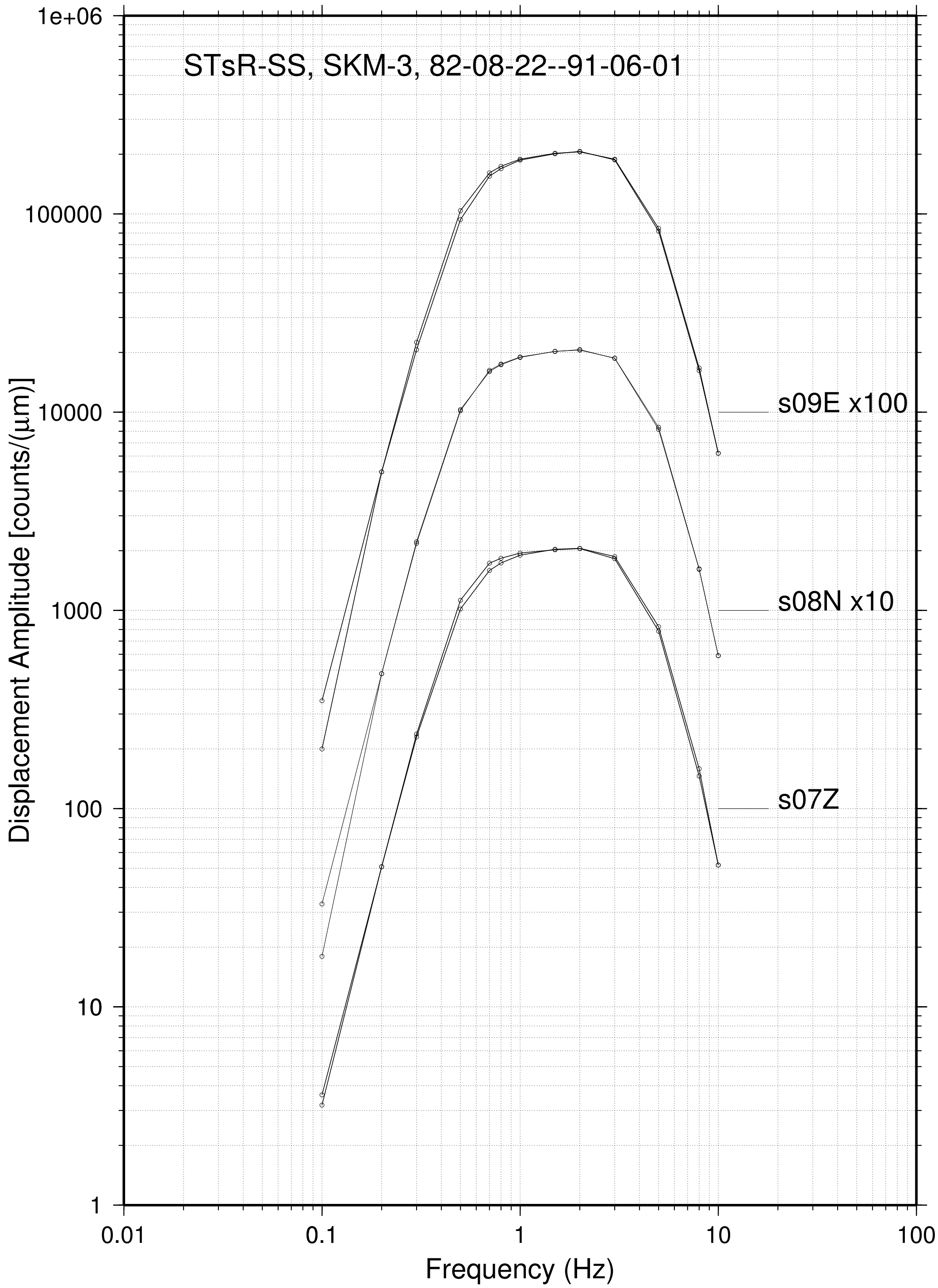

Figure 22: Frequency-amplitude calibration curves of 3-component short-period SKM-3 channels during 1982–1991. s07Z = vertical-component, s08N = NS-component, and s09E = EW-component. The curves for the NS-component are plotted with their amplitudes multiplied by 10, and EW-component are plotted by multiplying the amplitude by 100 to show the response curves separately.

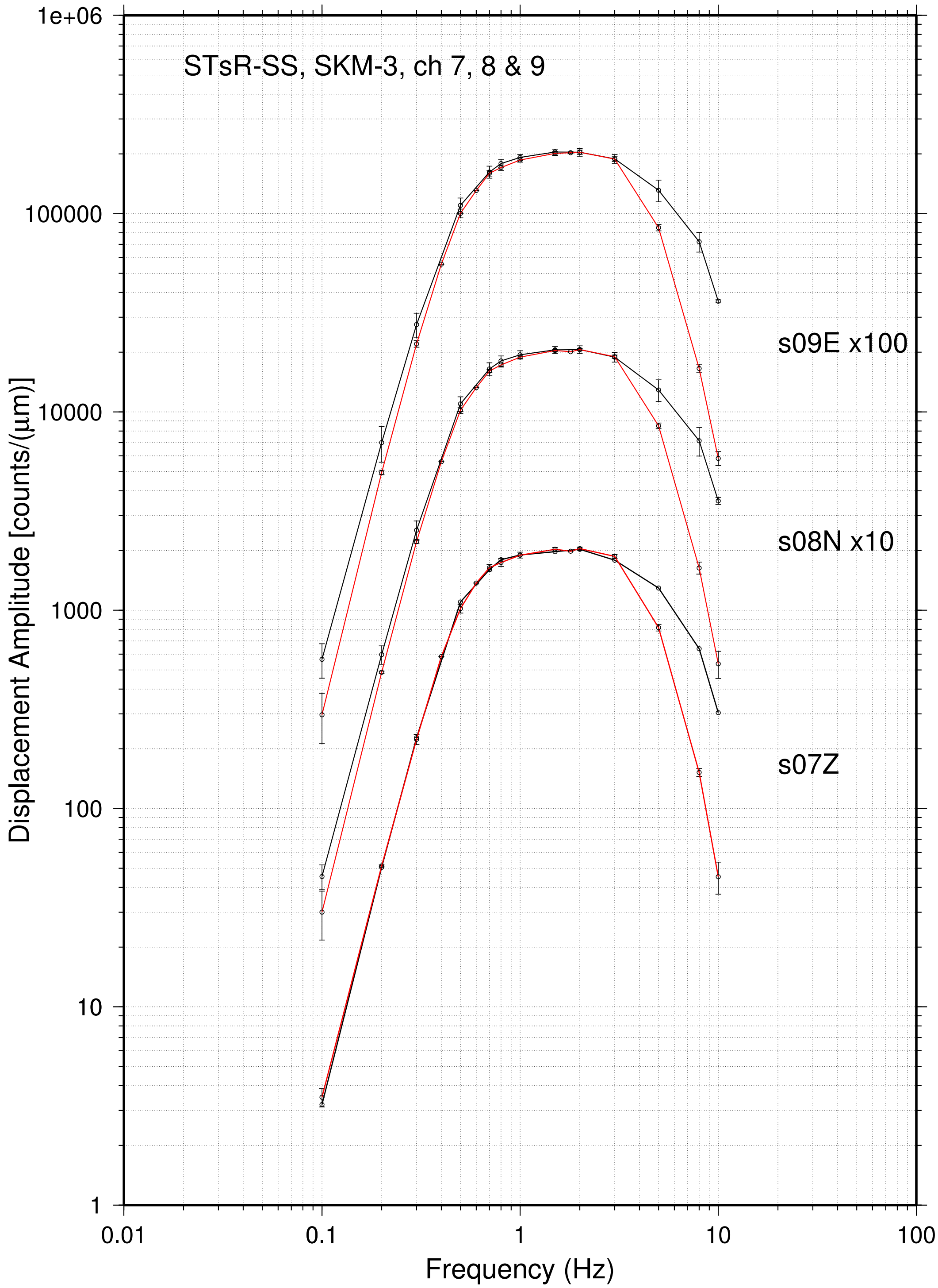

Figure 23: Comparison of frequency-amplitude calibration curves of 3-component short-period SKM-3 channels during 1973–1982 (*solid lines*) and 1982–1991 (*red lines*). Amplitude responses are nearly identical at frequencies up to 3 Hz for both periods. s07Z = vertical-component, s08N = NS-component, and s09E = EW-component. The curves for the NS-component are plotted with their amplitudes multiplied by 10, and EW-component are plotted by multiplying the amplitude by 100 to show the response curves separately.

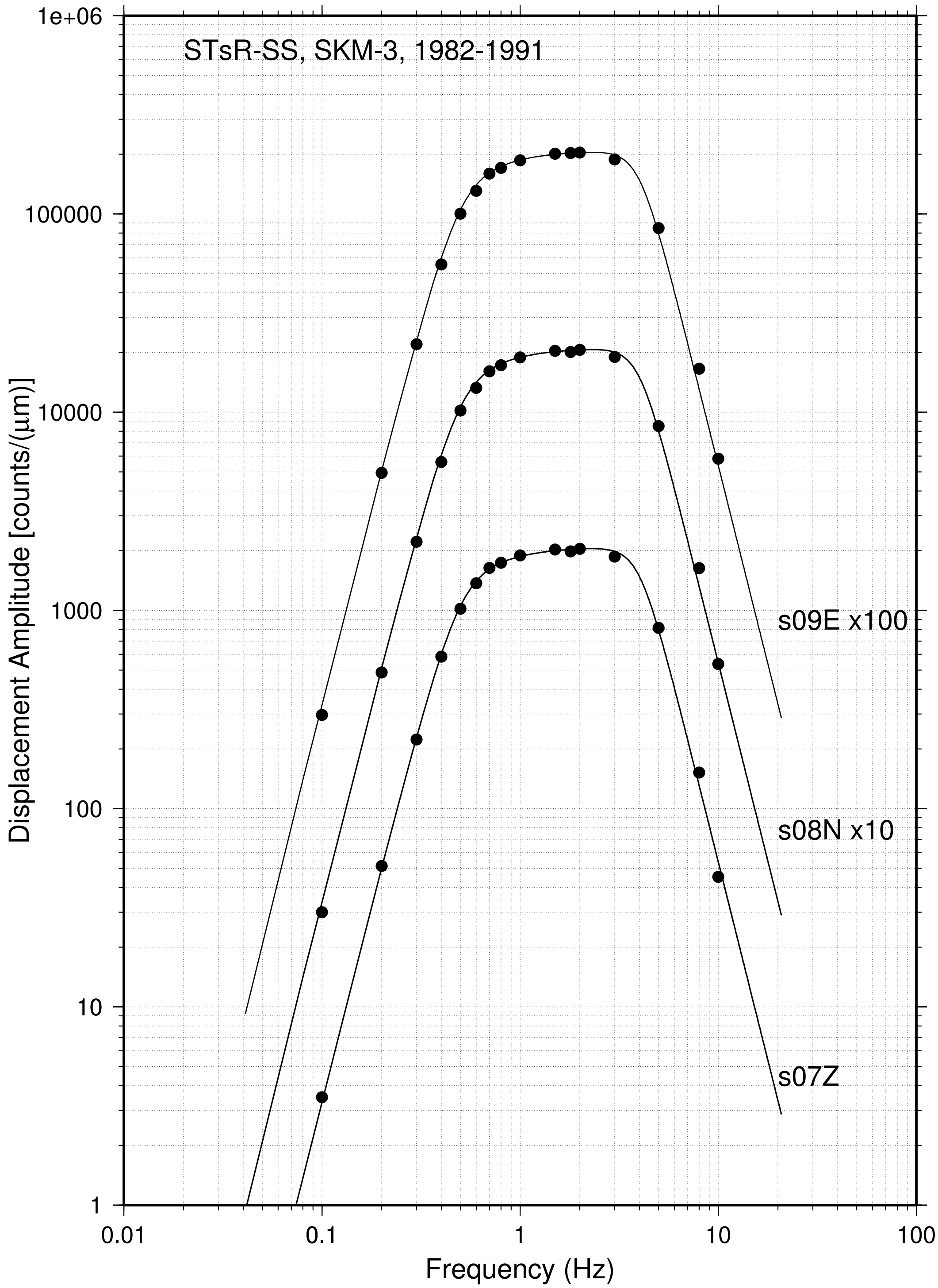

Figure 24: Comparisons of observed (*solid circles*) and theoretical (*solid lines*) frequency-amplitude curves of 3-component short-period SKM-3 channels during 1982–1989. s07Z = vertical-component, s08N = NS-component, and s09E = EW-component. The curves for the NS-component are plotted with their amplitudes multiplied by 10, and EW-component are plotted by multiplying the amplitude by 100 to show the response curves separately.

Table 15: Instrument constants of the high-gain SKM channels 7, 8 and 9, 1982–1991

Component	Z-component (s07Z)	NS-component (s08N)	EW-component (s09E)
Seismometer SKM-3	(-1.57080, 2.72070), (-1.57080, -2.72070) two zeros at origin (0.00, 0.00), (0.00, 0.00)		
2nd order RC high-pass filter	(-3.14159, 0.00), (-3.14159, 0.00) two zeros at origin (0.00, 0.00), (0.00, 0.00)		
4th order Butterworth low-pass filter	(-9.617798, 23.21964), (-9.617798, -23.21964) (-23.21964, 9.617798), (-23.21964, -9.617798) cutoff frequency= 4 Hz		

4) Channel 6 (s06Z; 1981-08-14–1991-07-15)

Short-period vertical-component signals from SKM-3 seismometer are recorded as low-gain on channel 6 with the gain of 20 counts/μm at 2 Hz and the sampling interval of 96 msec during 1981–1991. Figure 25 shows a frequency-amplitude curve on 1982-08-21. Notice that the frequency-amplitude curve is given up to 8 Hz, which is inconsistent with the sampling interval of 0.096 s with its Nyquist frequency of 5.2 Hz.

The instrument response of the channel 6 during 1981-08-04–1982-07-04 is the same as channel 1 during 1973-1981 shown in Figure 21.

Instrument Response: Poles and Zeros

This is the same data stream from the SKM-3 vertical-component but with low-gain recording. Figure 26 shows comparison of observed frequency-amplitude calibration curves with corresponding theoretical amplitude response calculated by using the instrument constants identical to high-gain vertical component s07Z shown in Figure 24. Notice that if this amplitude response is used as indicated by the available frequency-amplitude curves, then it may suggest that there must be some aliasing of signals with frequencies higher than 5.2 Hz into the lower frequencies due to insufficient anti-aliasing filters applied prior to the digitization.

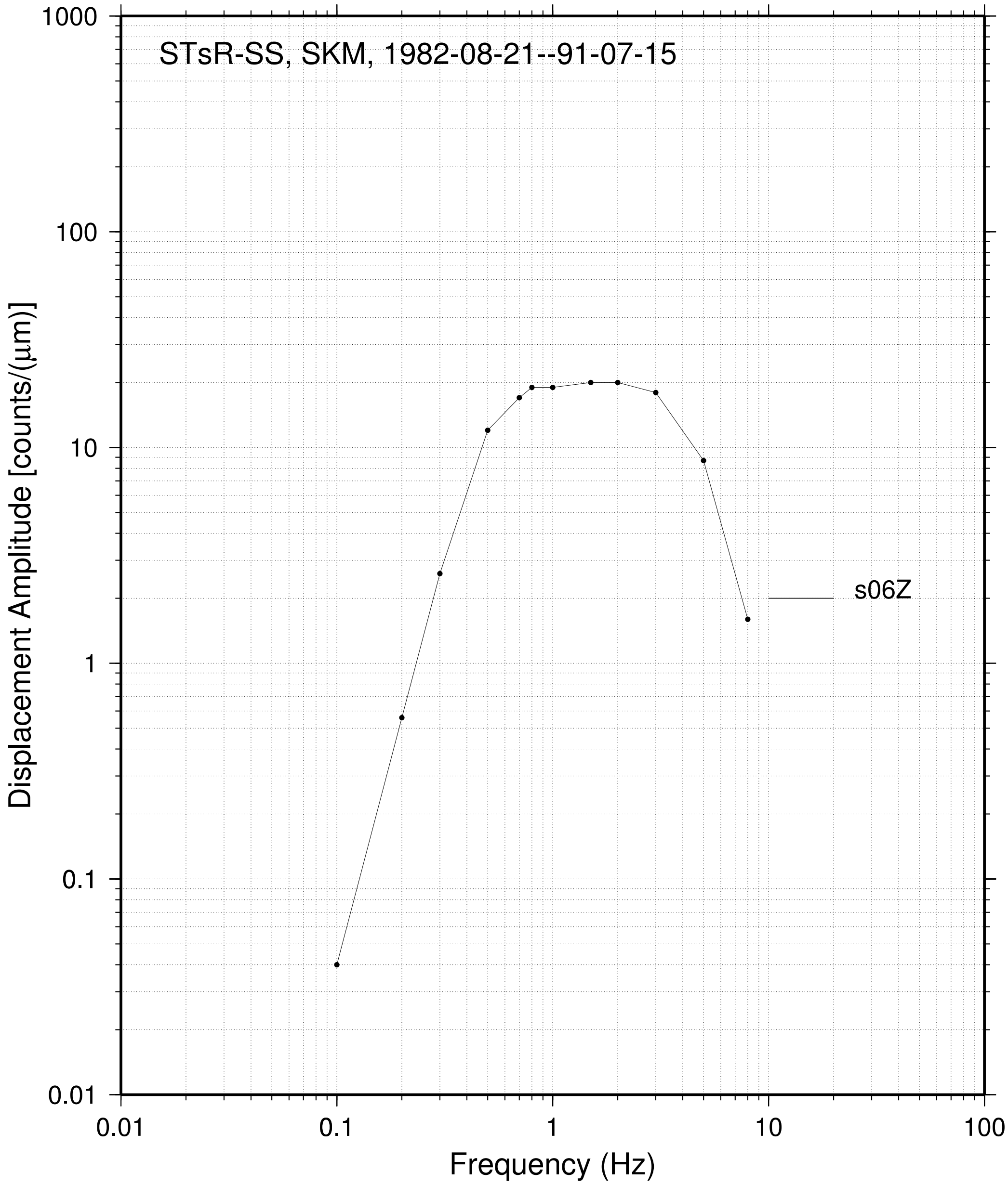

Figure 25: A frequency-amplitude calibration curve of vertical-component, low-gain short-period SKM-3 channels during 1981–1991. s06Z = low-gain vertical-component. The curve is similar to those of channel 7 (s07Z) shown in Figure 22 except the gain.

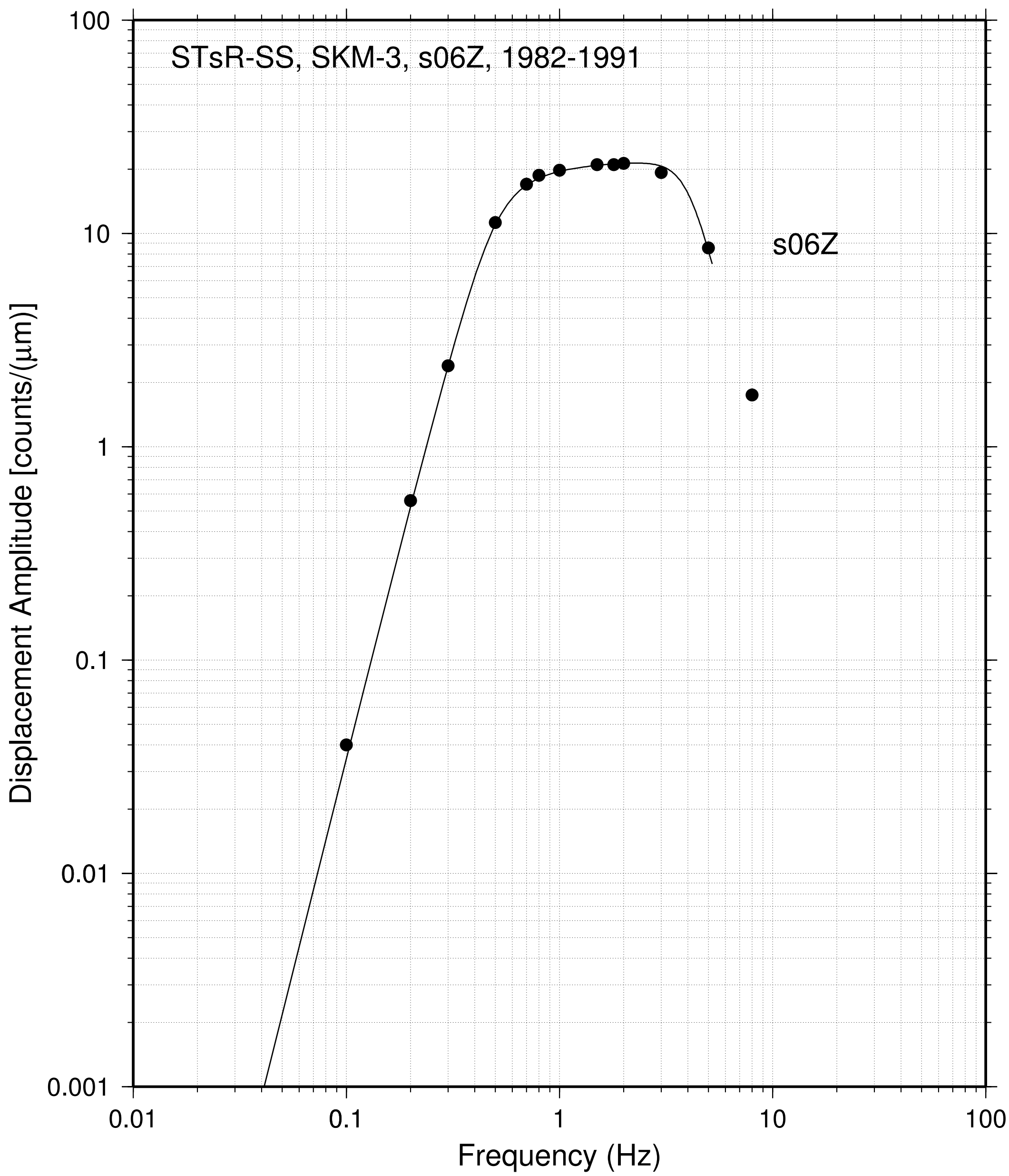

Figure 26: Comparisons of observed (*solid circles* with *dashed line*) and theoretical (*solid line*) frequency-amplitude curves of low-gain vertical-component short-period SKM-3 channels (s06Z) during 1982–1991.

SKD Extended-period Seismometer

1) Channel 2, 3 and 4 (l02Z, l03N, l04E; 1973–1982)

This is the main data stream for 3-component, extended-period SKD seismometers of the STsR-SS system. Signals are recorded on channels 2, 3 and 4, for vertical-, NS-, and EW-component, respectively. The channel names are assigned as l02Z, l03N and l04E for vertical-, NS-, and EW-component, respectively. Although Adushkin & An (1990) reported that these channels had the nominal gains of 5 counts/μm and recorded with a sampling interval of 0.192 s during their operation, the waveform data and frequency-amplitude calibration curves available indicate that there must have been at least two different instrument responses as in the case of 3-component short-period SKM-3 data.

During 1973–1981-06-30, the gains of these channels were 3.31, 3.36 and 3.36 counts/μm at 0.1 Hz for vertical-, NS-, and EW-component, respectively, which is given by a frequency-amplitude calibration curve oon 1973-03-17 as shown in Figure 27.

It is noted that these frequency-amplitude curves plotted in Figure 27 are not consistent with the system configuration, that is, the Nyquist frequency of the extended-period channels is 2.60 Hz (for 0.192 sec sampling interval), and hence, the frequency-amplitude curve on 1973-03-17 that listed amplitude beyond 3 Hz must be incorrect. These frequency-amplitude curves seem to lack anti-alias filter component prior to digitizing.

Instrument Response: Poles and Zeros

Two available frequency-amplitude calibration curves during this period for the channels 2, 3 and 4 are inconsistent with the data stream with sampling interval of 0.192 sec. The frequency-amplitude calibration curves covering 1973–1982 and for frequency band 0.02 and 1 Hz are plotted in Figure 28 and are compared with the amplitude response calculated with the instrument response for 1982–1991.

The amplitude response and the calibration curves are fairly well fit in the frequency band from 0.02 to 0.2 Hz. Hence, the instrument response for these channels may be the same as those of the later years.

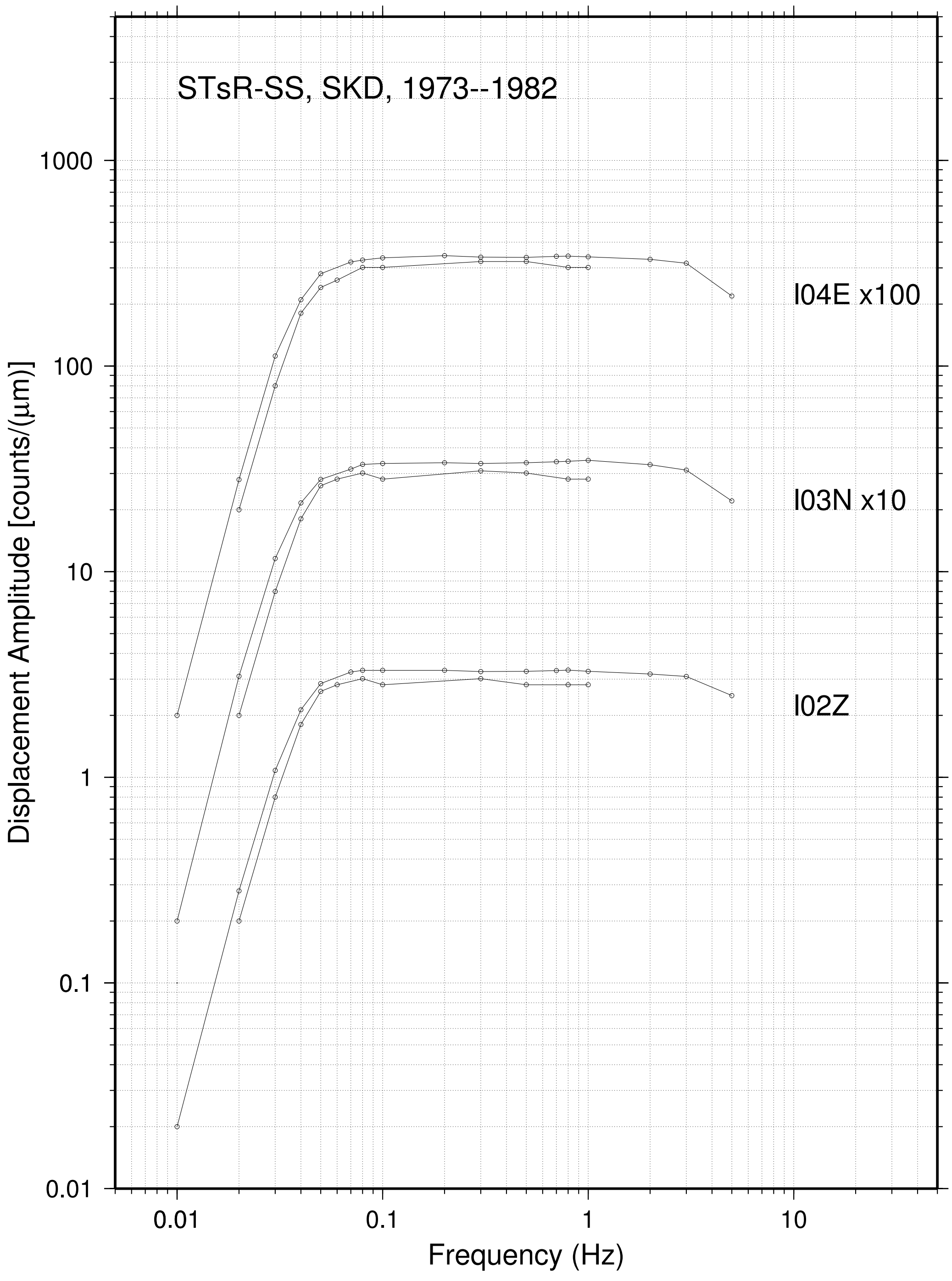

Figure 27: Frequency-amplitude calibration curves of 3-component extended-period SKD channels during 1973–1982. l02Z = vertical-component, l03N = NS-component, and l04E = EW-component. The curves for the NS-component are plotted with their amplitudes multiplied by 10, and EW-component are plotted by multiplying the amplitudes by 100 to show the response curves separately.

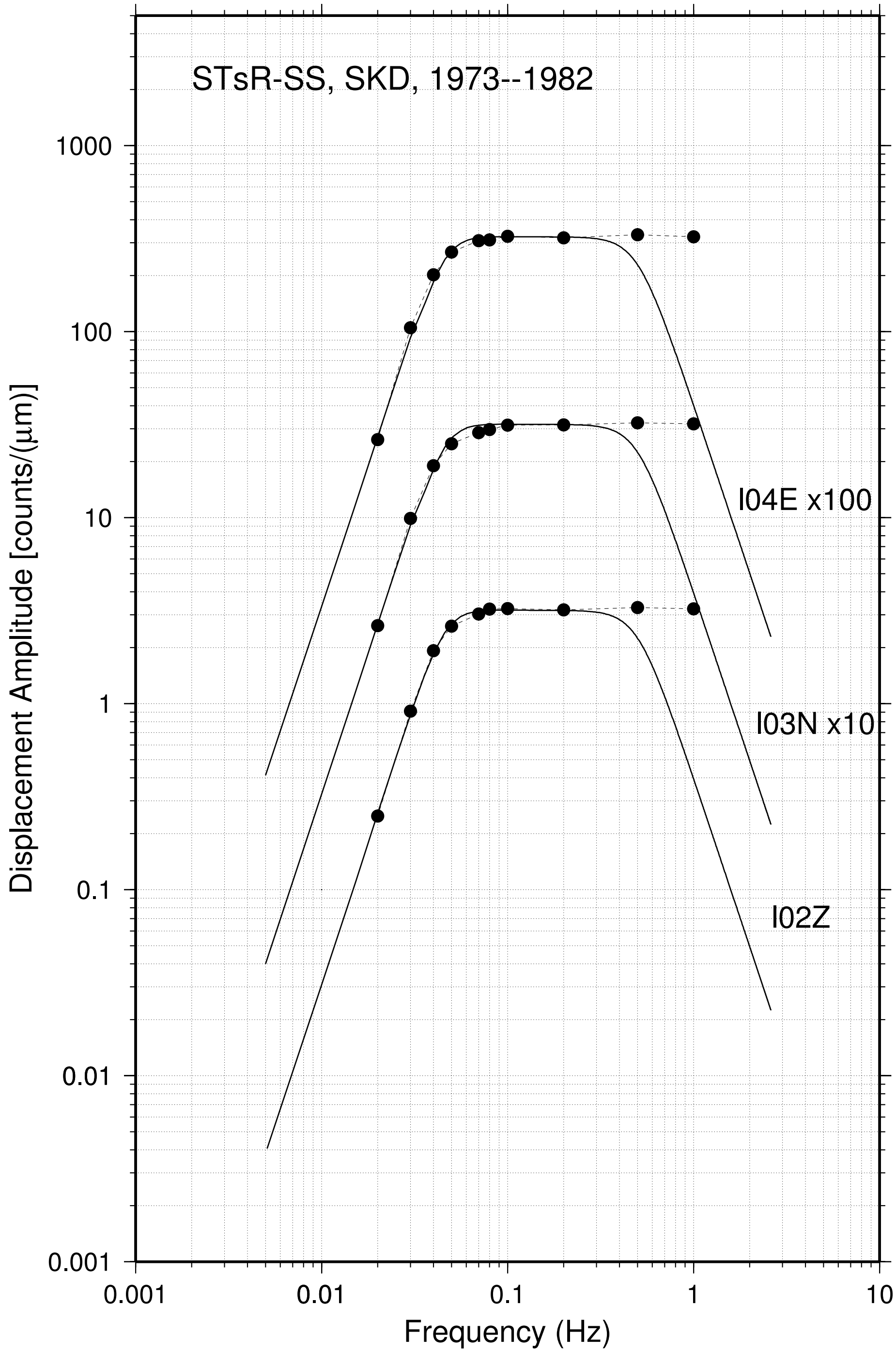

Figure 28: Comparisons of observed (*solid circles*) and theoretical (*solid lines*) frequency-amplitude curves of 3-component extended-period SKD channels during 1973–1982. l02Z = vertical-component, l03N = NS-component, and l04E = EW-component. The theoretical amplitude response is calculated using the instrument response for the later time period 1982–1991. The curves for the NS-component are plotted with their amplitudes multiplied by 10, and EW-component are plotted by multiplying the amplitude by 100 to show the response curves separately.

Table 16: Gains, Poles and Zeros of the instrument response of the Extended-period SKD Channels 2, 3 and 4, 1973-1982

Component	Z-component (l02Z)	NS-component (l03N)	EW-component (l04E)
Gain at 0.1 Hz (73-06-06–81-06-30)	3.31 counts/μm	3.36 counts/μm	3.36 counts/μm
Gain at 0.1 Hz (81-08-14–82-07-4)	2.82 counts/μm	2.82 counts/μm	3.02 counts/μm
Seismometer T_0=22 s, Ds=0.45	(-0.128520, 0.255048), (-0.128520, -0.255048) two zeros at origin (0.00, 0.00), (0.00, 0.00)		
1st order RC high-pass filter	cutoff at 0.05 Hz, one pole (-0.314159, 0.00) one zero at origin (0.00, 0.00)		
3rd order Butterworth low-pass filter	cutoff at 0.5 Hz, three poles (-3.14159, 0.00) (-1.57080, -2.72062), (-1.57080, 2.72062)		

2) Channel 2, 3 and 4 (l02Z, l03N and l04E; 1982–1991)

During 1982–1991, these channels recorded the signals from 3-component, extended-period SKD seismometer with the gains of 5.18, 5.14 and 5.17 counts/μm at 0.1 Hz for vertical-, NS-, and EW-component, respectively. A frequency-amplitude curve available during 1982–1991 is plotted in Figure 29. This is the instrument response shown in Adushkin & An (1990).

Instrument Response: Poles and Zeros

Instrument response of these channels can be represented by 6 poles and 3 zeros, which consists of seismometer with natural period T_0=25 s and damping constant of D_s=0.5; a first order RC high-pass filter with cutoff frequency at 0.05 Hz and a third-order Butterworth low-pass filter with cutoff at 0.5 Hz. Comparison of observed and theoretical responses for vertical-, NS- and EW-component are plotted in Figure 30. The observed frequency-amplitude calibration curves can be best fit by using the instrument constants that are slightly different from the nominal values. The seismometer with natural period T_0=22s and damping constant of D_s=0.45 fits the best. Six poles and three zeros can represent instrument response of these channels during 1982–1989 as listed in Table 17.

Table 17: Instrument Constants of the Extended-period SKD Channels 2, 3 and 4, 1982–1991

<table>
<tr><th>Component</th><th>Z-component (l02Z)</th><th>NS-component (l03N)</th><th>EW-component (l04E)</th></tr>
<tr><td>Gain at 0.1 Hz</td><td>5.18 counts/μm</td><td>5.14 counts/μm</td><td>5.17 counts/μm</td></tr>
<tr><td>Seismometer
SKD, 82-08-23–91-07-15</td><td colspan="3">two poles (-0.128520, 0.255048), (-0.128520, -0.255048)
two zeros at origin (0.00, 0.00), (0.00, 0.00)</td></tr>
<tr><td>1st order RC
high-pass filter</td><td colspan="3">cutoff at 0.05 Hz, one pole (-0.314159, 0.00)
one zero at origin (0.00, 0.00)</td></tr>
<tr><td>3rd order Butterworth
low-pass filter</td><td colspan="3">cutoff at 0.5 Hz, three poles (-3.14159, 0.00)
(-1.57080, -2.72062), (-1.57080, 2.72062)</td></tr>
</table>

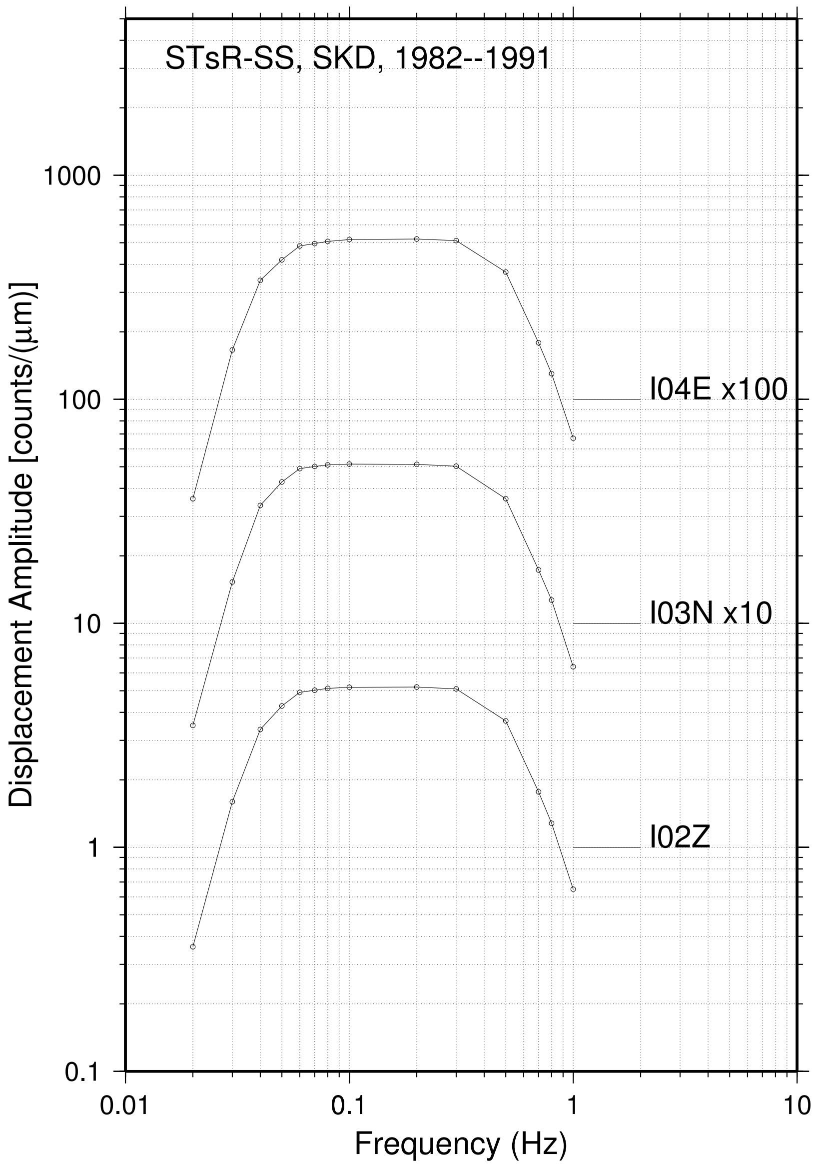

Figure 29: Frequency-amplitude calibration curves of 3-component extended-period SKD channels during 1982–1991. l02Z = vertical-component, l03N = NS-component, and l04E = EW-component. The curve for the NS-component is plotted with their amplitudes multiplied by 10, and EW-component is plotted by multiplying the amplitude by 100 to show the response curves separately.

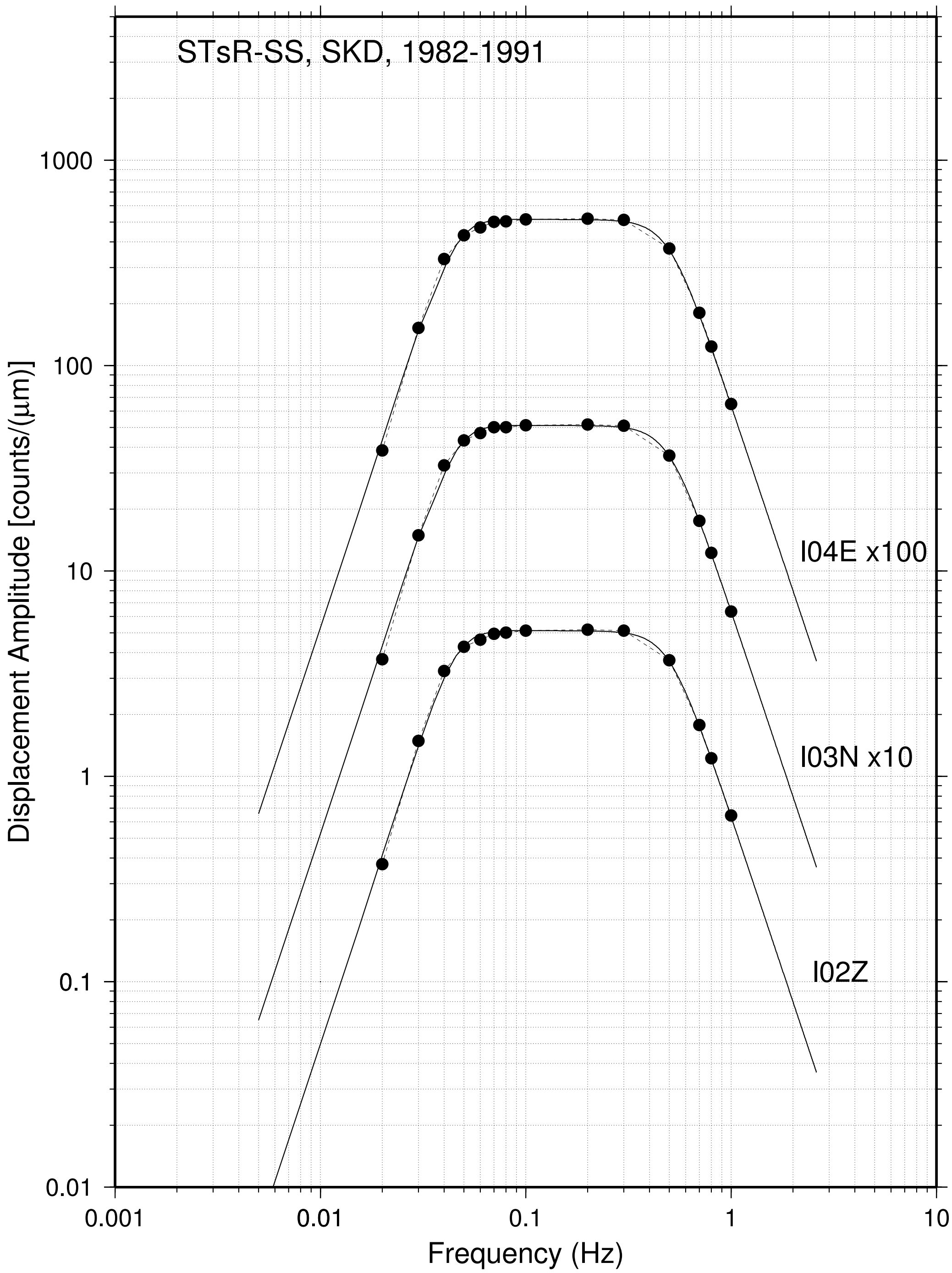

Figure 30: Comparisons of observed (*solid circles*) and theoretical (*solid lines*) frequency-amplitude curves of 3-component extended-period SKD channels during 1982–1991. l02Z = vertical-component, l03N = NS-component, and l04E = EW-component. The curves for the NS-component are plotted with their amplitudes multiplied by 10, and EW-component are plotted by multiplying the amplitude by 100 to show the response curves separately.

3) Channel 1, 5 and 10 (l01Z, l05N and l10E; 1982–1991)

These channels recorded signals from the 3-component, extended-period SKD seismometer with a low-gain configuration. The channel names are assigned as l01Z, l05N and l10E for vertical-, NS-, and EW-component, respectively. These channels were recorded only during 1982–1991 when the STsR-SS system was reconfigured. The waveform data and the frequency-amplitude calibration curves available for the period indicate that the gains of these channels were 0.51 counts/μm at 0.1 Hz for vertical-, NS-, and EW-component, respectively and were recorded with a sampling interval of 0.192 sec (Figure 31). During the 2nd half of the STsR-SS system operation, all 10 channels of the system were utilized: 3-component short-period SKM-3 data stream (s07Z, s08N and s09E); a low-gain vertical-component SKM-3 (s06Z); 3-component extended-period SKD data stream (l02Z, l03N and l04E); and low-gain 3-component extended-period SKD data stream (l01Z, l05N and l10E).

Instrument Response: Poles and Zeros

These channels are low-gain 3-component SKD data stream with the similar instrument responses as those of channels 2, 3 and 4. These channels are added since 1982 when the STsR-SS system was reconfigured. Comparison of observed and theoretical amplitude responses for vertical-, NS- and EW-component are plotted in Figure 32. The observed frequency-amplitude calibration curves are fairly well fit by the curve calculated using instrument constants identical to channels 2, 3 and 4 given in Table 17. The gains of each component at 0.1 Hz are listed in Table 18.

Table 18: The gains of the Extended-period SKD Channels 1, 5 and 10, 82-08-23–91-07-15

Component	Z-component (l01Z)	NS-component (l05N)	EW-component (l10E)
Gain at 0.1 Hz	0.51 counts/μm	0.51 counts/μm	0.51 counts/μm

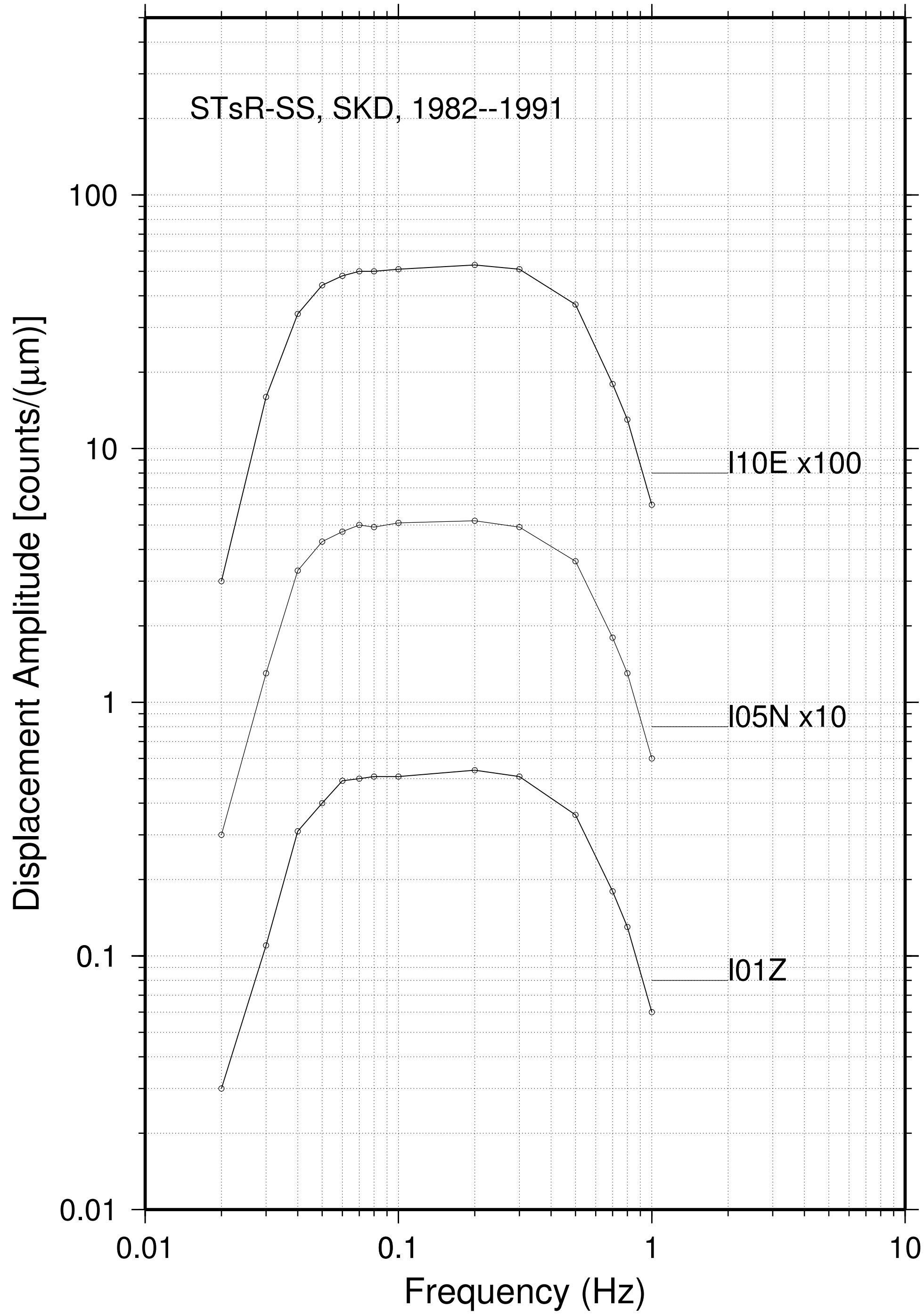

Figure 31: Frequency-amplitude calibration curves of 3-component extended-period SKD channels during 1982–1991. l01Z = vertical-component, l05N = NS-component, and l10E = EW-component. The curve for the NS-component is plotted with its amplitudes multiplied by 10, and EW-component is plotted by multiplying the amplitude by 100 to show the response curves separately.

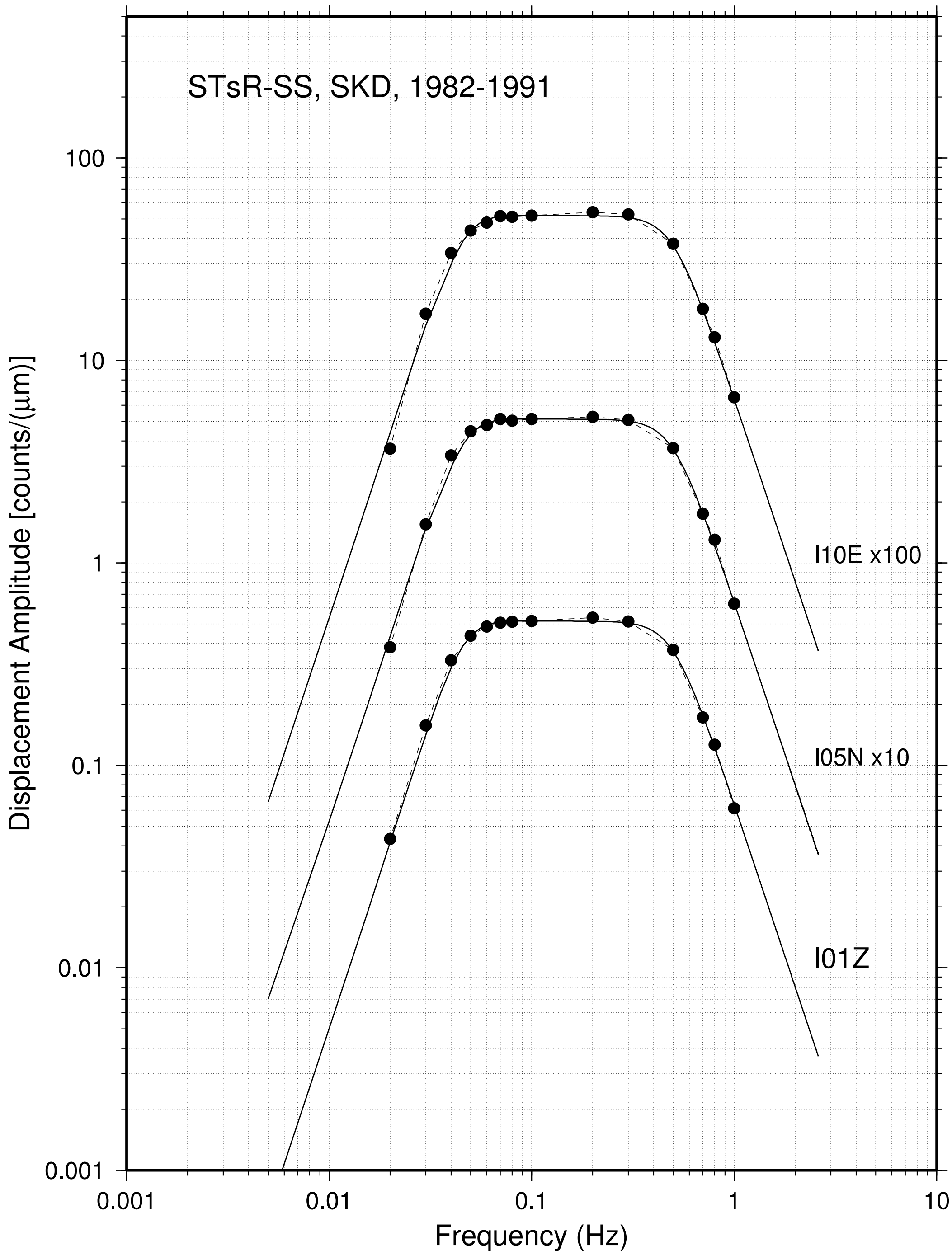

Figure 32: Comparisons of observed (*solid circles*) and theoretical (*solid lines*) frequency-amplitude curves of low-gain, 3-component extended-period SKD channels during 1982–1991. l01Z = vertical-component, l05N = NS-component, and l10E = EW-component. The curves for the NS-component are plotted with their amplitudes multiplied by 10, and EW-component are plotted by multiplying the amplitude by 100 to show the response curves separately.

Note on Instrument Types (Shishkevish, 1974)

SKD: Kirnos-Arkhangel'skiy broadband extended-period system or any of its three components:
    SGKD or SKD (N-S, E-W) – horizontal-component SKD seismographs
    SVKD or SKD (Z) – vertical-component SKD seismograph

SKM: Kirnos high-gain, short-period system or any of its three components:
    SGKM or SKM (N-S, E-W) – horizontal-component SKM seismographs
    SVKM or SKM (Z) – vertical-component SKM seismograph

SKM-3: Kirnos high-gain, short-period system (later model of SKM) or any of its three components:
    SGKM-3 or SKM-3 (N-S, E-W) – horizontal-component SKM-3 seismographs
    SVKM-3 or SKM-3 (Z) – vertical-component SKM-3 seismograph

KPCh: Low-gain seismograph channel obtained by connecting a galvanometer to the seismometer damping coil and used mostly with SK and SKD seismograph (SK-KPCh, SKD-KPCh).

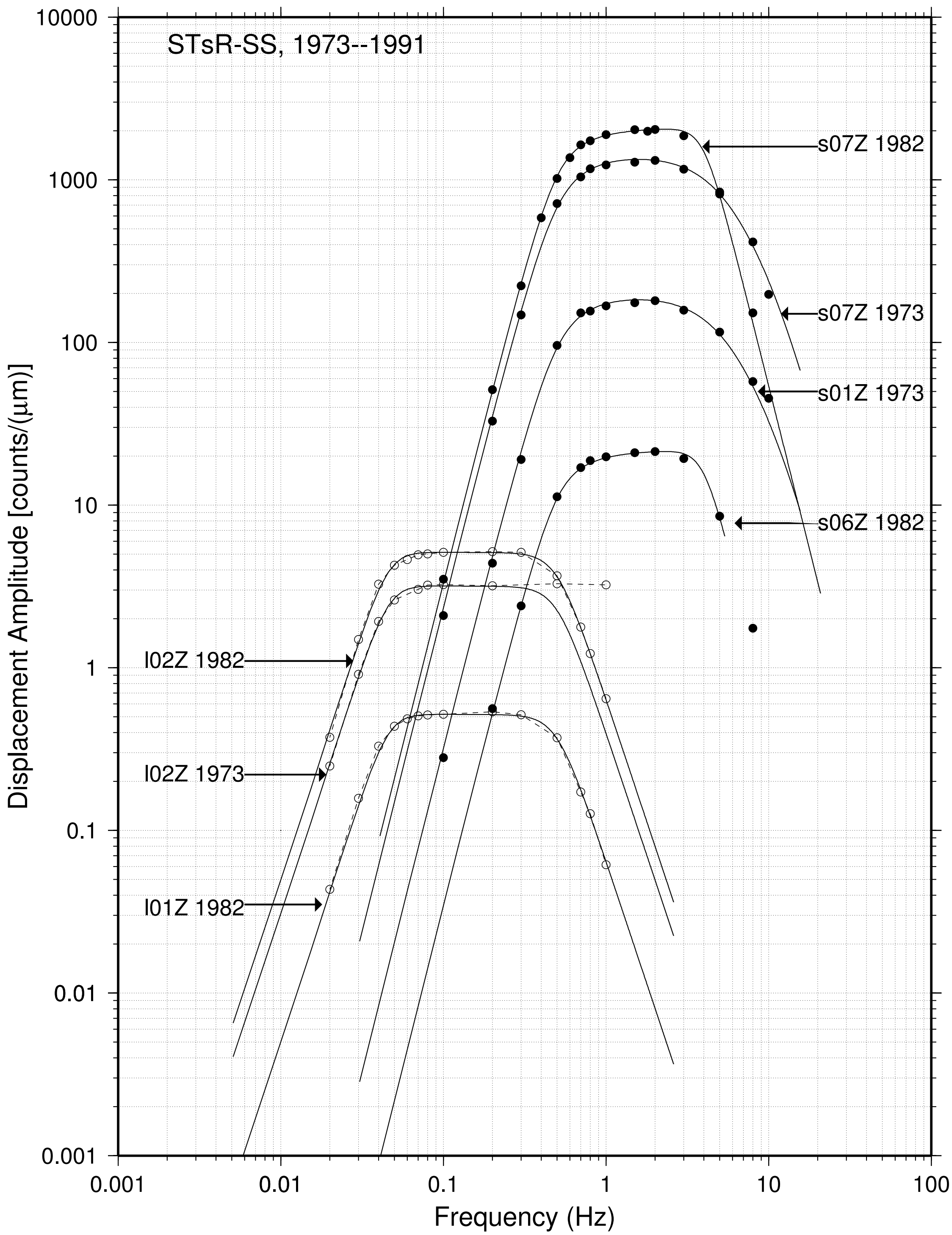

Figure 33: A summary plot of the averaged frequency-amplitude calibration curves of all data streams of the STsR-SS system (*open circles*=SKD and *solid circles*=SKM-3 seismometers). Theoretical amplitude responses are plotted by *solid lines*. SKM-3 data streams: s07Z 1982= 3-component (s07Z, s08N and s09E, 1982–1991); s07Z 1973= 3-component (s07Z, s08N and s09E, 1973–1982); s01Z 1973= low-gain vertical-component, 1973–1981; s06Z 1982= low-gain vertical-component, 1982–1991. SKD data stream: l02Z 1973= 3-component (l02Z, l03N and l04E, 1973–1982); l02Z 1982= 3-component (l02Z, l03N and l04E, 1982–1991); l01Z 1982= low-gain 3-component (l01Z, l05N and l10E, 1982–1991).

Table 19: Instrument Characteristics at Borovoye (BRV)(*)

System	Seismometer	$T_0^{(1)}$ (s)	$D_s^{(2)}$	Chan name	Gain(3) (C/μm)	fn(4) (Hz)	dt(5) (ms)	Chan no.	Time period
KOD	SKM-3	3.5	0.7	SHZ	3,386	1.8	30	1	67-02-26
				SHN	2,940	1.8	30	3	–73-10-26
				SHE	3,354	1.8	30	4	
	LG(Z)(6)			SLZb	423	1.8	30	2	
				SLZ	421	1.8	30	1	67-06-29
				SLN	321	1.8	30	3	–73-10-26
				SLE	371	1.8	30	4	
				SHZm	3,386	1.8	30	2	
SS	SKM-3	2.0	0.5	s07Z	1249	2.0	32	7	73-06-06
				s08N	1330	2.0	32	8	–82-07-04
				s09E	1336	2.0	32	9	
	LG(Z)			s01Z	175	2.0	32	1	–81-01-15
				s07Z	2059	2.0	24	7	82-08-21
				s08N	2054	2.0	24	8	–91-07-15
				s09E	2057	2.0	24	9	
	LG(Z)			s06Z	20	2.0	96	6	81-08-14–
	SKD	25.0	0.5	l02Z	3.31	0.10	192	2	73-06-06
				l03N	3.36	0.10	192	3	–82-07-04
				l04E	3.36	0.10	192	4	
				l02Z	5.19	0.10	192	2	82-08-23
				l03N	5.14	0.10	192	3	–91-07-15
				l04E	5.17	0.10	192	4	
	LG			l01Z	0.51	0.10	192	1	82-08-23
				l05N	0.51	0.10	192	5	–91-07-15
				l10E	0.51	0.10	192	10	
TSG	KSVM	1.5	0.5	sZ01	50	1.0	26	1	80-07-20–96-01-27
				sZ02	4,600	1.0	26	2	83-12-16–96-01-27
	KSM	1.5	0.5	sZ03	1,000	1.0	26	3	85-03-23
				sN04	1,000	1.0	26	4	–96-01-27
				sE05	1,000	1.0	26	5	
	KS	1.5	0.71	sZ06	1,000	1.5	26	6	85-03-23–96-01-27
				sZ07	2,000	1.5	26	7	74-12-16
				sN08	2,000	1.5	26	8	–82-01-30
				sE09	2,000	1.5	26	9	
				sZ07	4,500	1.5	26	7	82-03-24
				sN08	4,500	1.5	26	8	–91-01-27
				sE09	4,500	1.5	26	9	

continued on next page

System	Seismometer	$T_0^{(1)}$ (s)	$D_s^{(2)}$	Chan name	Gain[3] (C/μm)	fn[4] (Hz)	dt[5] (ms)	Chan no.	Time period
	KSM	1.5	0.5	sZ10	100,000	1.0	26	10	85-01-22
				sN11	100,000	1.0	26	11	–88-10-31
				sE12	100,000	1.0	26	12	
	DS	20.0	0.71	lZ19	50	0.1	312	19	74-07-12
				lN20	50	0.1	312	20	–88-06-28
				lE21	50	0.1	312	21	
	DSM	28.0	0.71	lZ22	1,000	0.07	312	22	75-11-19
				lN23	1,000	0.07	312	23	–88-12-02
				lE24	1,000	0.07	312	24	
				lZ15	10	0.07	312	15	85-01-26
				lN16	10	0.07	312	16	–88-12-02
				lN17	10	0.07	312	17	
	DS	20.0	0.71	lZ13	50	0.1	312	13	83-11-03–84-01-18
				lN14	50	0.1	312	14	83-11-03–85-02-13

[*] KOD (KODB and KODM) systems were operated from 1966–Nov 1973 and had polarity reversal on all channels, STsR-SS (SS) and STsR-TSG (TSG) systems were operated from Feb. 1973 to 1995.
[1] T_0= Seismometer natural period in seconds.
[2] D_s= Seismometer damping constant, critical damping=0.71.
[3] Gain = Sensitivity in counts/μm for ground displacement.
[4] fn = Normalization frequency where the gain is measured.
[5] dt = Sampling interval in millisecond.
[6] LG = low-gain channels and (Z) indicates that it is only vertical-component.

4. RESULTS

More than 3700 deglitched and calibrated seismograms are the main result of this project. Prior to this project, personnel at Los Alamos National Laboratory had become familiar with some of these data, in particular with waveforms recorded on the TSG system. In this current project we have approximately trebled the number of waveforms analyzed, by successfully processing the data recorded by earlier systems, which, prior our work, had not been usable. Here we give examples of, the waveforms from all three systems.

From Table 1 on page 4 we see that these thousands of waveforms can be organized into 497 sets, each set corresponding to one particular underground nuclear explosion (UNE), as recorded on one of the three different systems at Borovoye. These waveforms, now deglitched and documented with instrument responses, are the main result of this project, together with preliminary analyses of these data as presented at Monitoring Research Reviews in 2007, 2008, and 2009 (Kim et al, 2007, 2008; Baker et al., 2009). Details of the sampling rate and instrument response of the three systems emerged for all three years in which we did our work. Difficulties of the KOD system included Soviet publications describing the impulse response that did not match our own information from stations operators in Kazakhstan. Difficulties of the SS system included changes in sampling rate and an appreciation that the data are aliased to some degree—details described here on page 39 and following, and that that were not thoroughly understood until late in the project.

We have prepared all 497 of these waveform sets as a series of PDF documents to enable potential users to get a sense of which seismograms are likely to be useful for reading arrival times (a high-gain channel may be best), or for computing spectra (a low-gain channel may be best for this purpose), or for coda studies (both low-gain and high-gain channels are relevant). We are making these files available to interested users online via

http://www.ldeo.columbia.edu/res/pi/Monitoring/Arch/BRV_arch_deglitched.html

but there are far too many to include in this Final Report. Instead, to present our results in an orderly way in this section, we give 36 sets of examples, in Figures 34 through 69, each set representing the seismograms from one particular underground nuclear test as recorded on a particular digital seismographic system—either KOD, or SS, or TSG.

Our choice, in culling the 497 sets down to 36 has been to show data from the first and and the last UNE for each region, as recorded on a particular system. But we make two exceptions. The first is in Figure 39, which is the set of TSG seismograms for an overburied shot on 1989 July 8 in the Balapan sub-region of the Semipalatinsk Test Site. (This shot was set off at the depth appropriate for a yield of about 150 kt, though its actual yield was about 35 kt. At that time, in the summer of 1989, strong opposition to nuclear testing was developing in Kazakhstan and local committees of concerned people were invited to the test site to witness monitoring activities indicating that all radioactive products of the test were contained underground.) The second exception is in Figure 65, which shows the only KOD recording of a UNE at Lop Nor, China. (This was the first

Figure 34. First of seven sets of BRV seismograms on the KOD system for a UNE at the Balapan area of the Semipalatinsk Test Site, Kazakhstan; test of 1968 June 19

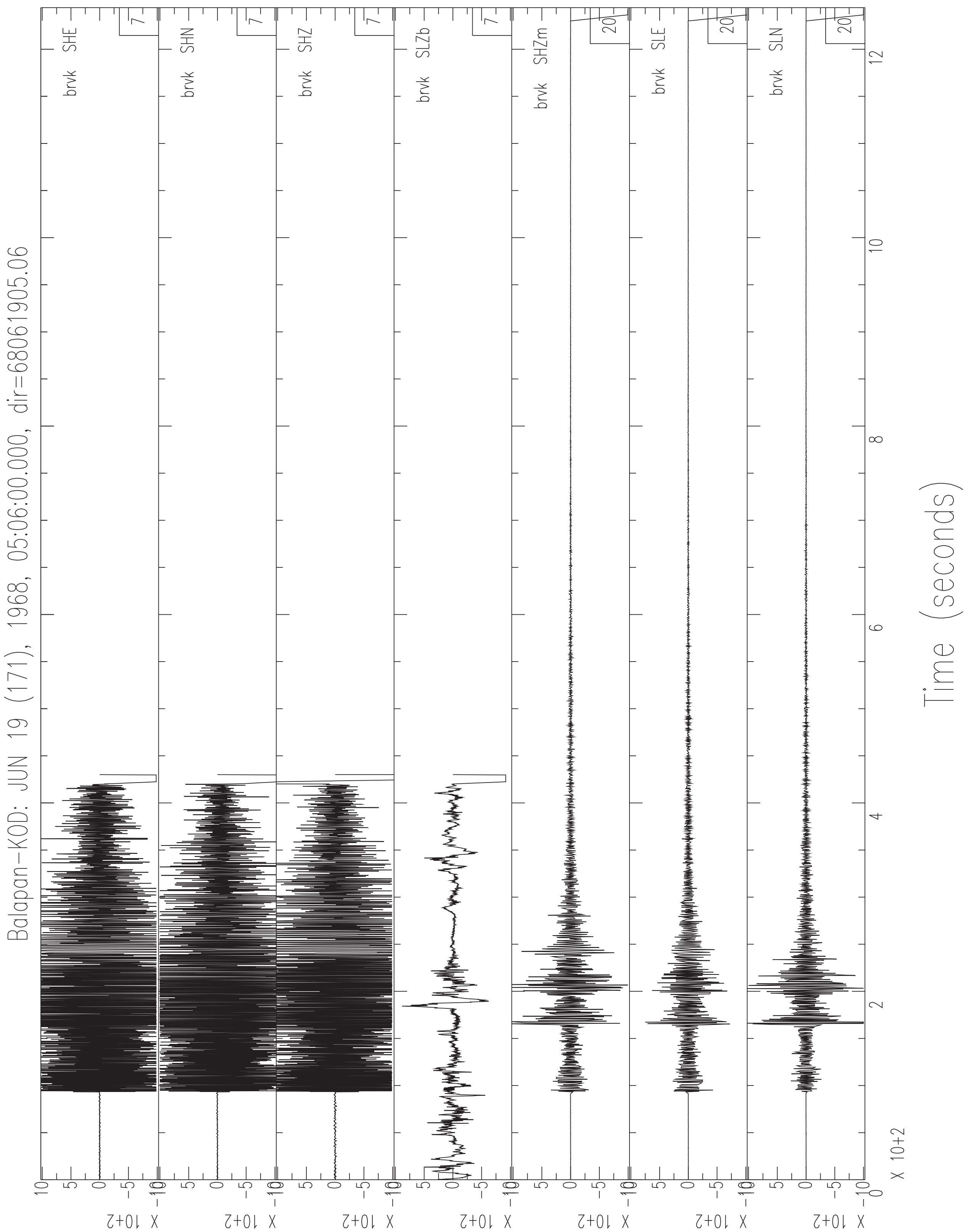

Figure 35. Last of seven sets of BRV seismograms on the KOD system for a UNE at the Balapan area of the Semipalatinsk Test Site, Kazakhstan; test of 1973 July 23

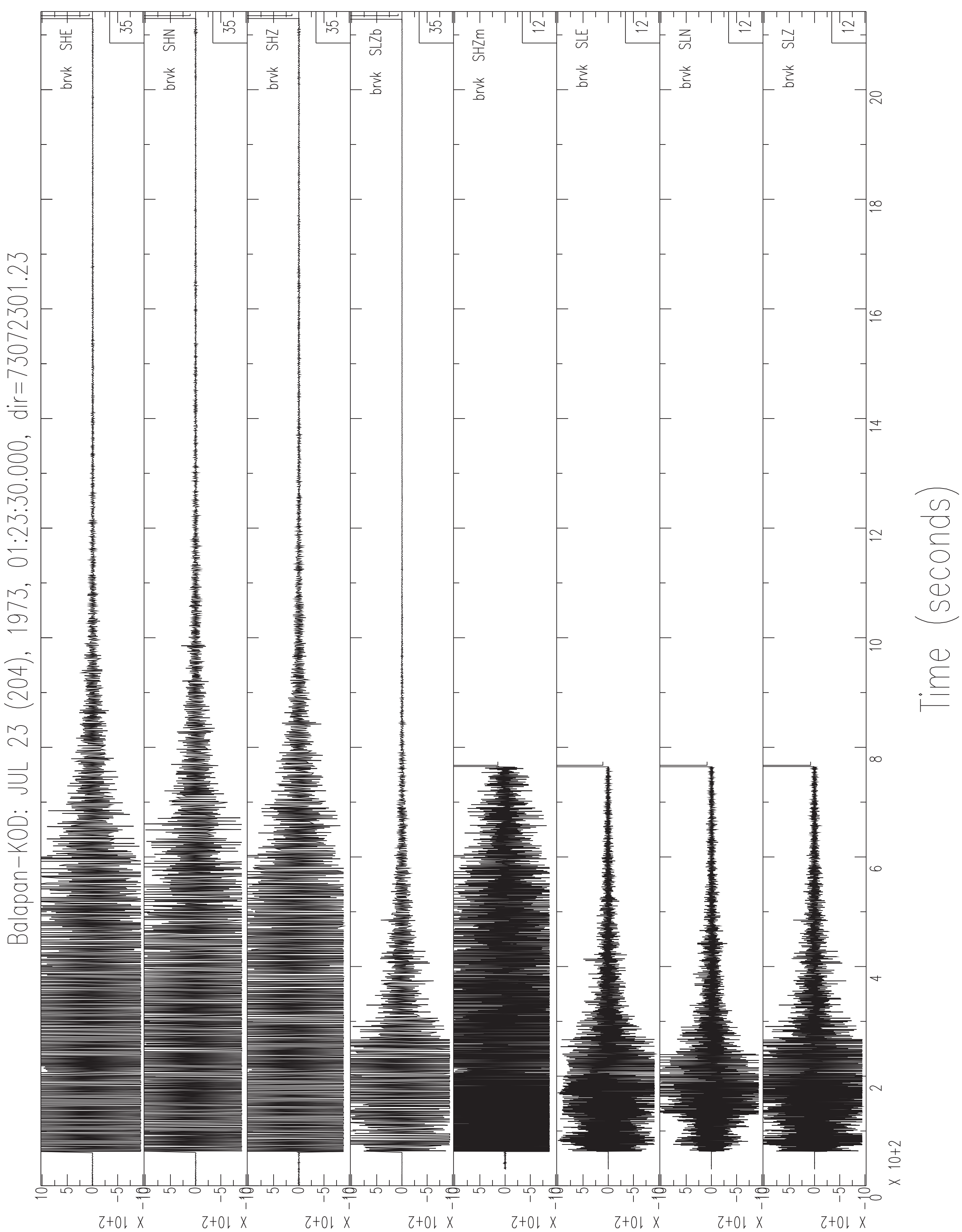

Figure 36. First of 78 sets of BRV seismograms on the SS system for a UNE at the Balapan area of the Semipalatinsk Test Site, Kazakhstan; test of 1975 October 29

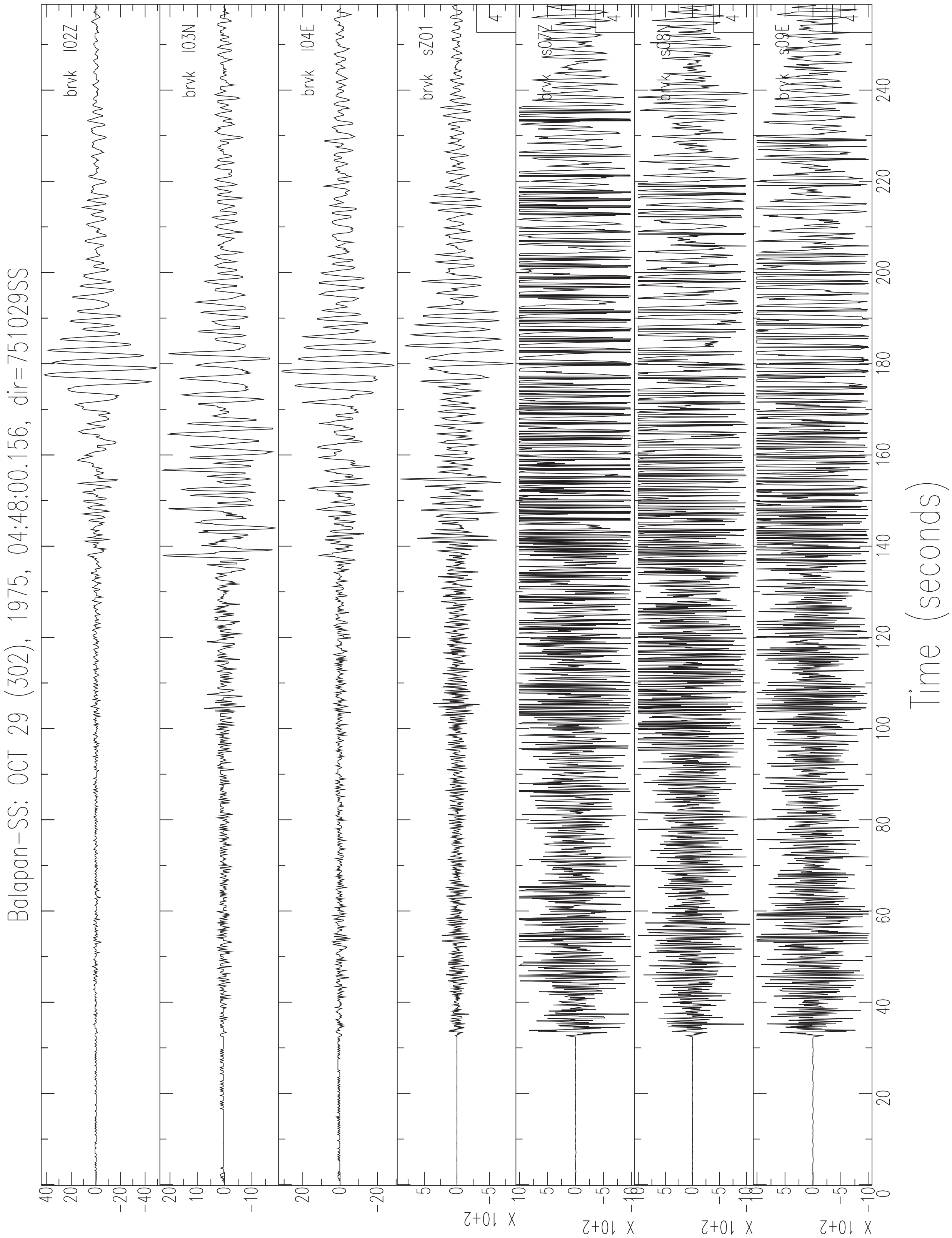

Figure 37. Last of 78 sets of BRV seismograms on the SS system for a UNE
at the Balapan area of the Semipalatinsk Test Site, Kazakhstan; test of 1989 October 19

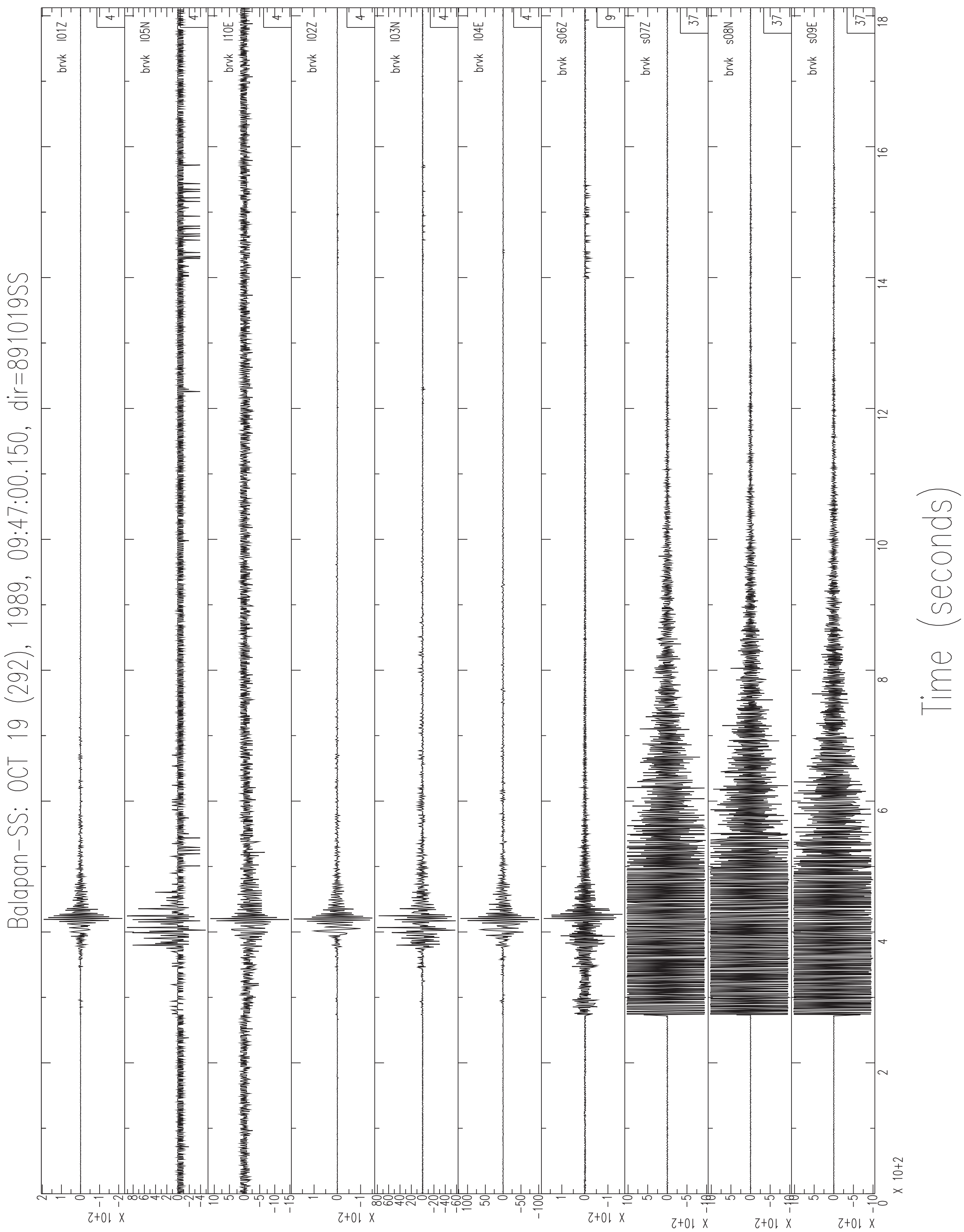

Figure 38. First of 73 sets of BRV seismograms on the TSG system for a UNE
at the Balapan area of the Semipalatinsk Test Site, Kazakhstan; test of 1974 December 27

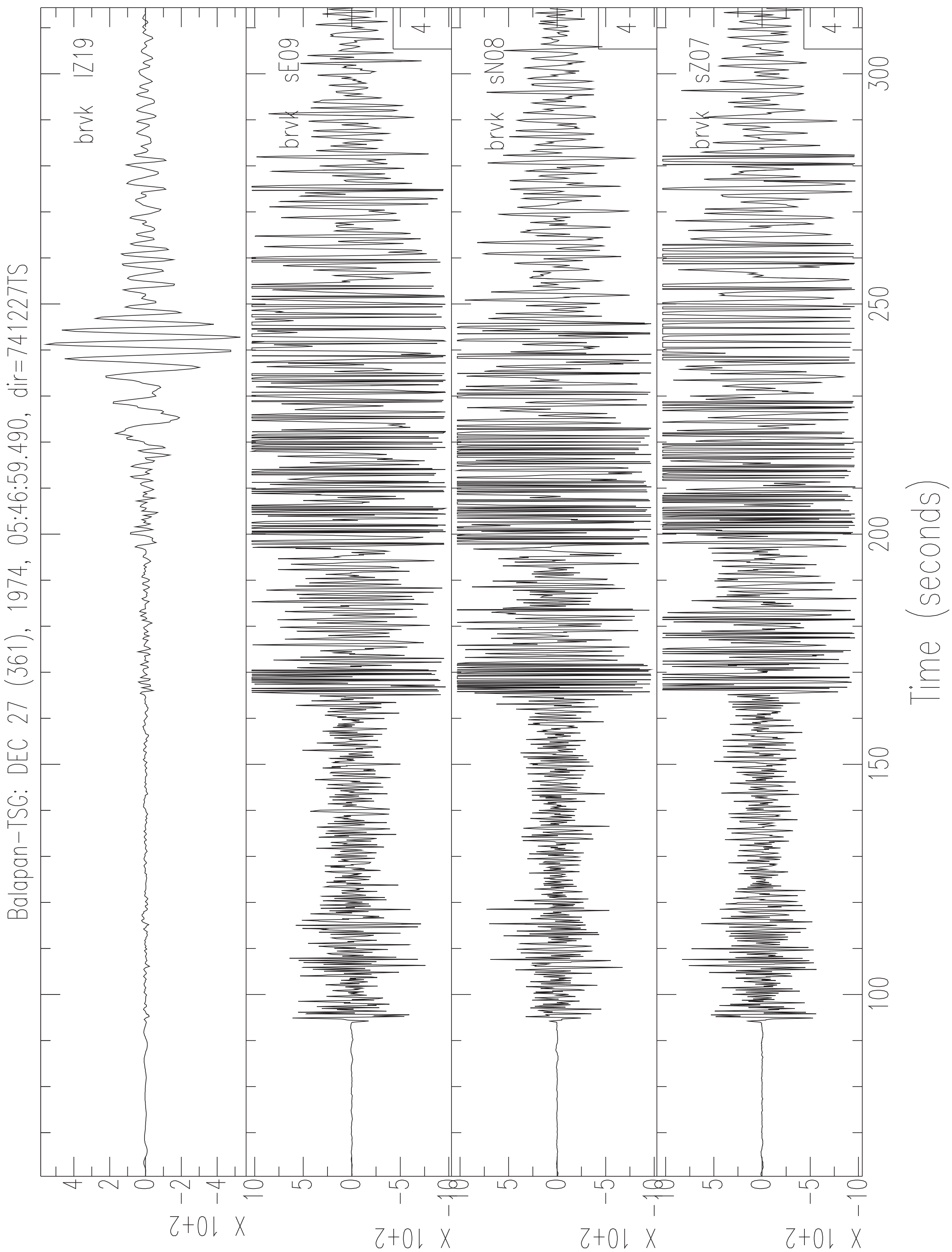

Figure 39. BRV seismograms on the TSG system for an overburied UNE
at the Balapan area of the Semipalatinsk Test Site, Kazakhstan; test of 1989 July 8

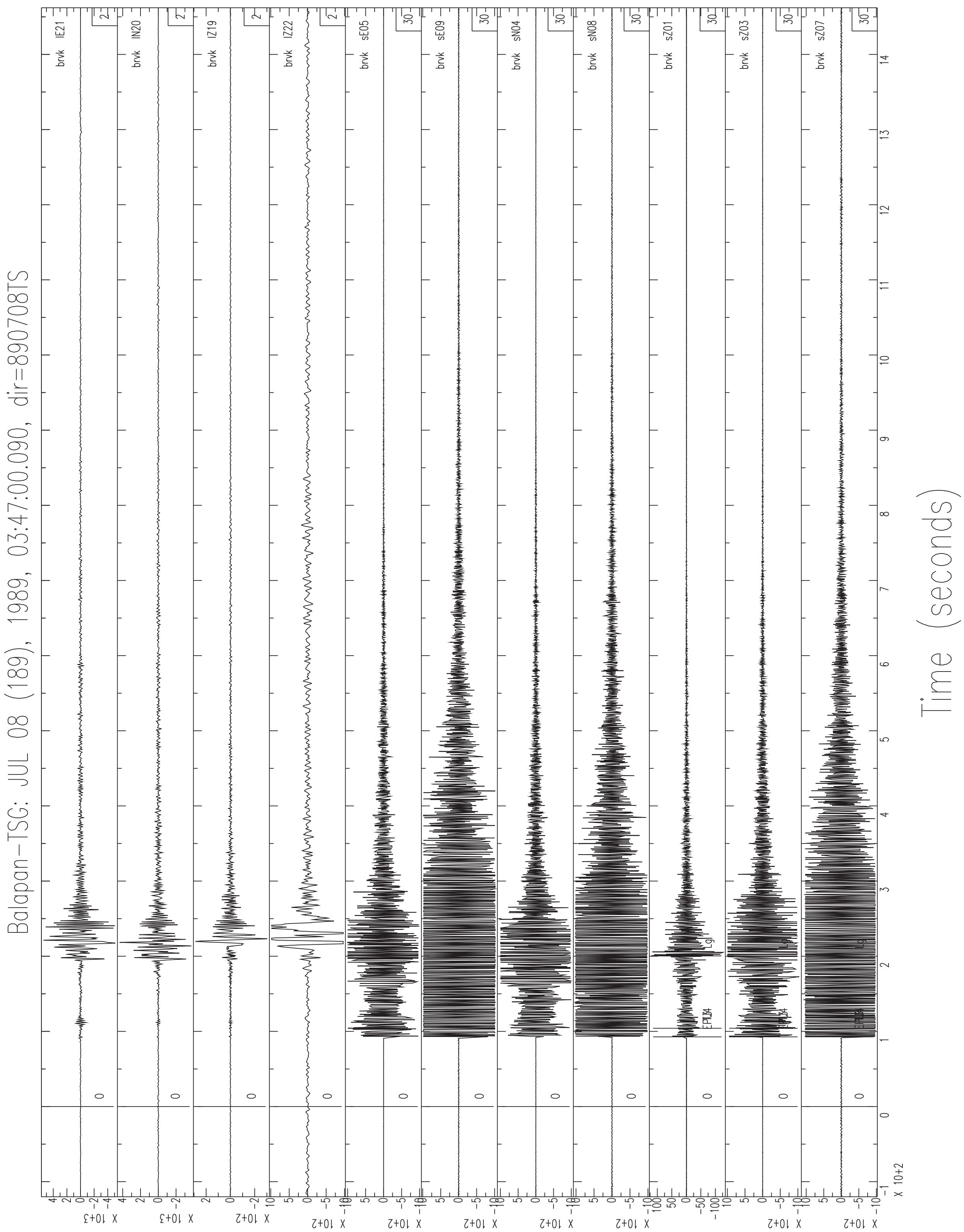

Figure 40. Last of 73 sets of BRV seismograms on the TSG system for a UNE at the Balapan area of the Semipalatinsk Test Site, Kazakhstan; test of 1989 October 19

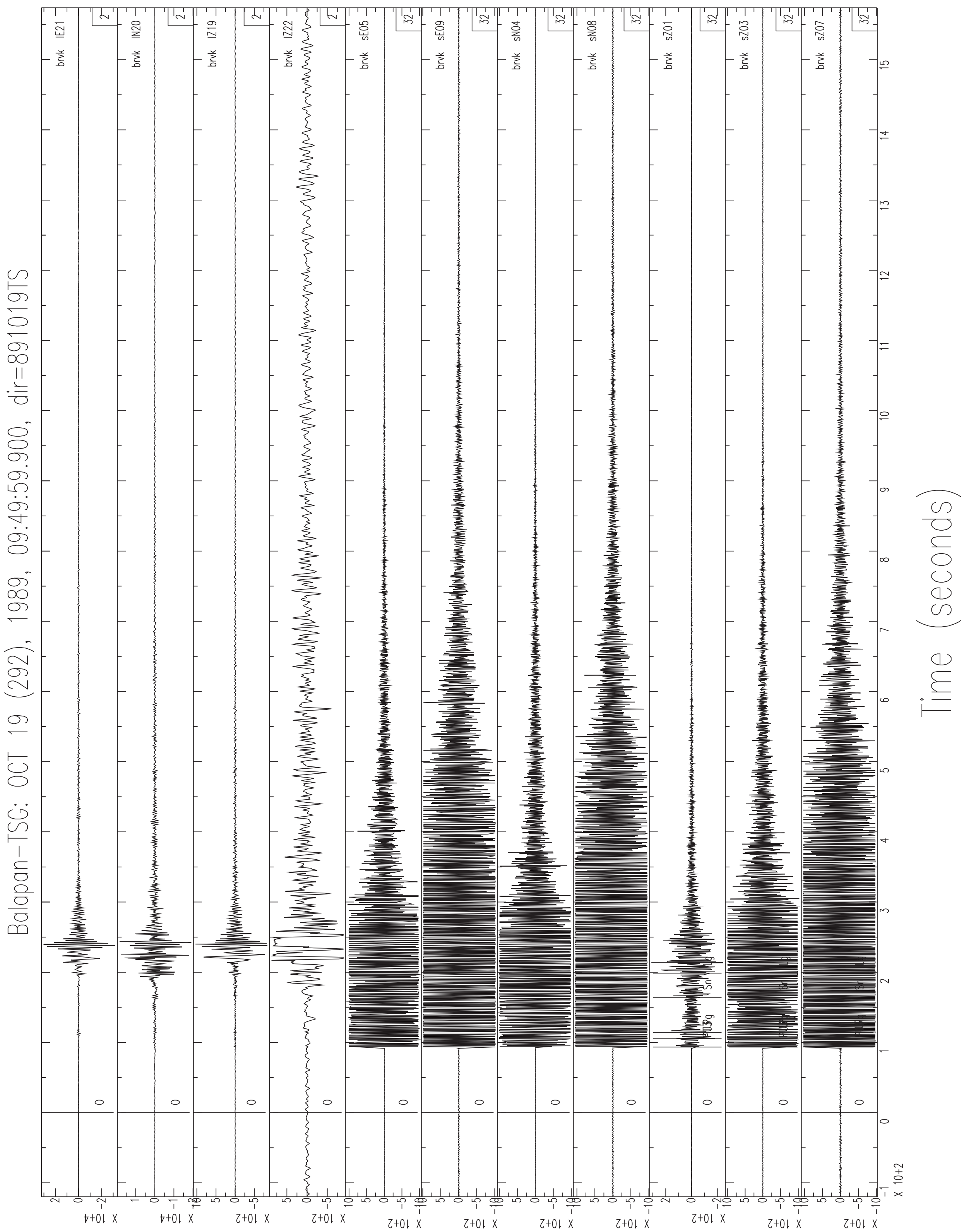

Figure 41. First of 45 sets of BRV seismograms on the KOD system for a UNE at the Degelen area of the Semipalatinsk Test Site, Kazakhstan; test of 1967 February 26

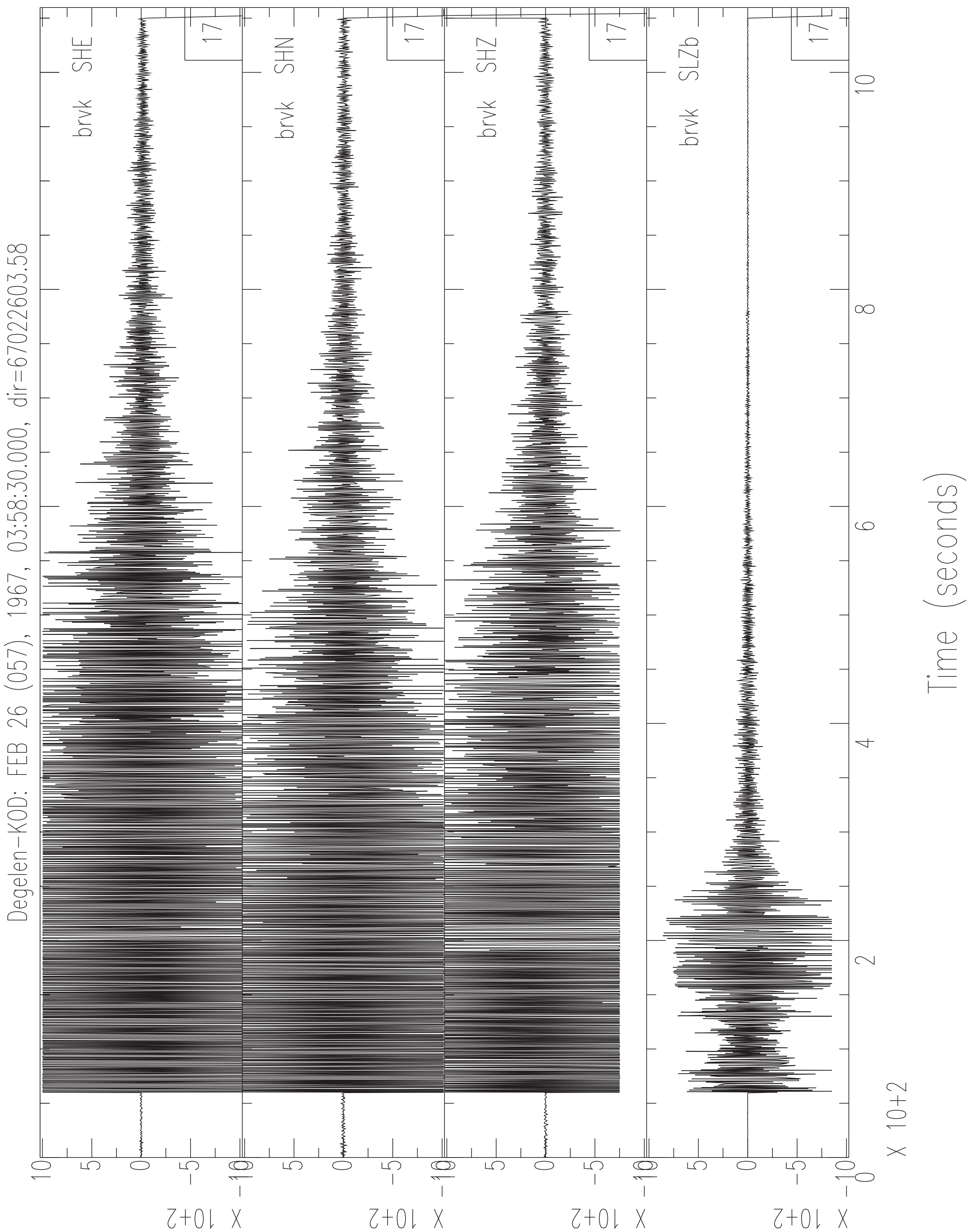

Figure 42. Last of 45 sets of BRV seismograms on the KOD system for a UNE at the Degelen area of the Semipalatinsk Test Site, Kazakhstan; test of 1973 October 26

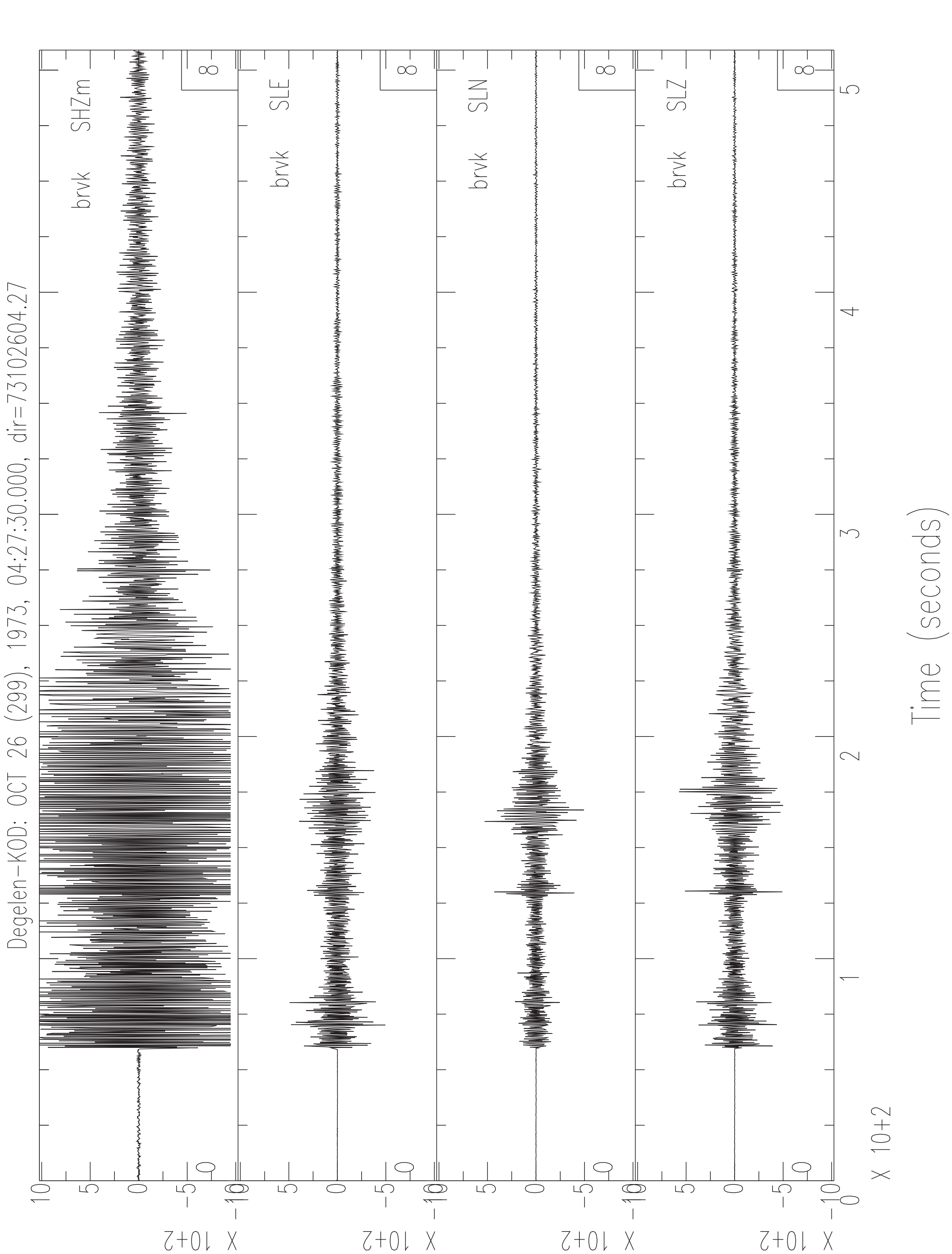

Figure 43. First of 59 sets of BRV seismograms on the SS system for a UNE at the Degelen area of the Semipalatinsk Test Site, Kazakhstan; test of 1975 December 13

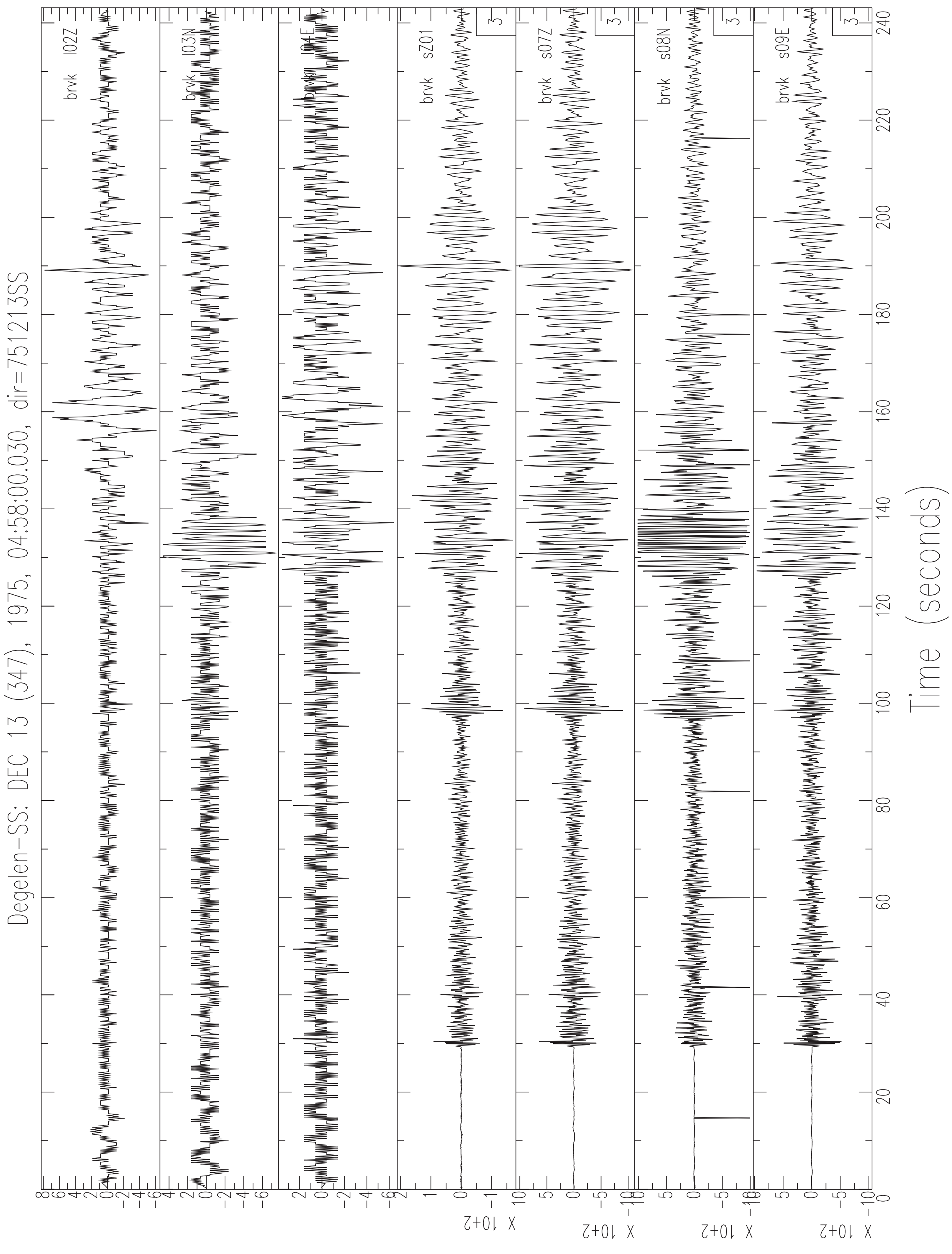

Figure 44. Last of 59 sets of BRV seismograms on the SS system for a UNE at the Degelen area of the Semipalatinsk Test Site, Kazakhstan; test of 1989 October 4

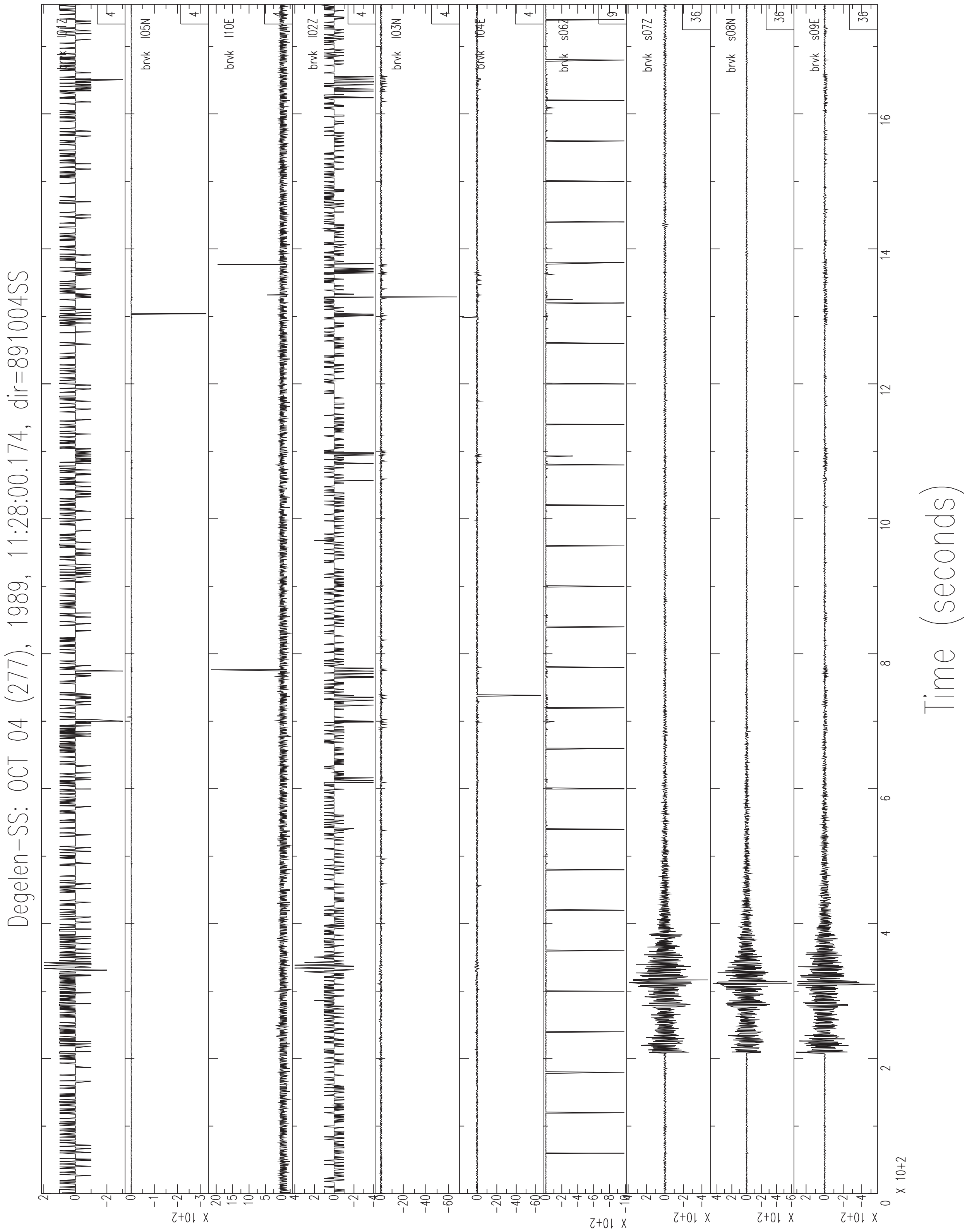

Figure 45. First of 59 sets of BRV seismograms on the TSG system for a UNE at
the Degelen area of the Semipalatinsk Test Site, Kazakhstan; test of 1974 December 16

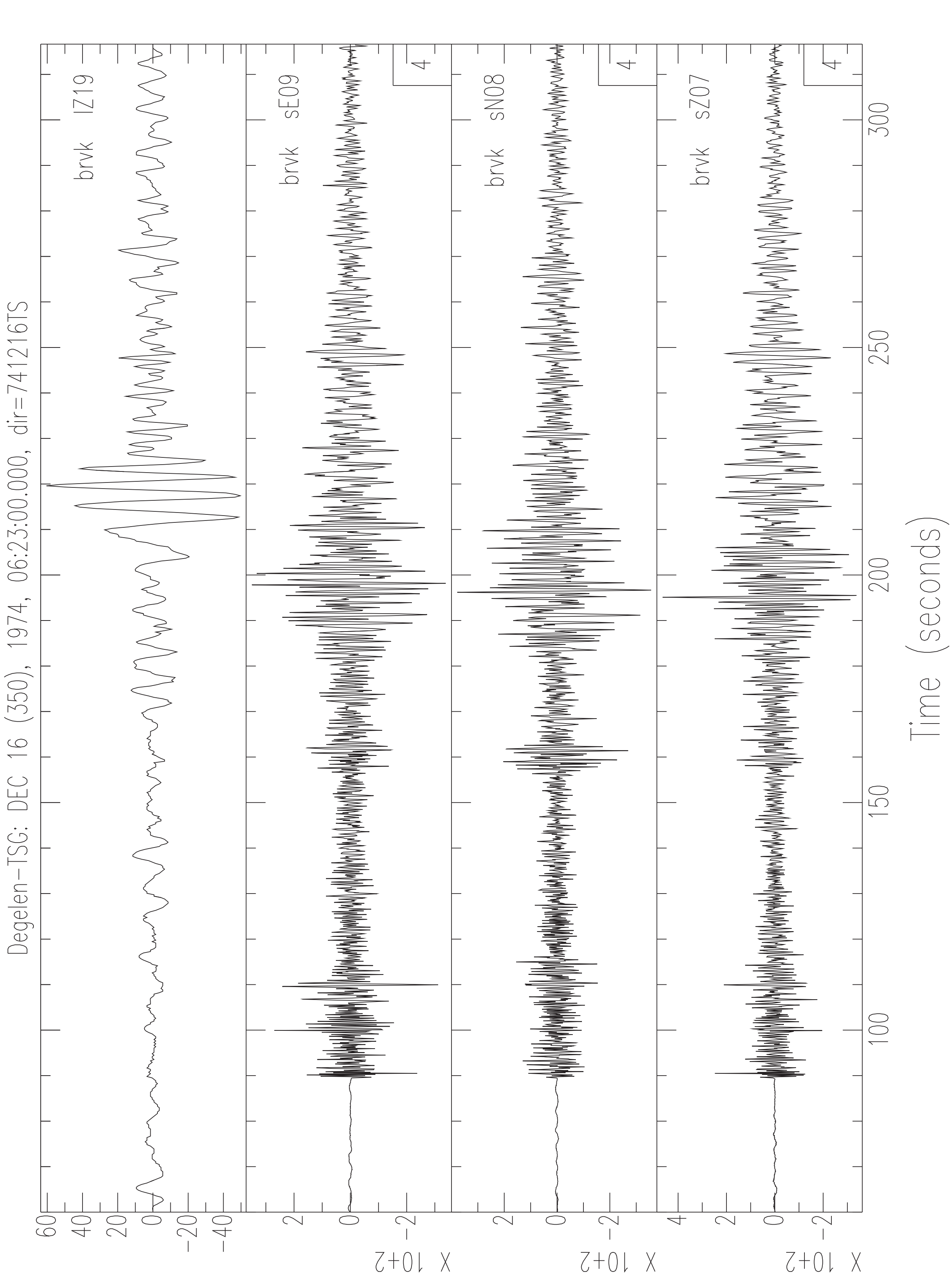

Figure 46. Last of 59 sets of BRV seismograms on the TSG system for a UNE at the Degelen area of the Semipalatinsk Test Site, Kazakhstan; test of 1989 October 4

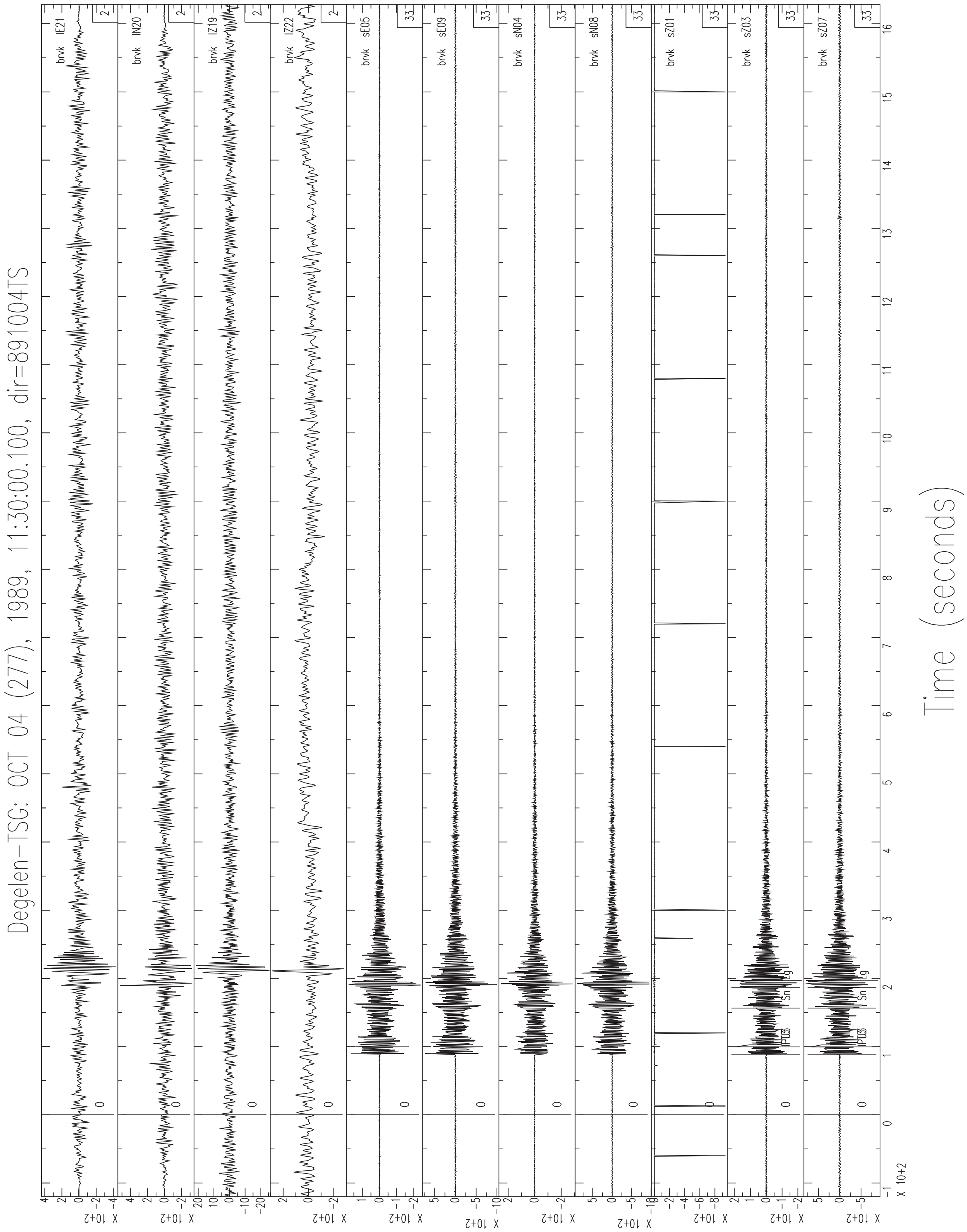

Figure 47. First of 14 sets of BRV seismograms on the KOD system for a UNE at the Murzhik area of the Semipalatinsk Test Site, Kazakhstan; test of 1966 December 18 (the earliest Eurasian nuclear test digitally recorded at Borovoye)

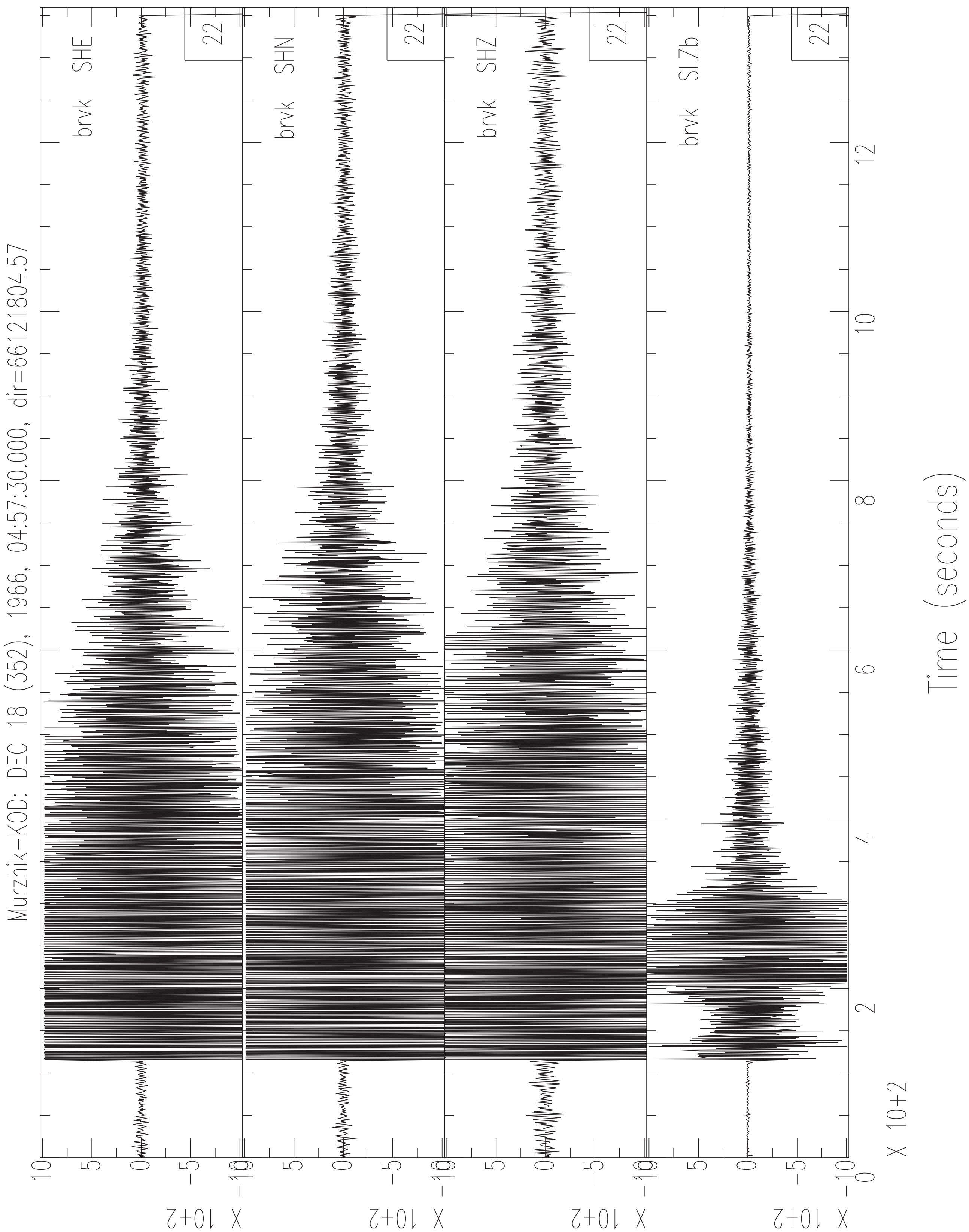

Figure 48. Last of 14 sets of BRV seismograms on the KOD system for a UNE at the Murzhik area of the Semipalatinsk Test Site, Kazakhstan; test of 1973 April 19

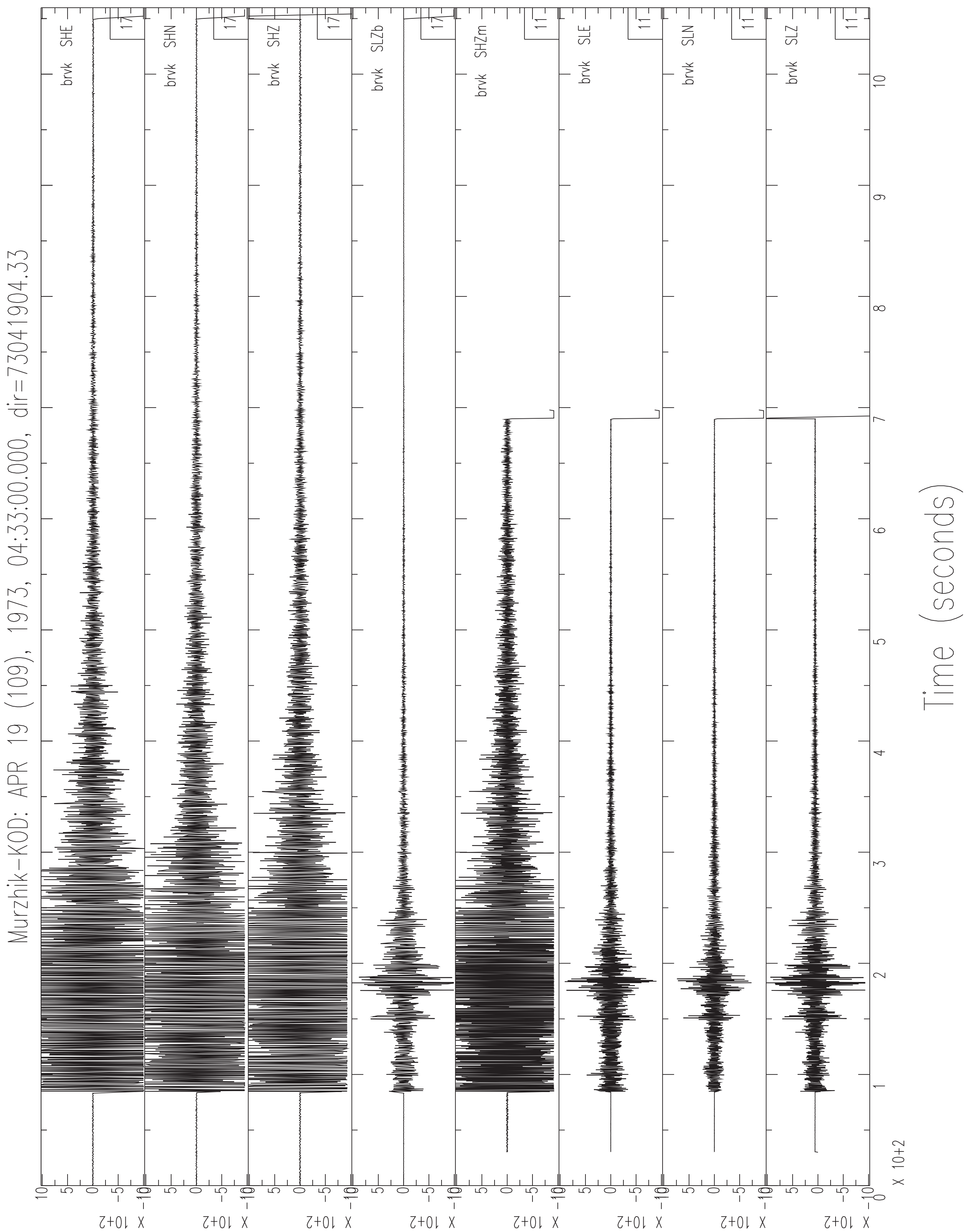

Figure 49. First of five sets of BRV seismograms on the SS system for a UNE at the Murzhik area of the Semipalatinsk Test Site, Kazakhstan; test of 1976 August 4

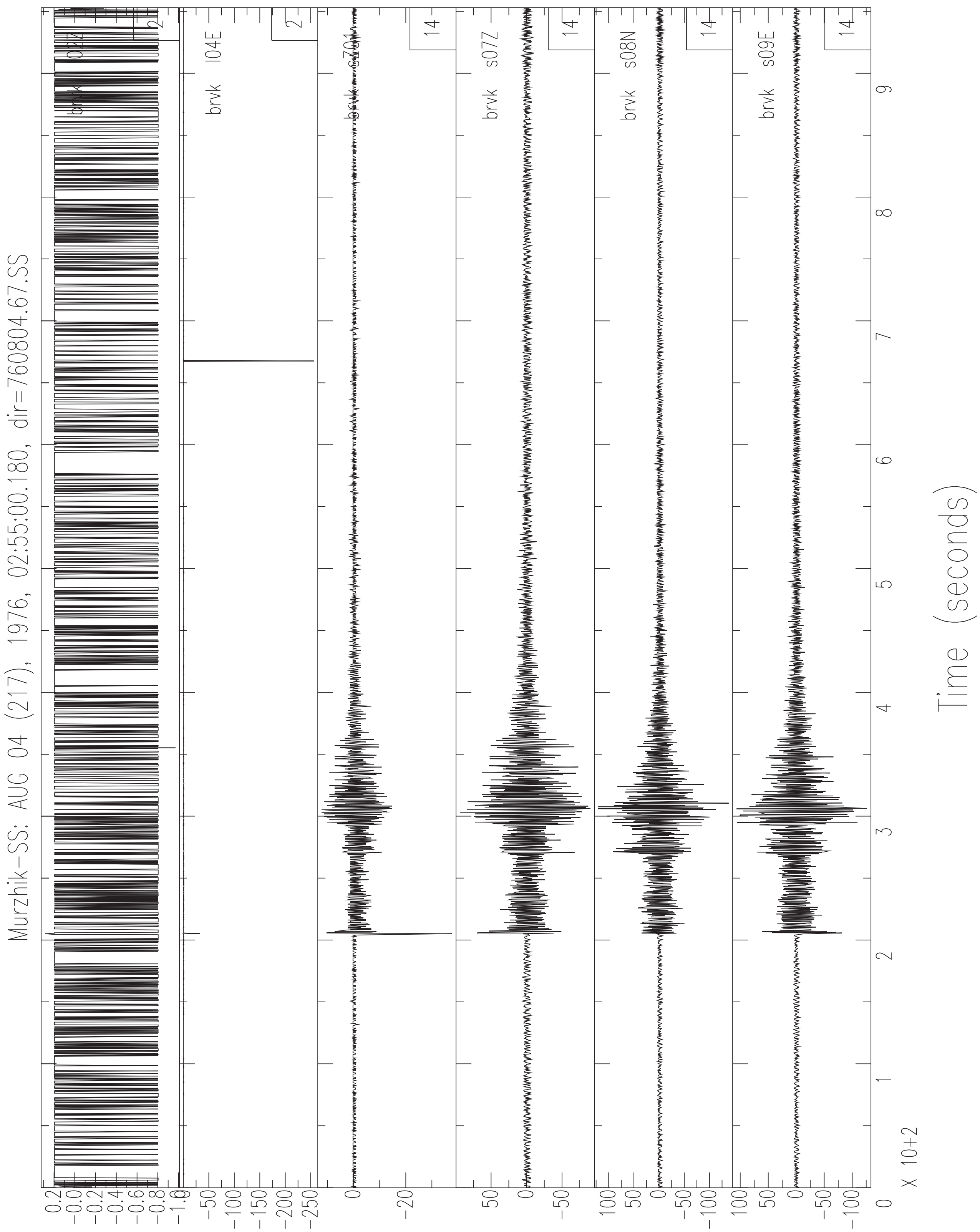

Figure 50. Last of five sets of BRV seismograms on the SS system for a UNE at the Murzhik area of the Semipalatinsk Test Site, Kazakhstan; test of 1980 April 4

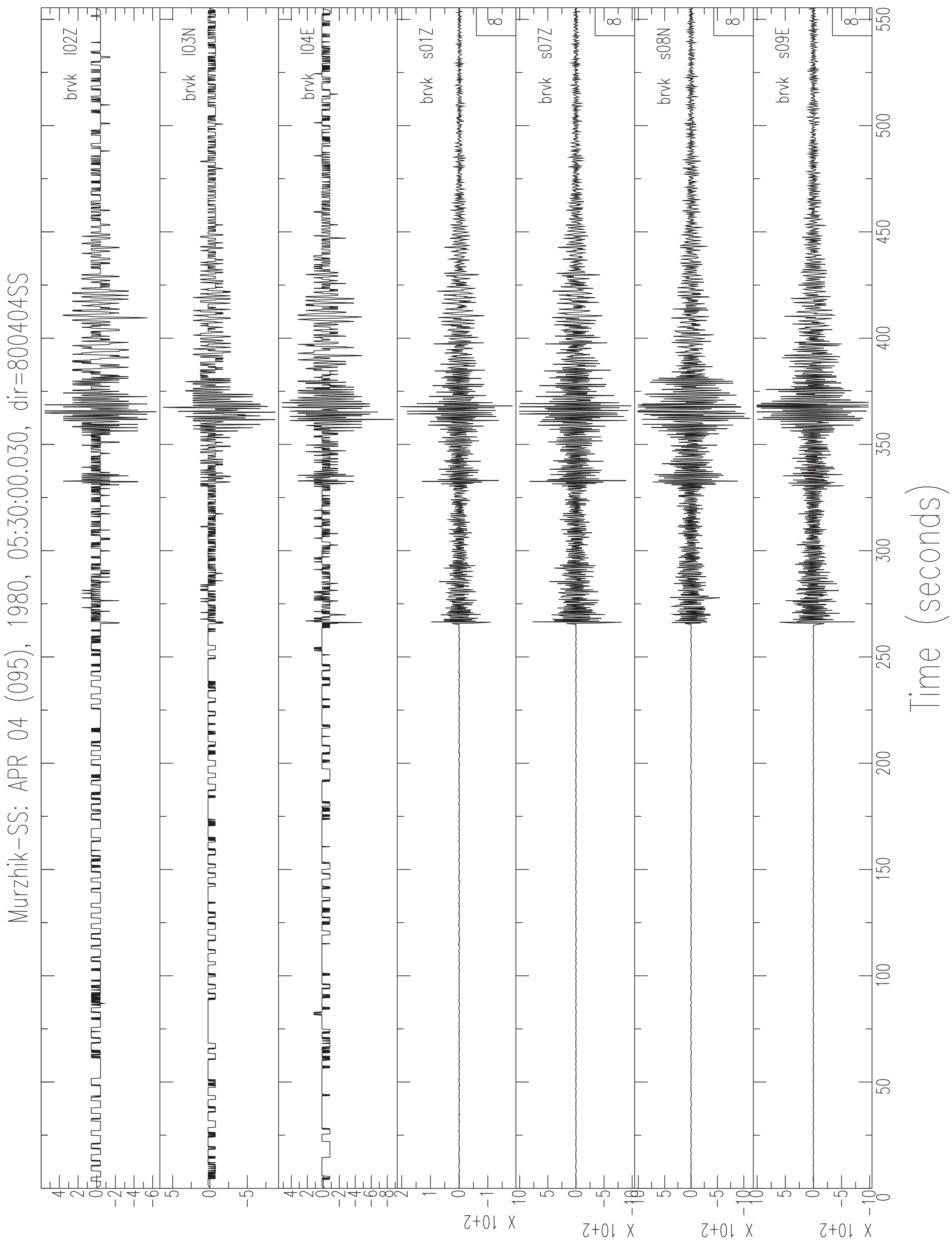

Figure 51. First of four sets of BRV seismograms on the TSG system for a UNE at the Murzhik area of the Semipalatinsk Test Site, Kazakhstan; test of 1978 March 19

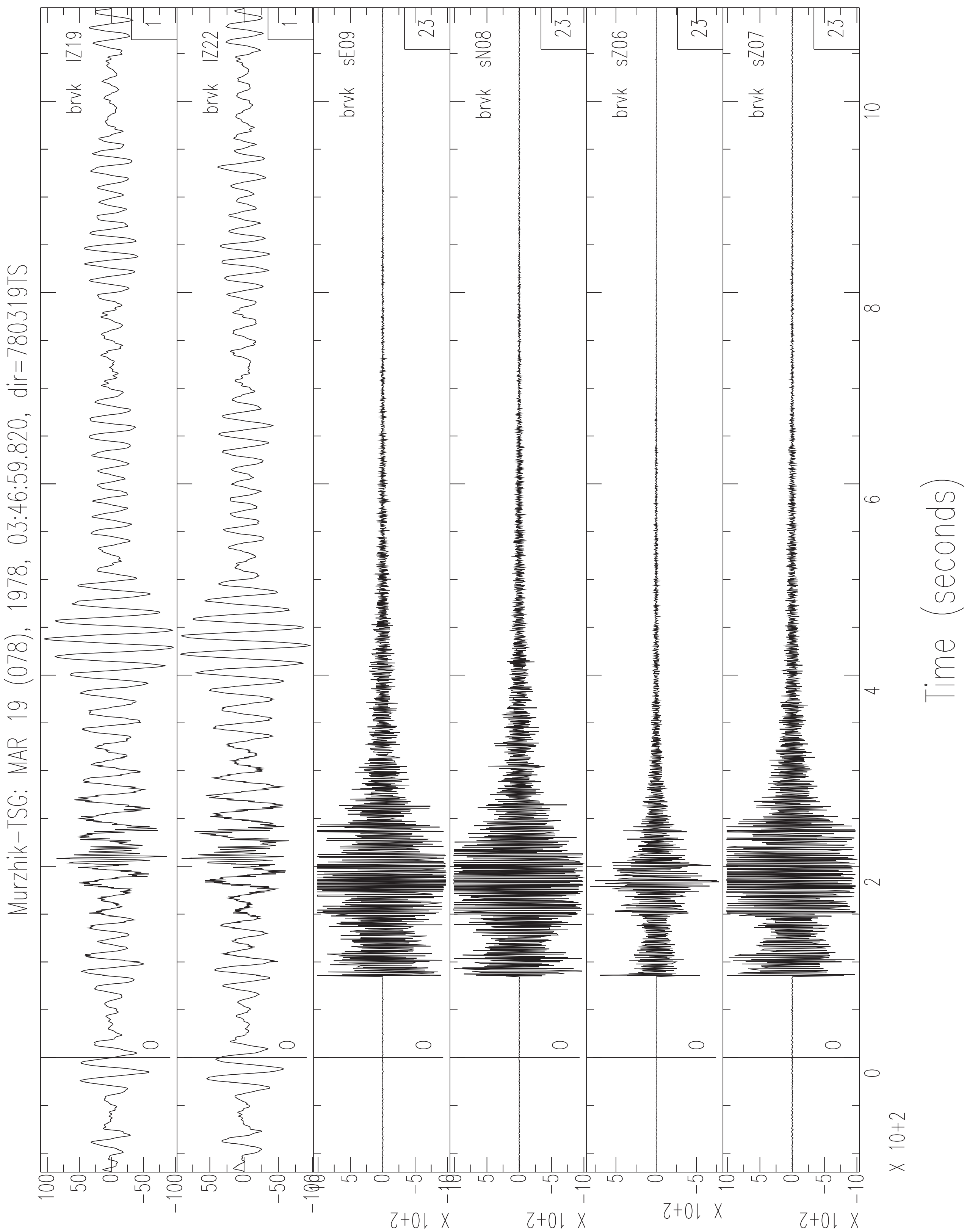

Figure 52. Last of four sets of BRV seismograms on the TSG system for a UNE at the Murzhik area of the Semipalatinsk Test Site, Kazakhstan; test of 1980 April 4

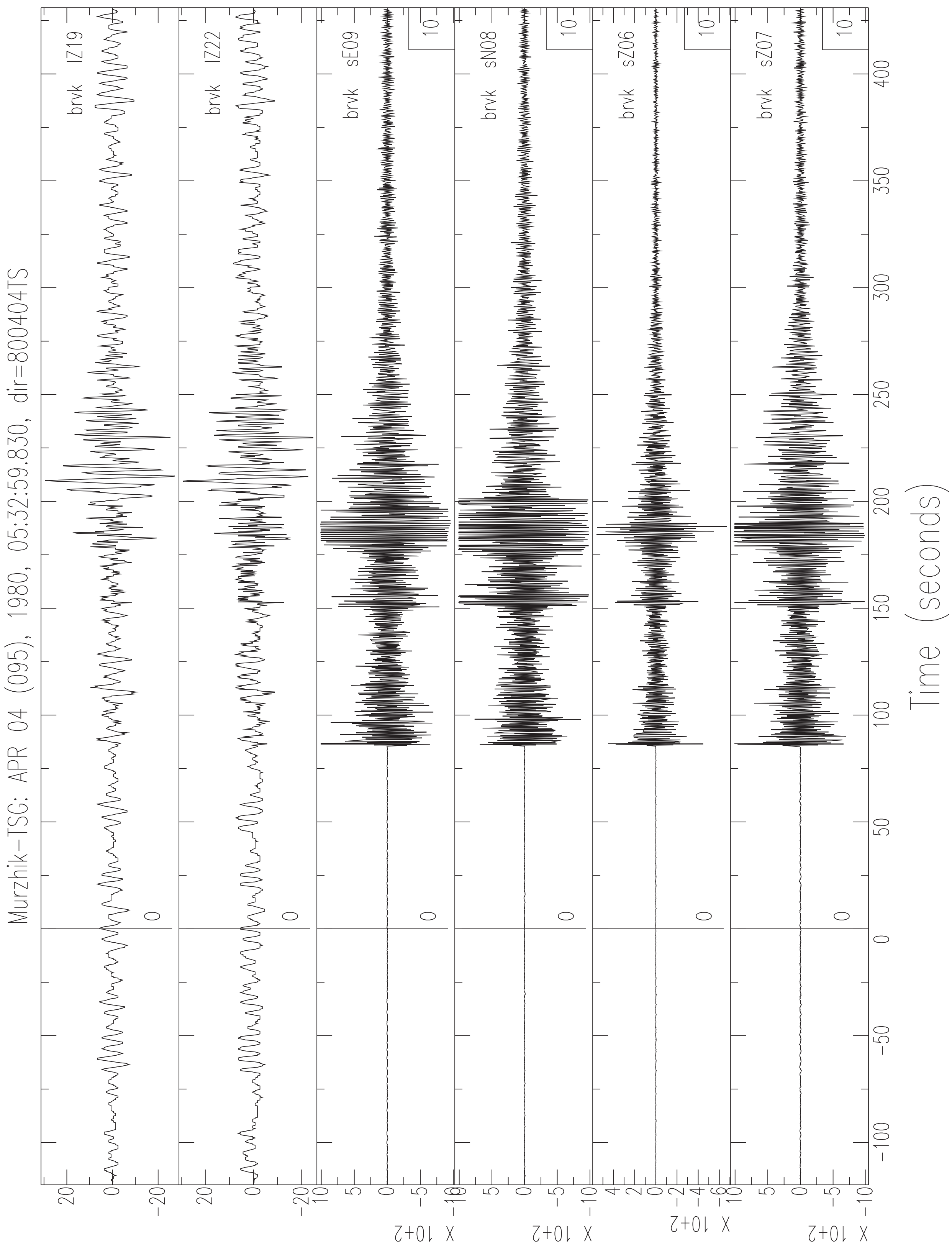

Figure 53. First of nine sets of BRV seismograms on the KOD system for a UNE at the Novaya Zemlya Test Site, Russia; test of 1967 October 21

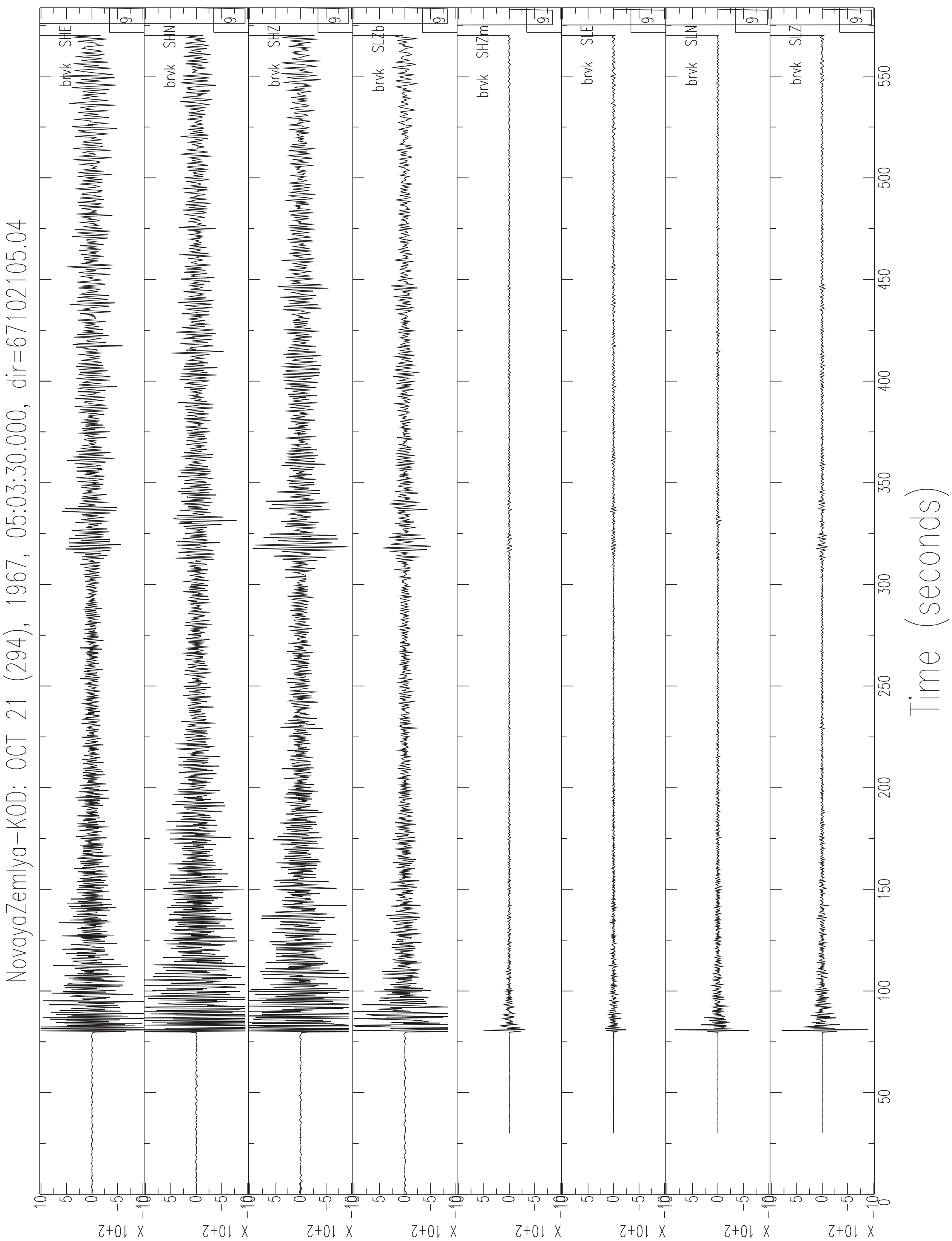

Figure 54. Last of nine sets of BRV seismograms on the KOD system for a UNE at the Novaya Zemlya Test Site, Russia; test of 1973 October 27

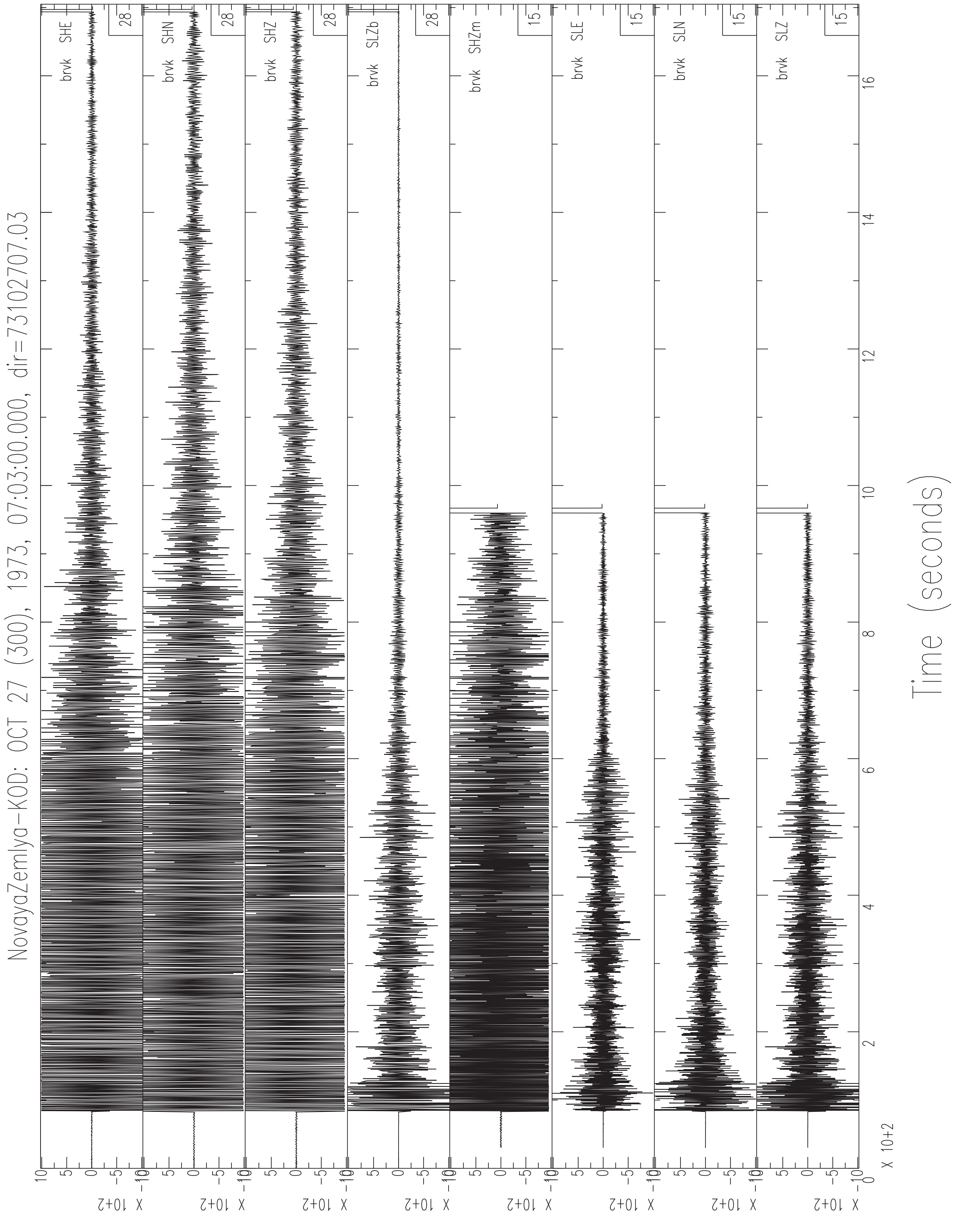

Figure 55. First of 17 sets of BRV seismograms on the SS system for a UNE at the Novaya Zemlya Test Site, Russia; test of 1973 September 27

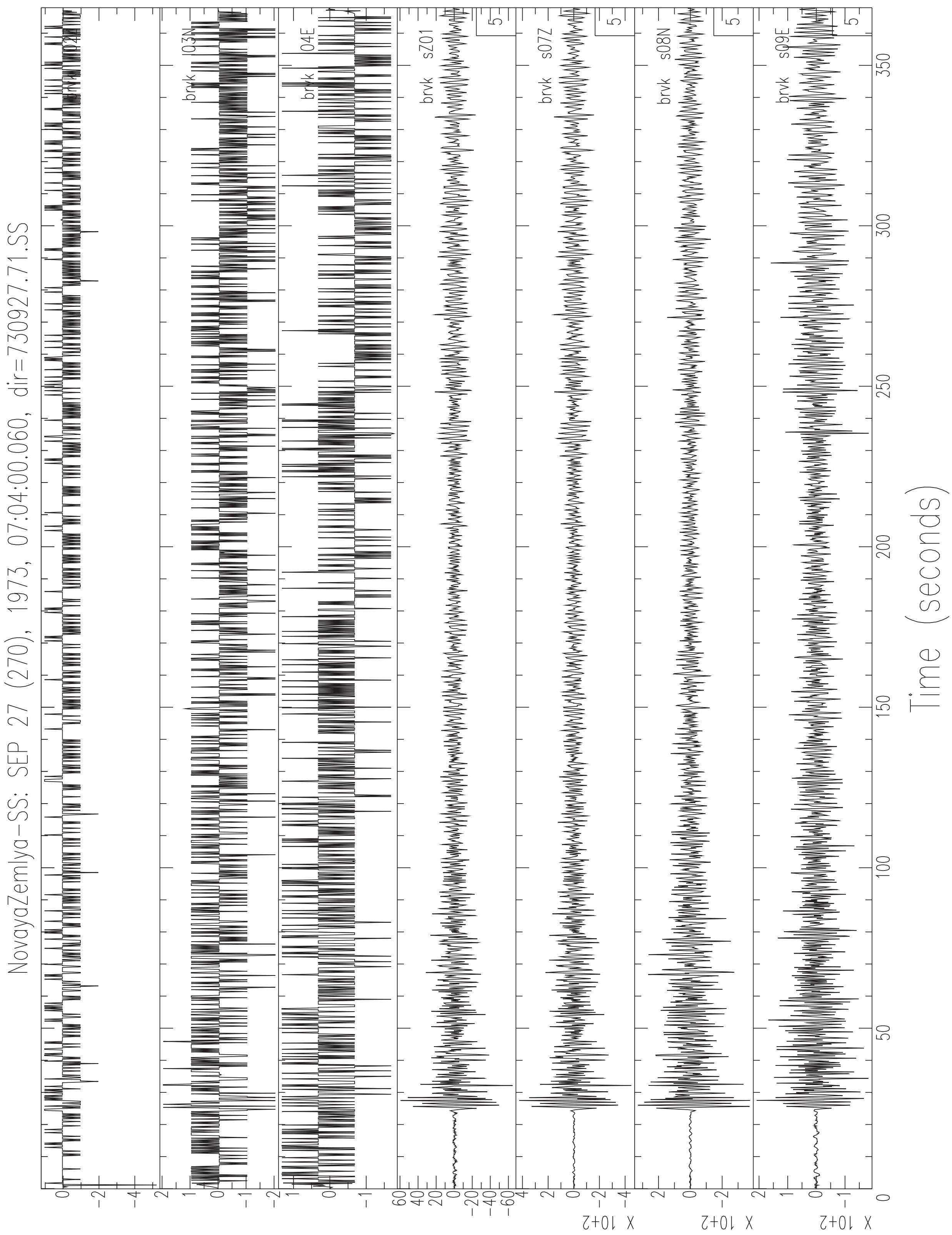

Figure 56. Last of 17 sets of BRV seismograms on the SS system for a UNE at the Novaya Zemlya Test Site, Russia; test of 1990 October 24

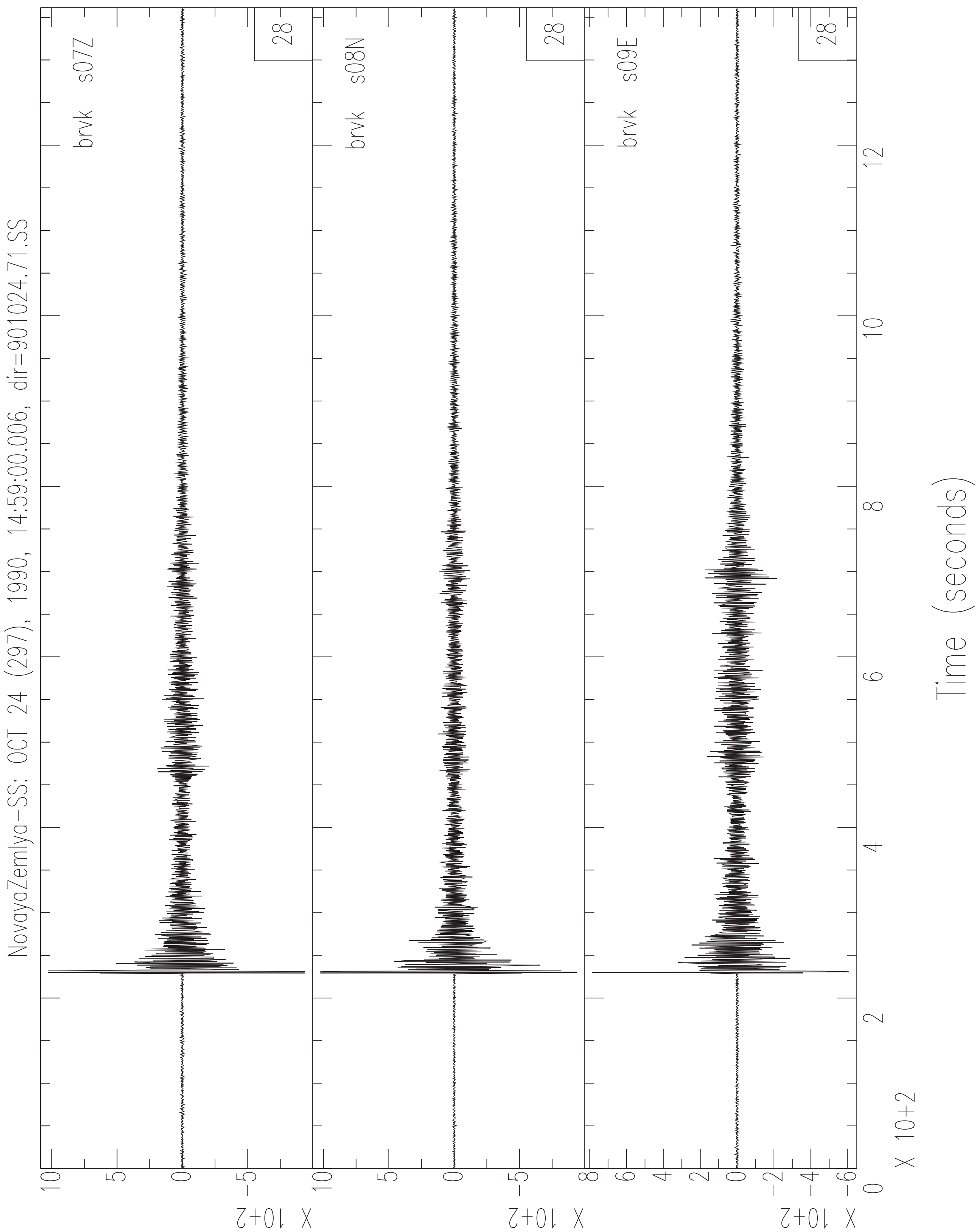

Figure 57. First of 19 sets of BRV seismograms on the TSG system for a UNE at the Novaya Zemlya Test Site, Russia; test of 1975 August 23

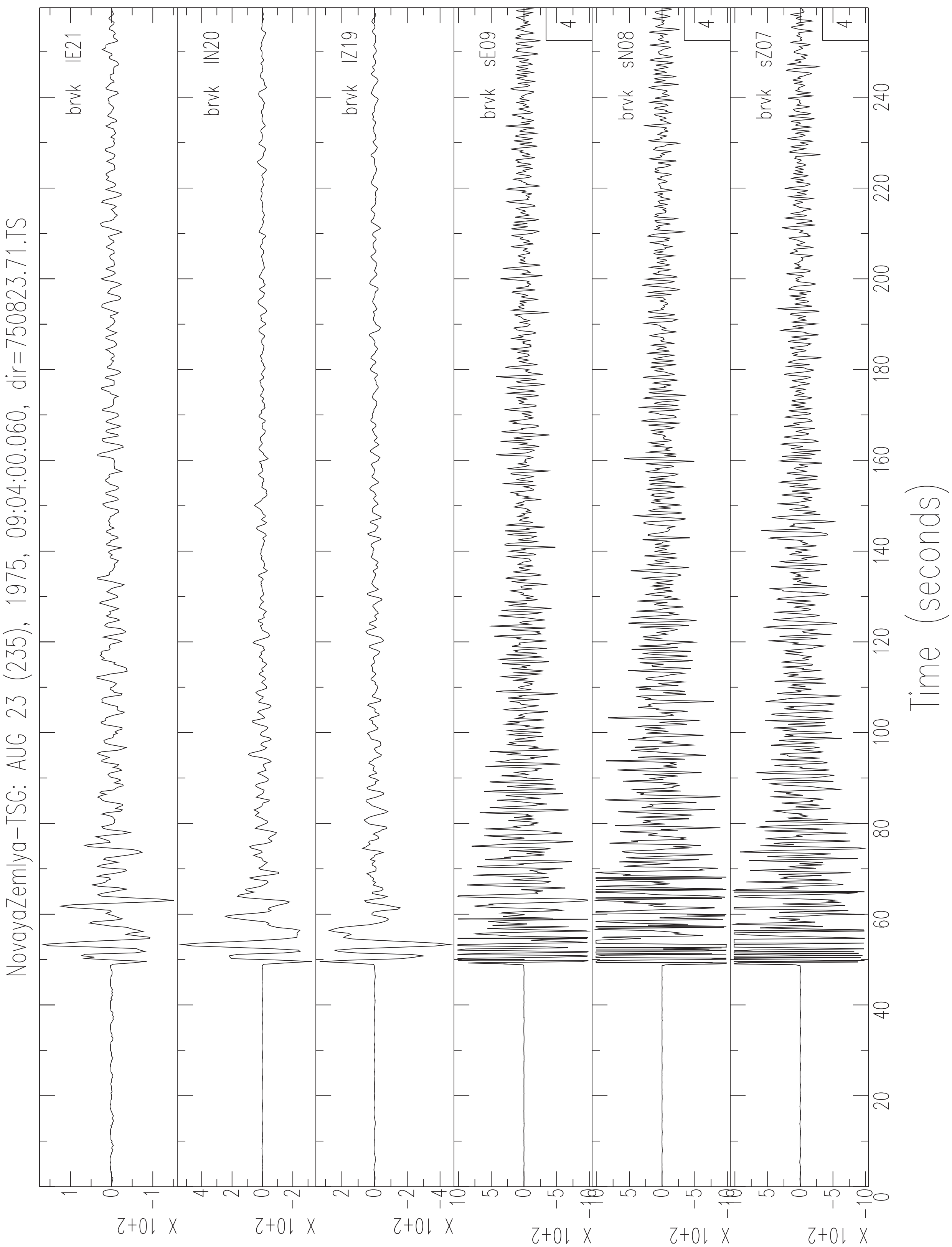

Figure 58. Last of 19 sets of BRV seismograms on the TSG system for a UNE at the Novaya Zemlya Test Site, Russia; test of 1990 October 24

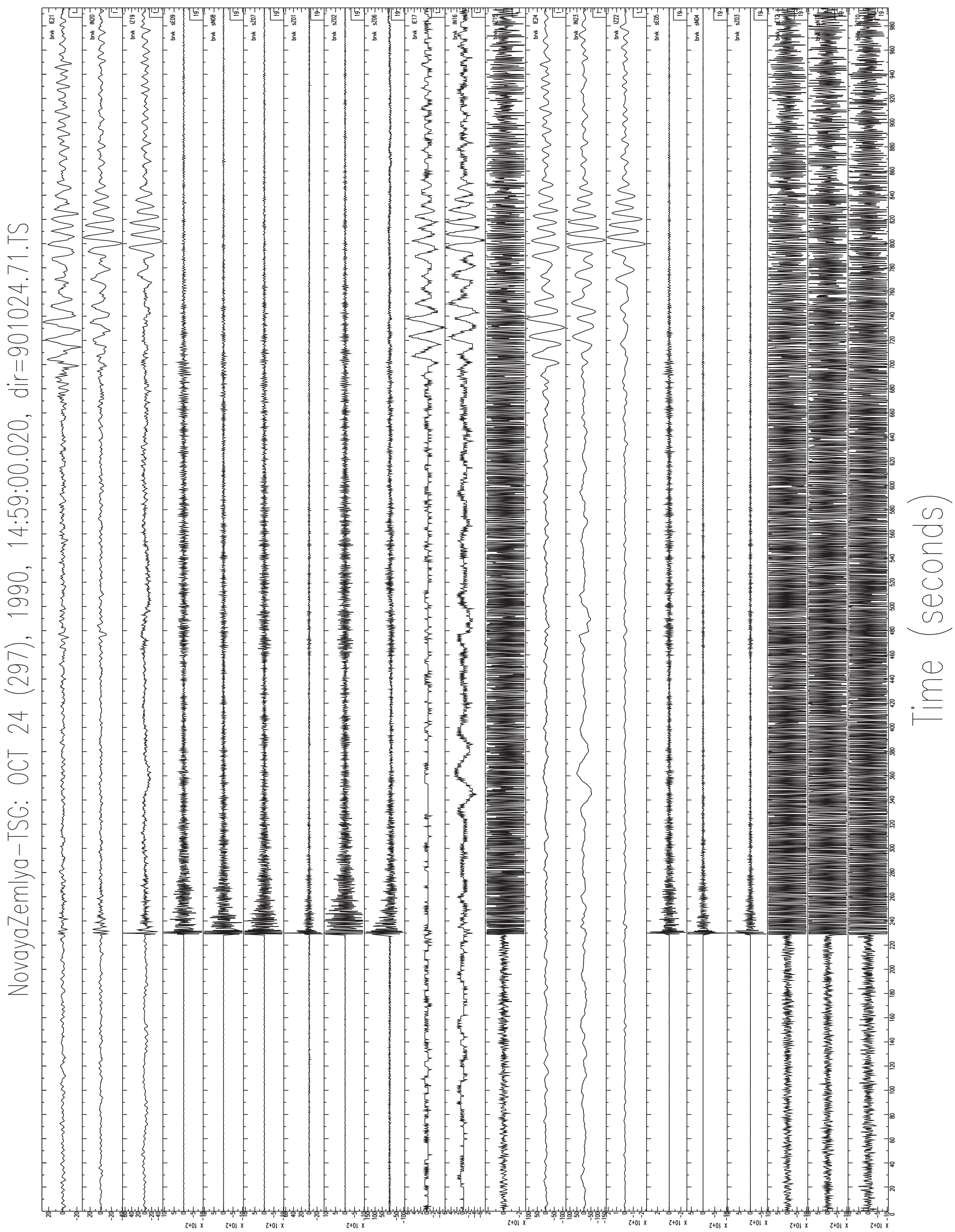

Figure 59. First of 27 sets of BRV seismograms on the KOD system for a PNE in the Soviet Union; test of 1967 October 6, at (57.7°N, 65.2°E), depth 172 m, 0.3 kt, mb 4.7

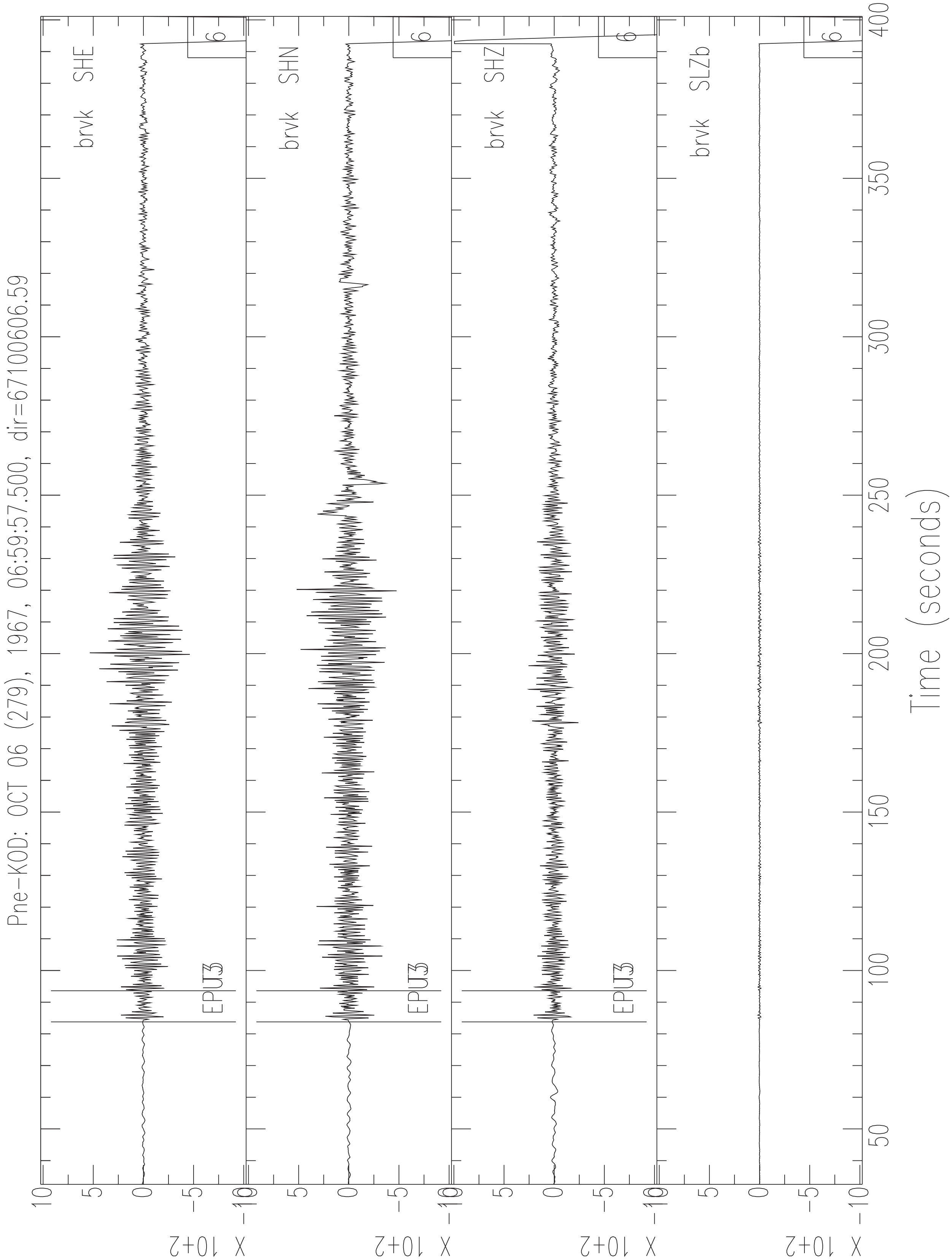

Figure 60. Last of 27 sets of BRV seismograms on the KOD system for a PNE in the Soviet Union; test of 1973 October 26, at (53.65°N, 55.4°E), depth 2036, 10 kt, mb 4.8

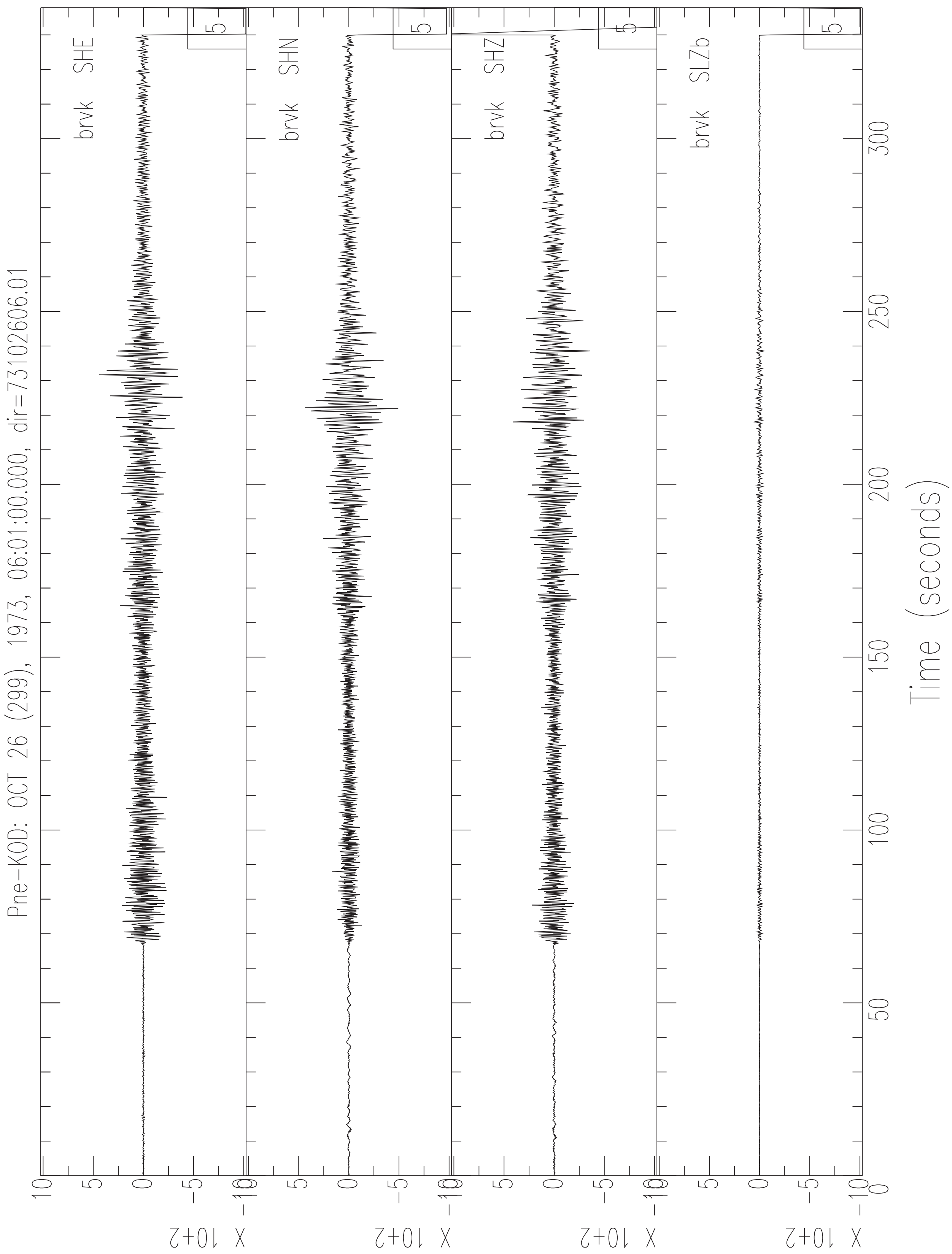

Figure 61. First of 38 sets of BRV seismograms on the SS system for a PNE in the Soviet Union; test of 1973 August 15, at (42.775°N, 67.408°E), depth 600 m, 6.3 kt, mb 5.3

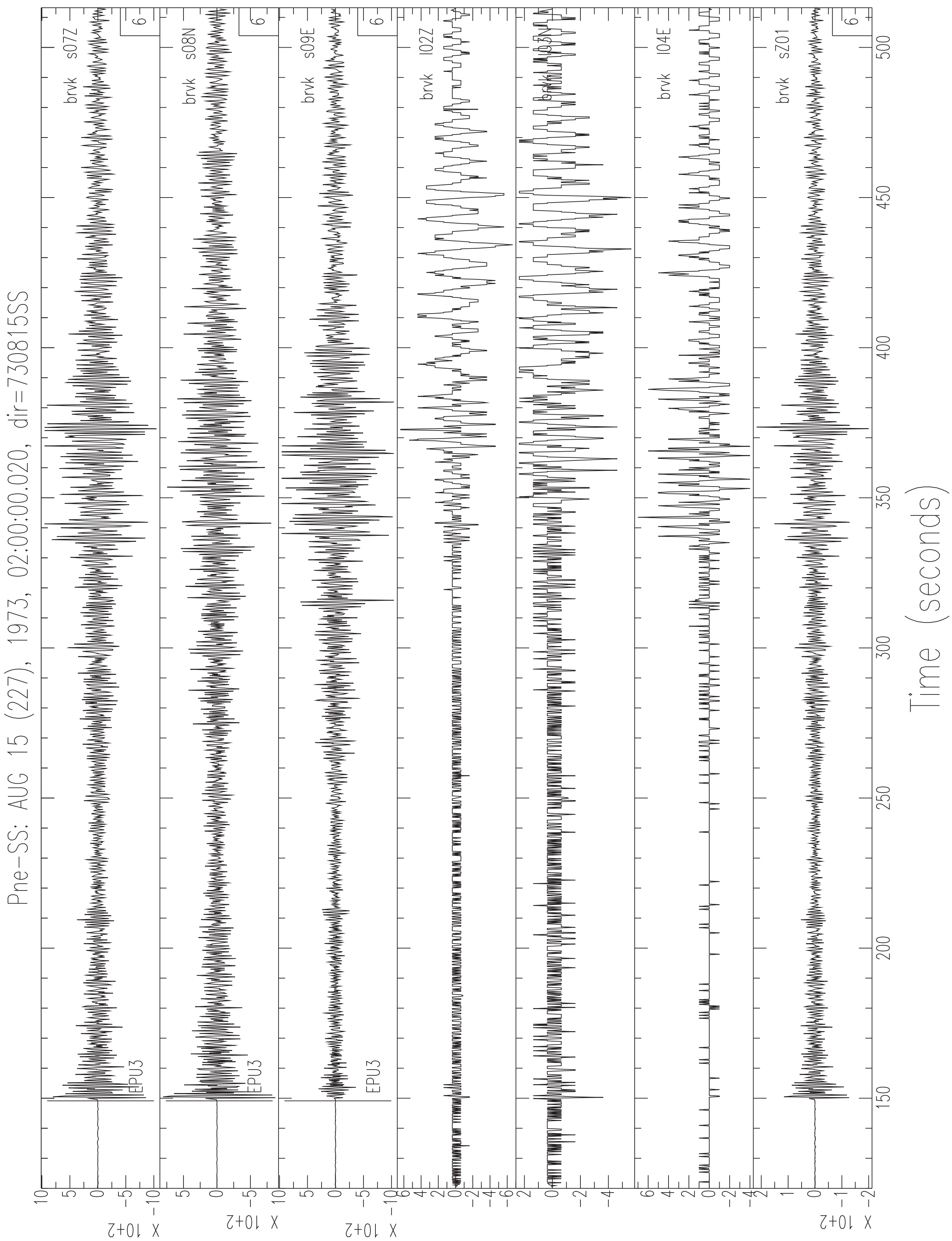

Figure 62. Last of 38 sets of BRV seismograms on the SS system for a PNE in the Soviet Union; tests of 1984 July 21, being three separate shots five minutes apart, centered at (51.37°N, 53.34°E), depth 900, 15 kt, mb 5.

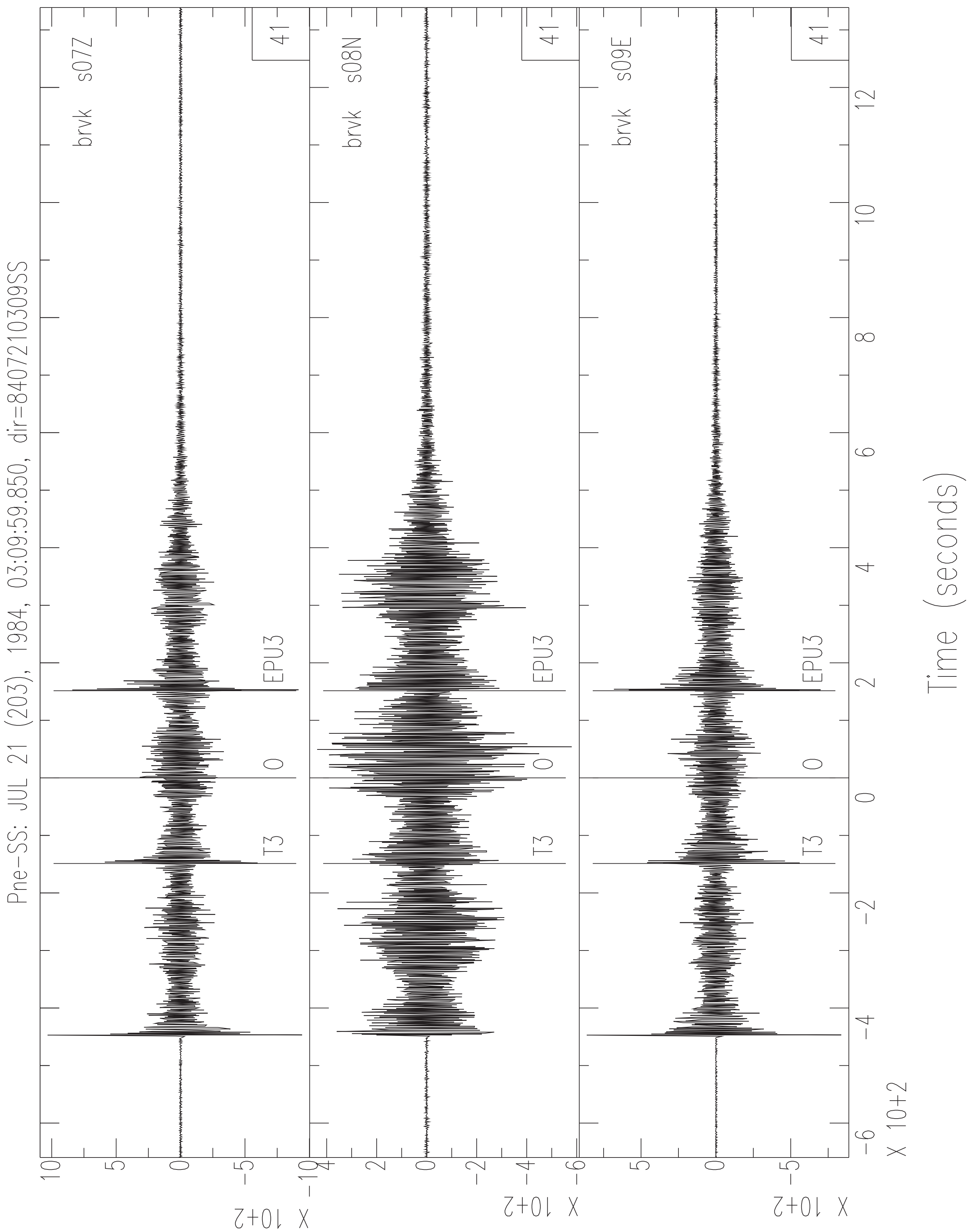

Figure 63. First of 27 sets of BRV seismograms on the TSG system for a PNE in the Soviet Union; test of 1976 March 29, at (47.897°N, 48.133°E), depth 986 m, 8 to 10 kt, mb 4.3. This was a partially decoupled shot in Azgir, Western Kazakhstan, but although it was detected teleseismically there is minimal signal at BRV. Signals are also available on the SS system. The 64 kt mb 6.0 shot on 1971 December 22 which made the cavity was well recorded on the KOD system.

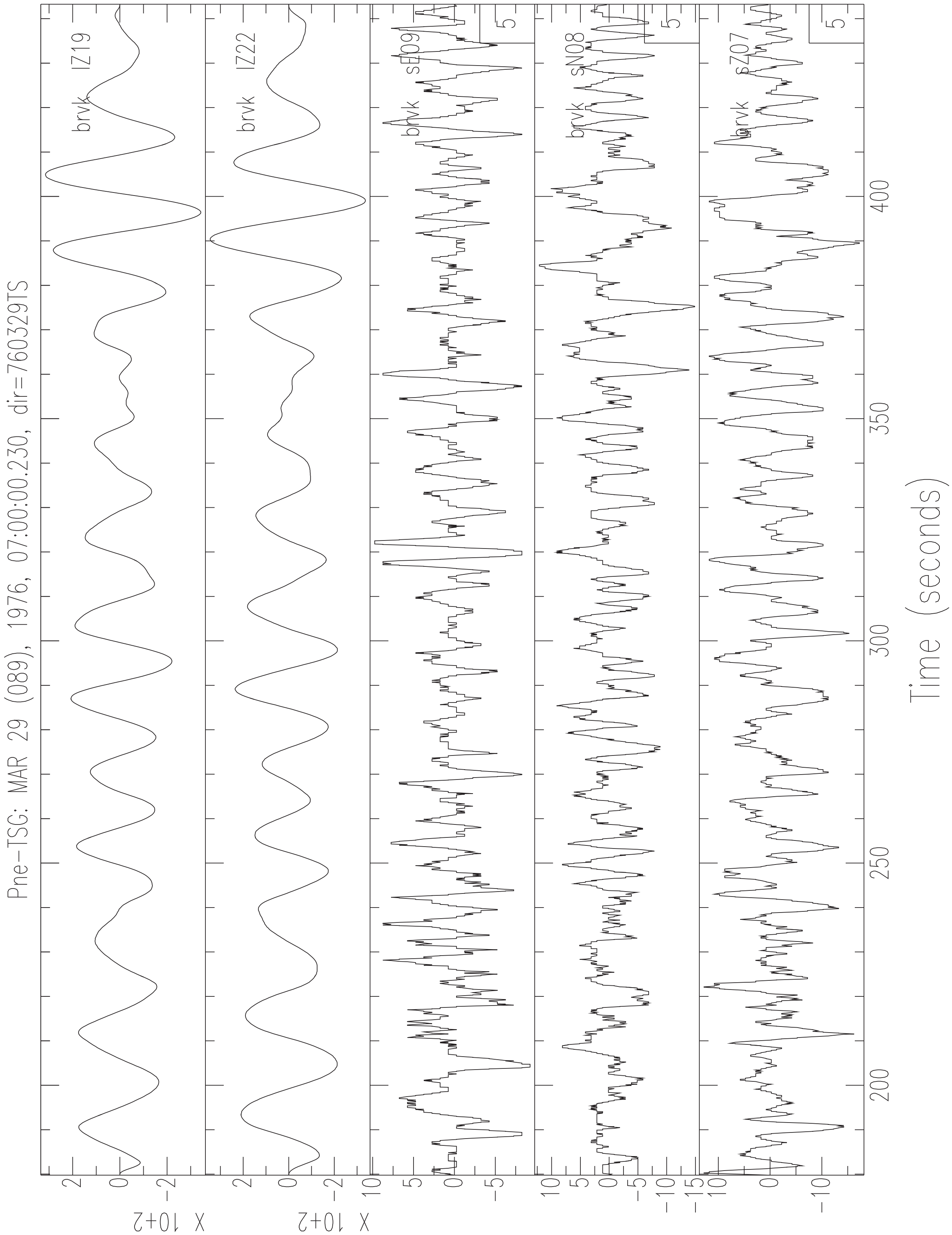

Figure 64. Last of 27 sets of BRV seismograms on the TSG system for a Soviet PNE; test of 1984 October 27, at (46.9°N, 48.10°E), depth 1000, 3.2 kt, mb 5.0 in salt

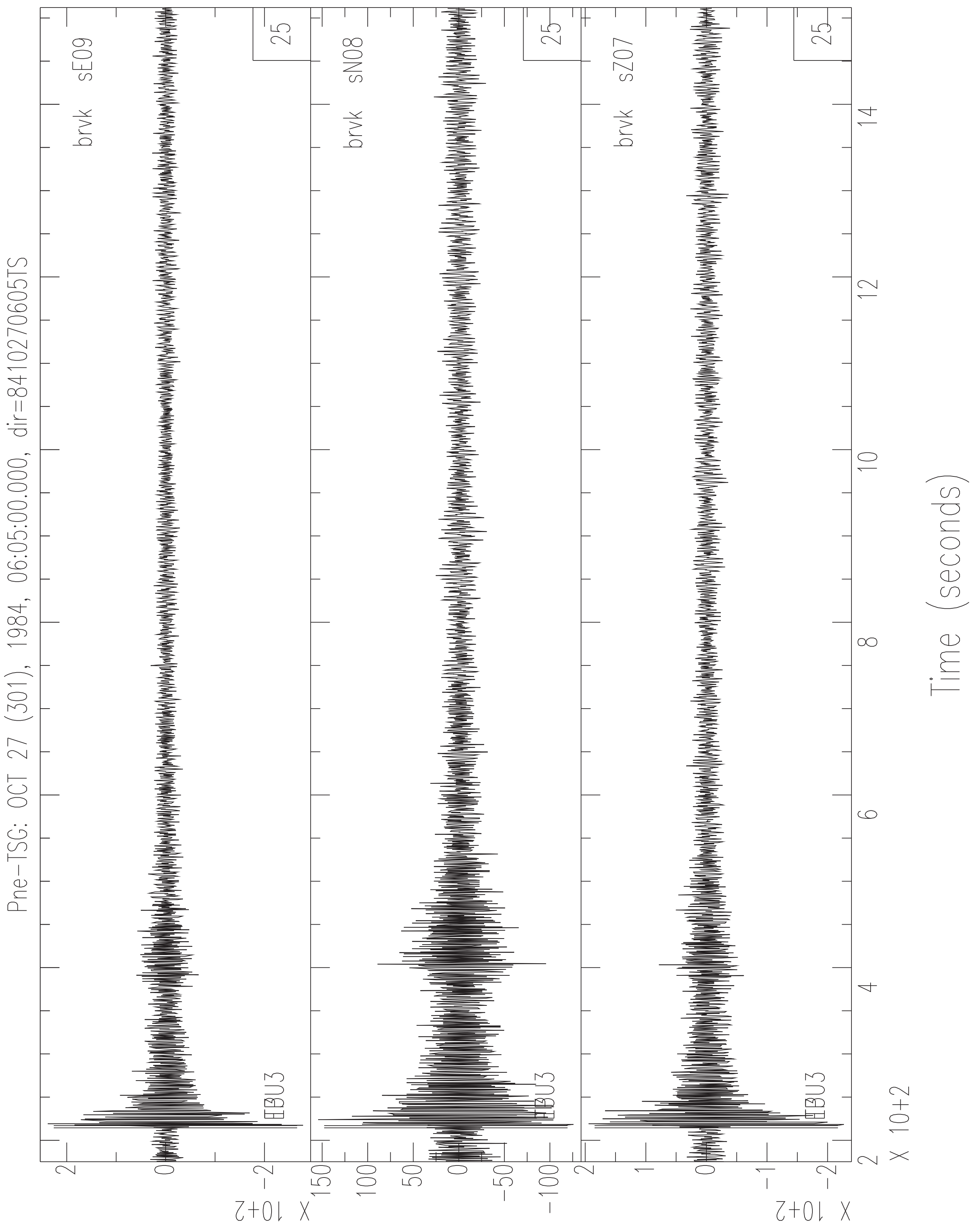

Figure 65. The only set of BRV seismograms on the KOD system for a UNE at the Lop Nor Test Site, China; China's first UNE, of 1969 September 22

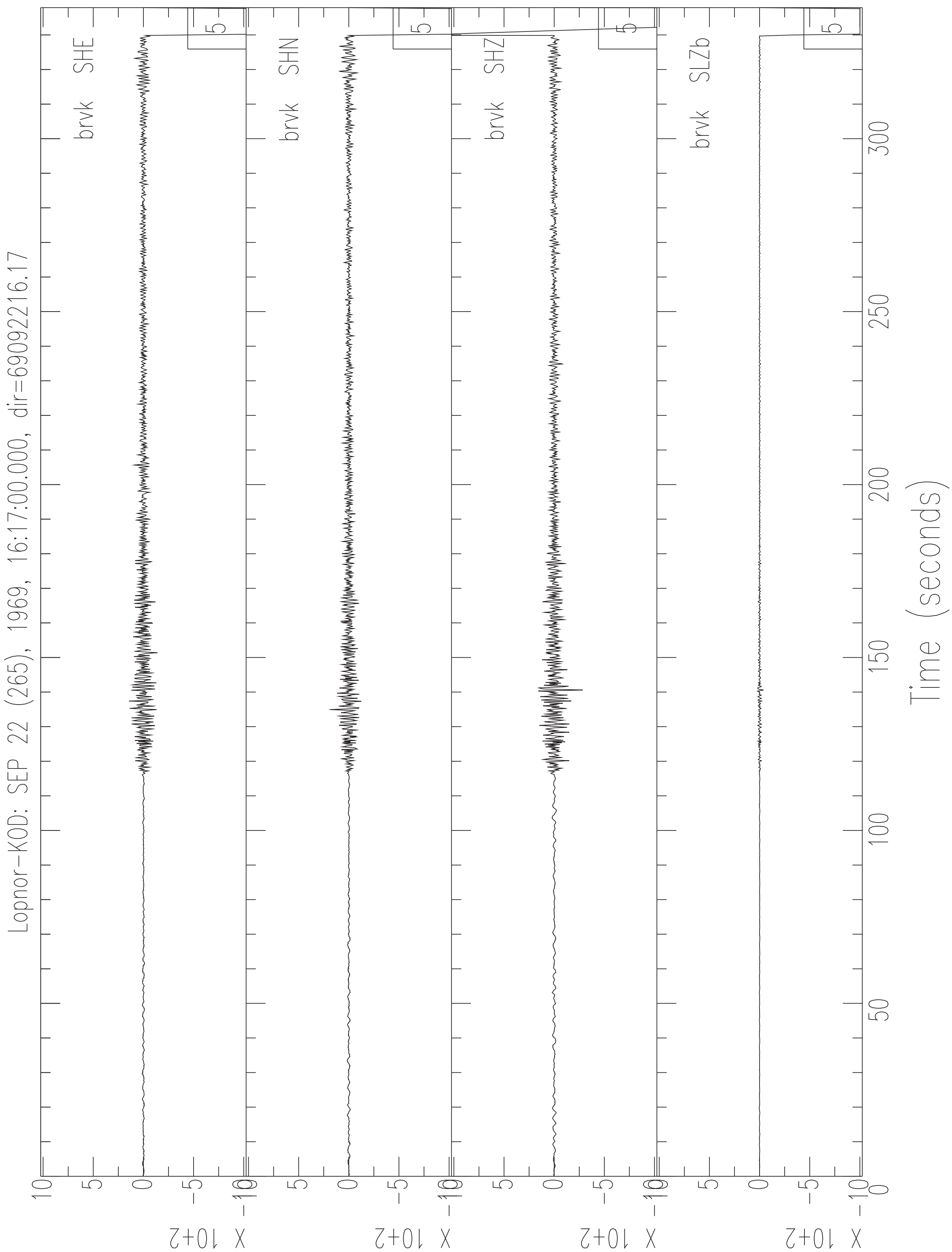

Figure 66. First of seven sets of BRV seismograms on the SS system for a UNE at the Lop Nor Test Site, China; test of 1976 October 17

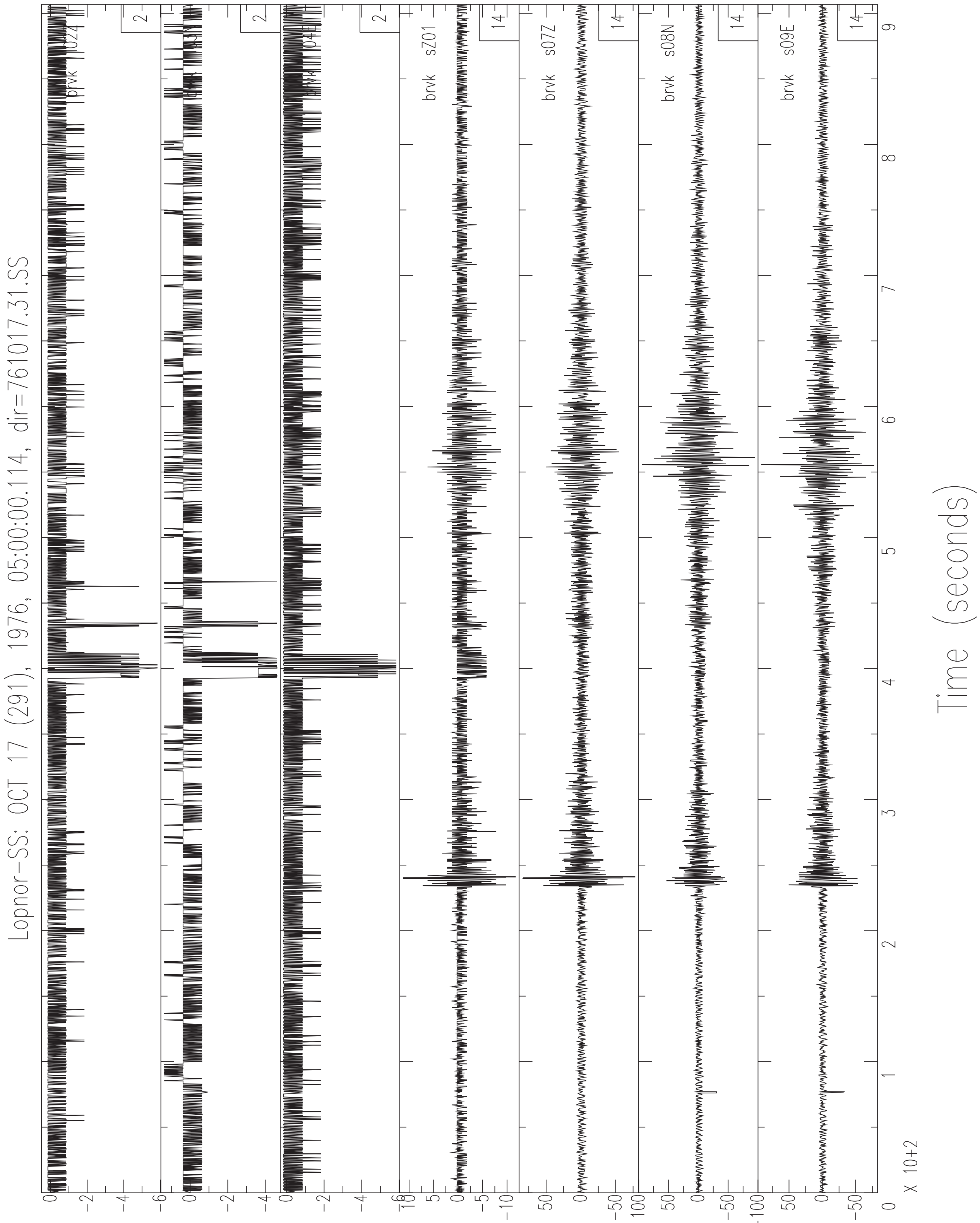

Figure 67. Last of seven sets of BRV seismograms on the SS system for a UNE at the Lop Nor Test Site, China; test of 1983 October 06

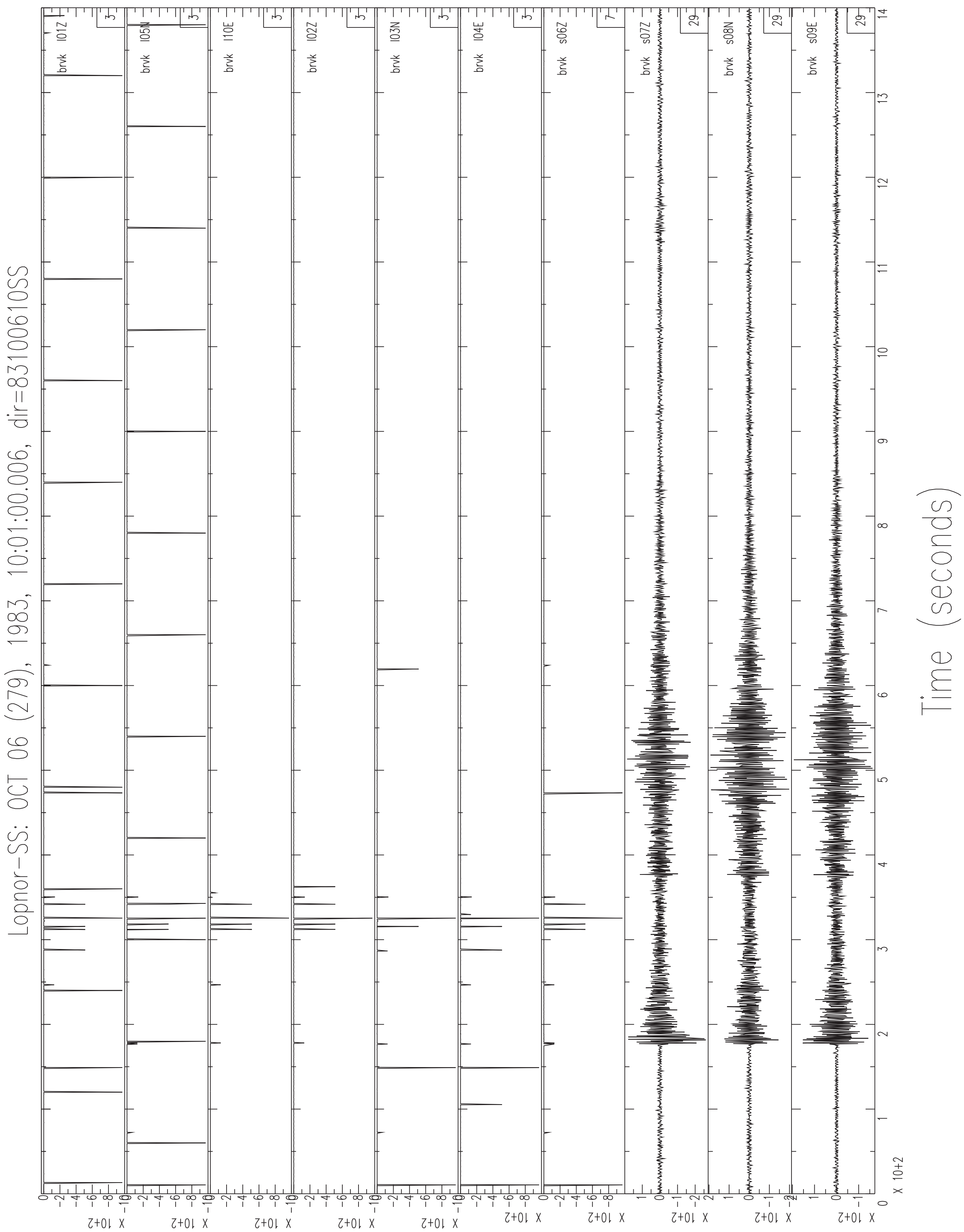

Figure 68. First of eight sets of BRV seismograms on the TSG system for a UNE at the Lop Nor Test Site, China; test of 1978 October 14

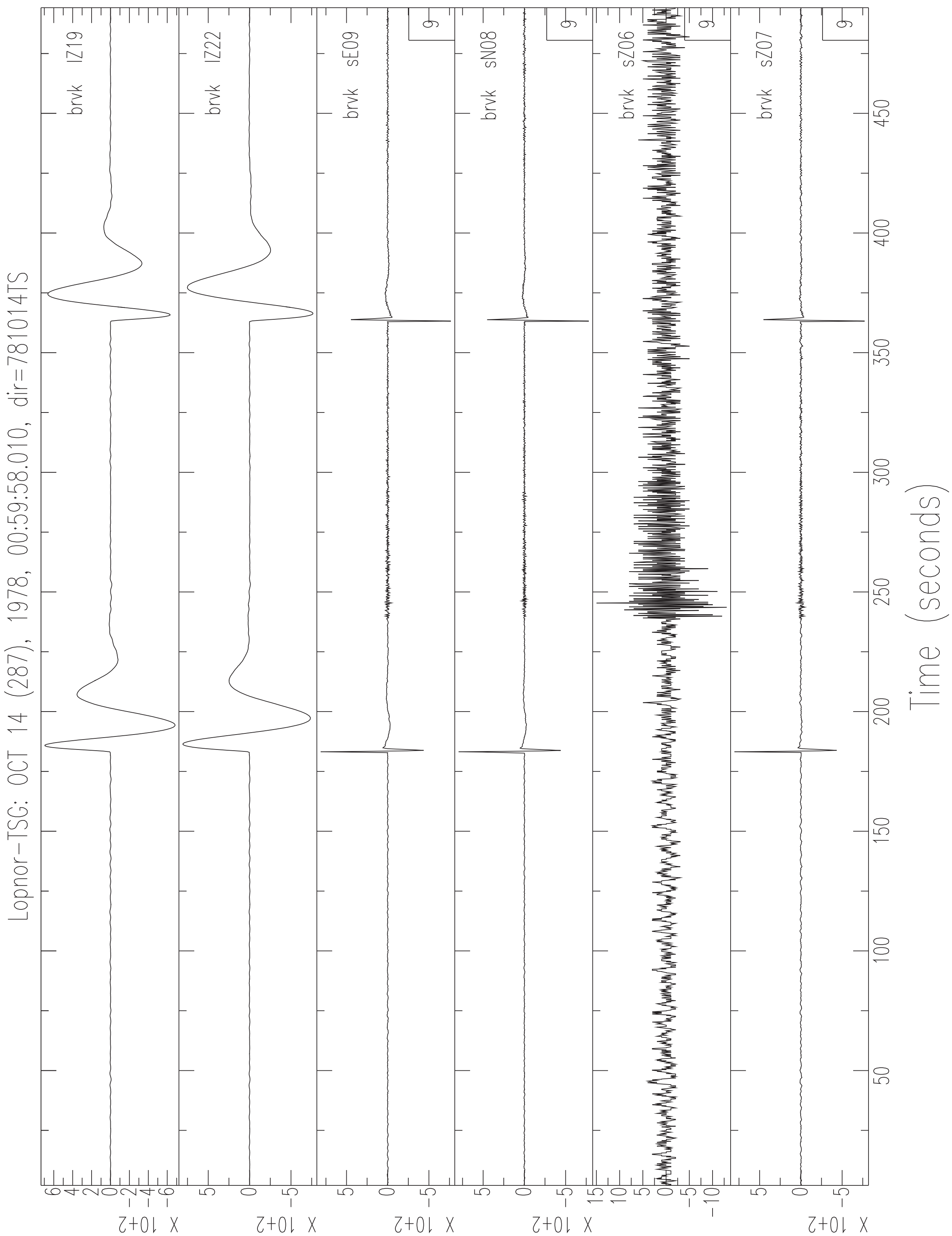

Figure 69. Last of eight sets of BRV seismograms on the TSG system for a UNE at the Lop Nor Test Site, China; test of 1995 May 15

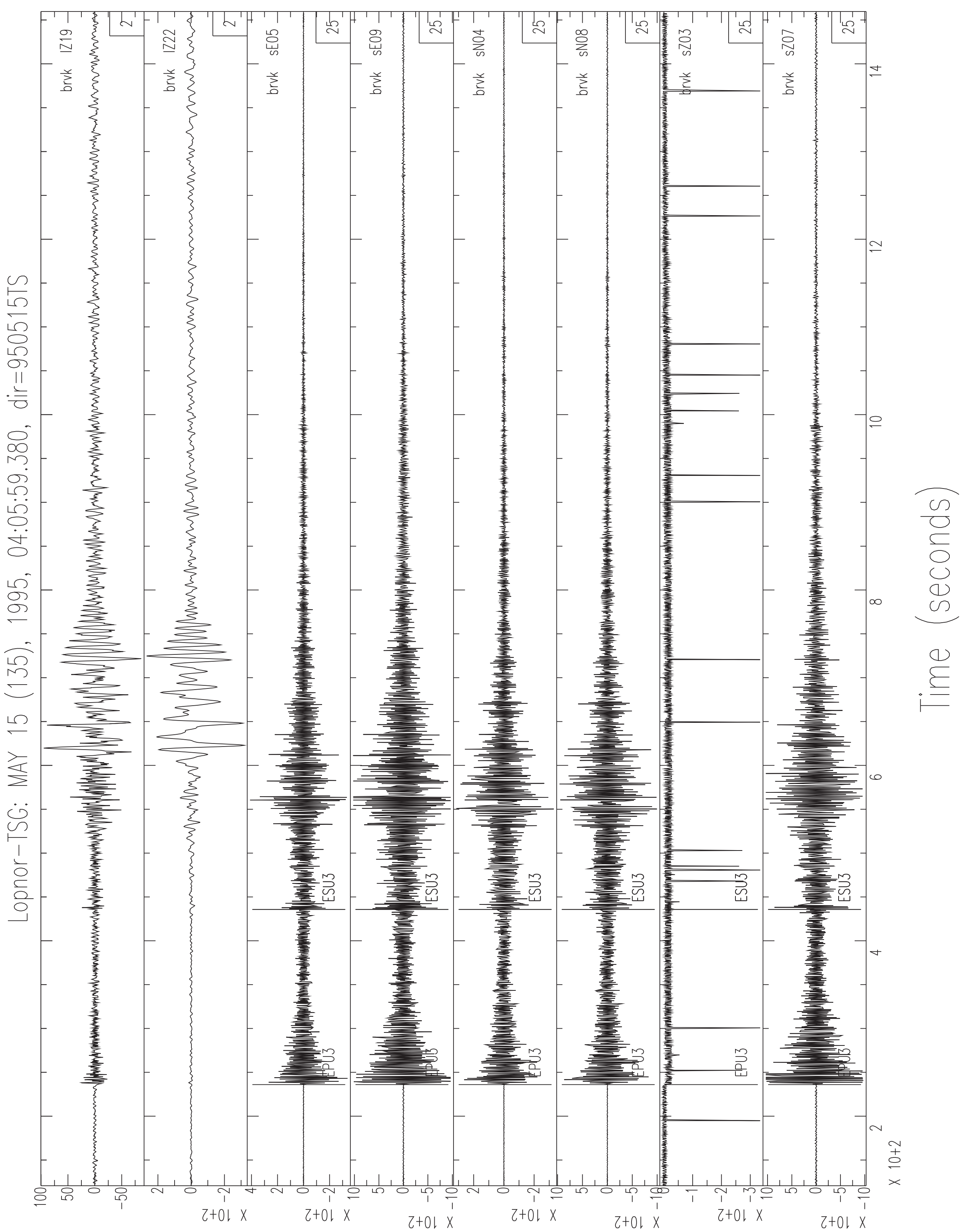

underground nuclear explosion at that site. Atmospheric nuclear explosions at Lop Nor continued until 1980.)

4.1. Example Seismograms

Thus, Figure 34 shows the first of seven sets of BRV seismograms on the KOD system for a UNE at the Balapan area of the Semipalatinsk Test Site, Kazakhstan (the test of 1968 June 19). It shows high-gain and low-gain channels, and immediately it is apparent which channels are appropriate for picking arrival times (high-gain), measuring spectral levels (low-gain) and quantifying coda (both high-gain and low-gain).

Figure 35 shows the last of the KOD recordings for a Balapan UNE (1973 July 23). These two sets, Figures 34 and 35, are short-period records, and contrast with information from an extended bandwidth contained in Figures 36 and 37 (the first and last UNEs at Balapan recorded on the SS system); and Figures 38 and 39 (the first and last UNEs at Balapan recorded on the TSG system). The longer-period records have *Rg* as the strongest phase at this regional distance.

The earliest Eurasian UNE, digitally recorded at Borovoye, is shown in Figure 47, and is for an explosion at the Murzhik sub-region of the Semipalatinsk Test Site.

There is a total of 343 sets of records for UNEs at all sub-regions of the Semipalatinsk Test Site, and these regional signals with their *Pg*, *Pn*, *Sn*, *Lg*, and *Rg* phases are now available for study of different source effects as documented by a digital station that long operated at the same distance from the test site. In contrast with these regional signals, the recordings from Novaya Zemlya UNEs in Figures 53–58 are show impulsive teleseismic *P*-wave arrivals.

CONCLUSIONS

We have produced nearly 500 sets of digital seismograms of underground nuclear explosions in Eurasia. They are an outcome of decades of operation of a sophisticated and long-term effort to acquire monitoring data in Central Asia that involved Russia, Kazakhstan, and (at a later stage) personnel from the United States. This was an enormous project, with two earlier phases. First, there was a phase that lasted about thirty years during which the data were acquired (1966 to 1995), then a second stage during which the digital data were salvaged from deteriorated magnetic tapes. The present project, described in detail in this Final Report, was the effort to remove glitches and add instrument responses to make the data usable in by researchers using modern methods of data management. This work has now been completed, with details to be found in this report, and the data are now openly available to the research community.

REFERENCES

Adushkin, V. V. and V. A. An (1990). Seismic observations and underground nuclear shot monitoring at Borovoye Geophysical Observatory, Izvestiya Akademii Nauk SSSR: Fizika Zemli, 47-59, No. 12, (also available in English as Physics of the Solid Earth, 1023-1031, #12 for 1990).

Adushkin, Vitaly V. and Vadim A. An (1993). Teleseismic Monitoring of Underground Nuclear Explosions at the Nevada Test Site from Borovoye, Kazakhstan, *Science & Global Security* **3**, 289-309.

Baker, D. W.-Y.Kim, H. Patton, G. Randall, and P. Richards (2009). Improvements to a major digital archive of seismic waveforms from nuclear explosions: the Borovoye Seismogram Archive, Proceedings of the 31st Monitoring Research Review, Tucson, Arizona.

Bocharov, V.S., S.A. Zelentsov, and V.N. Mikhailov (1989). Characteristics of 96 UNTs at the STS. *Atomic Energy*, **67**, 210-214.

Engdahl, R., Relocation of Chinese underground nuclear explosions by cluster analysis, personal comm., March, 2001.

Khalturin, V.I., T.G. Rautian and P.G. Richards (2001). A study of small magnitude seismic events during 1961-1989 on and near the Semipalatinsk Test Site, Kazakhstan, Pure and Applied Geophysics, 158, 143-171.

Kim, W-Y. and G. Ekström (1996). Instrument responses of digital seismographs at Borovoye, Kazakstan, by inversion of transient calibration pulses, *Bull. Seism. Soc. Am.* **86**, 191-203.

Kim, W-Y., P.G. Richards, V. Adushkin and V. Ovtchinnikov (2001). Borovoye digital seismogram archive for underground nuclear tests during 1966-1996, A report of Lamont-Doherty Earth Observatory, 41 pages, April 2001, available online as http://www.ldeo.columbia.edu/Monitoring/Data/Brv_arch_ex/brv_text_table.pdf

Kim, W.-K., H. Patton, G. Randall, and P. Richards (2007). Improvements to a major digital archive of seismic waveforms from nuclear explosions: Borovoye Seismogram Archive, Proceedings of the 29th Monitoring Research Review, Denver, Colorado.

Kim, W.-K., H. Patton, G. Randall, and P. Richards (2008). Improvements to a major digital archive of seismic waveforms from nuclear explosions: Borovoye Seismogram Archive, Proceedings of the 30th Monitoring Research Review, Portsmouth, Virginia.

Leith, W. (1998). Degelen Nuclear Test and Tunnel Data, Technical Memorandum dated June 26, 1998, to the Defense Threat Reduction Agency, US Geological Survey; and Technical Reports to the Defense Threat Reduction Agency (formerly Defense Special Weapons Agency; formerly Defense Nuclear Agency), under Contract DNA001-95-C-1079.

Lilwall, R.C. and J. Farthing (1990). Joint Epicenter Determination of Soviet Underground Nuclear Explosions 1973-89 at the Semipalatinsk Test Site, AWE Report No.O 12/90, HMSO, London.

Marshall, P.D., D. Porter, J.B. Young and P.A. Peachell (1994). Analysis of short-period seismograms from explosions at the Novaya Zemlya test site in Russia, AWE Report No. O 2/94, HMSO, London.

Marshall, P.D., T.C. Bache and Lilwall R.C. (1985). Body wave magnitude and location of Soviet Underground Explosions at the Semipalatinsk Test Site, AWRE Report No. O 16/84, HMSO, London.

Mikhailov, V. N., chief editor (1996). "USSR Nuclear Weapons Tests and Peaceful Nuclear Explosions, 1949 through 1990," Ministry of Atomic Energy and Ministry of Defense, Russian Federation, Russian Federation Nuclear Center - VNIEF, Sarov, 63 pages.

Osadchiy, A.P. (1972). Magnification of a Digital Seismograph System, Seysmicheskiye pribory, AN USSR, Institut fiziki Zemli, No. 6, 108-110.

Osadchiy, A.P. and S.K. Daragan (1966). The KOD Digital Seismograph System, Vychislitel'naya seysmologiya, Mashinnaya interpretatsiya seysmicheskikh voln (Computational Seismology, Computer Interpretation of Seismic Waves), AN USSR, Institut fiziki Zemli, No. 2, 183-195.

Richards, P.G. (2000). Accurate estimates of the absolute location of underground nuclear tests at the northern Novaya Zemlya Test Site, Proceedings of Second Workshop on IMS Location calibration, 10-24 March 2000 (Oslo, Norway).

Richards, Paul G., Won-Young Kim, and Göran Ekström (1992). The Borovoye Geophysical Observatory, Kazakhstan, feature article in EOS, Transactions of the American Geophysical Union, 73, 201 and 205-6.

Ringdal, F., Marshall, P.D., and Alewine, R.W. (1992), Seismic yield determination of Soviet underground nuclear explosions at the Shagan River test site, Geophys. J. Int., 109, 65 - 77.

Rousseeuw, P.J. and C. Croux, (1993), Alternatives to the median absolute deviation, J. Am. Stat. Assoc., 88, 1273-1283.

Shishkevish, Charles (1974). Soviet Seismographic Stations and Seismic Instruments, Part I, A report for DARPA, R-1647-ARPA, RAND Cooperation, Santa Monica, CA 90406.

Shishkevish, Charles (1975). Soviet Seismographic Stations and Seismic Instruments, Part II, A report for DARPA, R-1647-ARPA, RAND Cooperation, Santa Monica, CA 90406.

Sultanov, D. D., J.R. Murphy and Kh.D. Rubinstein (1999). A seismic source summary for Soviet peaceful nuclear explosions, Bulletin of the Seismological Society of America, 89, 640-647.

List of Symbols, Abbreviations, and Acronyms

AFRL	Air Force Research Laboratory
BRV	Borovoye (a small village in Northern Kazakhstan)
CTBT	Comprehensive Nuclear-Test-Ban Treaty
DARPA	Defense Advanced Research Projects Agency
KOD	The Russian abbreviation for the first seismographic system used at Borovoye
LANL	Los Alamos National Laboratory
LDEO	Lamont-Doherty Earth Observatory of Columbia University
MAD	Median Absolute Deviation
NZ	Novaya Zemlya
NZTS	Novaya Zemlya Test Site
PNEs	Peaceful Nuclear Explosions (meaning a nuclear explosion in Russia conducted at a location other than a recognized nuclear weapons test site)
SS	An abbreviation for STsR-SS (see below), in turn the Russian abbreviation for the second seismographic system used at Borovoye
STS	Semipalatinsk Test Site
STsR-SS	A Russian abbreviation for the second seismographic system used at Borovoye
STsR-TSG	A Russian abbreviation for the third seismographic system used at Borovoye
TSG	An abbreviation for STsR-TSG (see above), in turn the Russian abbreviation for the third seismographic system used at Borovoye
UK	United Kingdom
USA	United States of America
USSR	Union of Soviet Socialist Republics